DEVELOPMENT AND APPLICATION OF CHEMICALLY MODIFIED GRAPHITE ELECTRODES FOR USE IN CONTINUOUS-FLOW SYSTEMS

BY

FAKHRILDEEN NIEMA ALBAHADILY

Bachelor of Science
Basrah University
Basrah, Iraq
1976

Master of Science
Texas A&M University
College Station, Texas
1984

Submitted to the Faculty of the
Graduate College of the
Oklahoma State University
in partial fulfillment of
the requirements for
the degree of
DOCTOR OF PHILOSOPHY
July, 1989

Thesis
1989
A325d
cop. 2

Oklahoma State Univ. Library

DEVELOPMENT AND APPLICATION OF
CHEMICALLY MODIFIED GRAPHITE
ELECTRODES FOR USE IN
CONTINUOUS-FLOW
SYSTEMS

Thesis Approved:

Horacio R. Mottola
Thesis Advisor

J. Paul Oberlin

Carl D. Mitchell Jr.

Norman N. Durham
Dean of the Gradute College

425853

PREFACE

I have dedicated this thesis to the memory of my father who strived hard all his life for the betterment of his children's education but missed seeing me fulfill his hopes and my goal by many years. Besides my father, my mother, my brothers, and my sisters all have given encouragement throughout my studies, for which I am grateful. Special appreciation goes to my wife Zaineb and my daughters Sarah and Nadia for their love and encouragement.

Special gratitude and appreciation go to my thesis advisor, Dr. Mottola, who spent an uncountable amount of time and effort in supervising and perfecting this piece of research. Besides being advisor, Dr. Mottola was the friend and the teacher who taught chemistry and fishing. His influence in my life will never be forgotten. Thanks are directed to Dr. Devlin, Dr. Gelder, Dr. McGown, and Dr. Mitchell, who served on my committee and gave invaluable advice during the time I spent in the chemistry department. Special thanks go to Dr. Dermer for proofreading this thesis.

Since this research stemmed from the knowledge of my chemistry study, I am grateful to all the professor at this university. I am also thankful to the department of

chemistry for the financial support and for the use of their facilities in the conduct of this research.

My sincere appreciation also goes to the past and the present members of Dr. Mottola's research group, Dennis, Monte, Shaker, Jim, Kazi, Frazier, Sudha, Matt, Al, Zack, Ricky, and Chris for their help and friendship.

TABLE OF CONTENTS

Chapter Page

LIST OF TABLES

LIST OF FIGURES

CHAPTER I

INTRODUCTION

There is an increased interest in the development of simple and efficient instrumental techniques for the determination of air pollutants of gaseous nature. Because of their toxicity and chemical reactivity, nitrogen dioxide (NO_2) and sulfur dioxide (SO_2) are of particular interest.

The work reported in this thesis is part of efforts to construct and optimize dependable input transducers (detectors) for the determination of NO_2 and SO_2 in air samples. Such determination is based on amperometric measurements since the two species are electrochemically active. The detector is expected to be part of a flow injection analysis system. Such systems with amperometric detection offer advantages over other instrumental methods in terms of sensitivity, speed, simplified hardware, and cost, yet results obtained with this approach are comparable to those reported for other methods of manipulating solutions. The success of the whole system, however, depends on the design of the flow cell and the type of electrode used.

Three common cell configurations are used under flow conditions: tubular, thin-layer, and wall-jet. Each has

its own advantages and limitations. Some characteristics of the three configurations are listed in Table 1. It seems, from the Table, that wall-jet and thin-layer configurations are more practical. This conclusion is clearly reflected in the literature by the number of publications using these two configurations in amperometric-based detectors. Nevertheless, criteria such as cell volume, nature of the flow, and type of electrode material usually decide the issue.

Regardless of the cell configuration used, amperometric sensors should meet the following requirements:

1. The sensor should display sufficient mechanical strength to insure stability under flow conditions.

2. The sensor should show low and predictable background current to achieve high sensitivity and low detection limits.

3. The sensor should have a wide dynamic range (i.e. response proportional to analyte content ration) regardless of interferences from other species in the system.

4. The time constant of the sensor should be low enough to allow high determination rates with minimum signal distortion.

5. The sensor materials should be chemically inert toward the analyte and the carrier.

Electrochemical sensors based on two-electrode

TABLE I

CHARACTERISTICS OF COMMONLY USED FLOW-THROUGH CELLS

	Wall-Jet	Thin-Layer	Tubular
Equation for Limiting Current	$I = knFAcD^{2/3}v^{-1/6}(u/l)^{1/2}$	$I = 0.68nFD^{2/3}Cbl^{1/2}u^{1/2}v^{-1/6}$	$I = 2.01nF\ D^{2/3}l^{2/3}u^{k}r^{2/3}C$
Flow Type Through the Cell	turbulant	laminar	laminar/turbulent
Useful Potential range in Citrate-Phosphate Buffer vis. SCE (V)	-0.8 to +1.2 (glassy carbon) -0.8 to +1.0 (carbon Paste)	-0.8 to +1.2 (glassy carbon) -1.5 to 1.2 (carbon paste)	-0.5 to +1.2
Residual Current (A)	1.0×10^{-5} (glassy carbon) 1.8×10^{-7} (carbon paste)	$2.4 \times 10^{-8} - 5.6 \times 10^{-8}$ $1.0 \times 10^{-7} - 2.0 \times 10^{-7}$	$3.0 \times 10^{-8} - 1.0 \times 10^{-5}$
Detection Limit of Adernaline (ng)	0.3 (glassy carbon) 0.03 (carbon paste)	0.5 (glassy carbon) 0.5 (carbon paste)	0.3
Linear Dynamic Range (ng)	0.3 to 3000 (glassy carbon) 0.03 to 3000 (carbon paste)	1 - 5000 (glassy carbon) 1 - 5000 (carbon paste)	0.3 - 2500
Relatively Minimum Acheivable Cell Volume	ver small (<0.1 ul)	small(<1 ul)	large (>10 ul)
Ease of Costruction	easy	easy	difficult
Signal to Noise Ratio (similar electrode areas)	$181.9\ r^{-1/2}$	$138.6\ l^{-1/2}$	$85.2\ (rl)^{-1/3}$

arrangements can be used under flow conditions (1,2). Such cells have the advantage of eliminating the need for a reference electrode and allows cell design with minimum volume. The two-electrode arrangements also minimize the IR drop problem. Application of such a cell is limited to zero-current conditions, which do not allow significant chemical information to be acquired. More attractive are cells with three electrodes (indicator or working electrode, reference electrode, and auxiliary electrode). This design does not solve the IR-drop problem completely. It has the advantages, however, of keeping the potential of the reference electrode constant since no current is drawn from it. Kissinger et al. (3) proposed five design options for thin-layer-based amperometric detectors. These displayed different levels of IR drop depending on the location of the reference and auxiliary electrodes with respect to the indicator electrode. While selecting electrode material for indicator electrodes is of prime importance, some consideration has to be given to the nature and position of the auxiliary electrode in cases were oxidation or reduction is expected to take place on its surface. This may be considered as advantageous for improving the detection limits since the product from the indicator electrode is converted back to reactant on the surface of the auxiliary electrode (4).

The nature of the indicator electrode material contributes significantly to the quality of the output

signal expected from electrochemical detectors. Mercury is an attractive electrode material for detecting reducible species. It produces a small and reproducible current. When used as the dropping mercury electrode (DME), it offers continuous surface renewal, which minimizes surface poisoning. These electrodes, however, have limited working anodic potentials and suffer from current oscillations because of continual drop re-formation. Flow cells based on the DME are very few (5,6) as the cell design imposes significant difficulties. It is possible, however, to deposit thin films of mercury on the surfaces of solid electrodes. This allows use of mercury electrodes in flow cells, but without the continuous surface renewal observed with the DME. Difficulties associated with the replication of the same mercury film thickness has to be considered also.

Amperometric detectors with platinum as indicator electrodes are commonly used in tubular cell configuration. They exhibit high sensitivity with a wide anodic working potential range but with limited cathodic potential owing to hydrogen evolution in aqueous media. They are expensive and not very useful for detection of many organic compounds owing to the formation of platinum oxide, which slows down the electrode reactions and increases the IR drop. Silver and copper are very seldom used in flow cells. Silver has been used for amperometric determination of cyanide (7), and copper for determination of amino acids (8).

Since detectors with graphite electrodes as sensing material are widely used in flow systems, the development of these electrodes is discussed in more detail in this introduction, and indeed is the main work reported in this thesis.

Development of Graphite Electrodes

Since their introduction in the early 50's, graphite electrodes have been found to be very useful electrochemical surfaces. Compared to other solid electrodes (e.g. platinum, silver, and copper), graphite is unique in terms of availability, ease of shaping, and surface renewability (9). Plain graphite electrodes suffer from high background current, memory effect, and low sensitivity. Gayler (10) took a major step in minimizing or eliminating problems associated with these electrodes. The enhancement process involved impregnating graphite rods with a high molecular weight wax. The new electrodes are more practical for analytical purposes (11).

Adams (12) realized the importance of the wax-impregnated graphite electrodes and tried to overcome the tedious impregnation step with a more practical procedure. Rather than using graphite rods, Adams wetted graphite powder uniformly with a viscous organic liquid. The new materials had a pasty form and were called "carbon paste electrodes". Since they are inexpensive, easy to prepare, exhibit very low residual current, and show

relatively good surface renewability, graphite paste electrodes became the material of choice for many applications. However, these electrodes display the following drawbacks: (a) their usage is mostly limited to aqueous media, (b) electrode reactions are relatively slower than those reported for well polished glassy carbon or metallic electrodes, and (c) they display insufficient mechanical strength to be used in wall-jet cell configurations or as rotating disk-electrodes.

The usefulness of carbon paste electrodes in nonaqueous media was recognized as soon as these electrodes were developed. Adams and his group (13) described a paste composition that can resist the action of many nonaqueous solutions with performance similar to electrodes used in aqueous solution. These electrodes included surfactants in their compositions and lost their characteristics when exposed to aqueous media.

Many ways have been considered to eliminate the slow electron transfer process on the surfaces of paste electrodes. Rice et al. (14) and Ravichandran and Baldwin (15) enhanced the rate of the electron transfer process significantly by pretreating the graphite electrodes electrochemically. Urbaniczky and Lundstrom showed that including alumina in the paste composition enhances the electrochemical oxidation of hexacyanoferrate(II) (16). We have reported recently (17) that treating the paste electrode surfaces with surfactant affected the rate of

reactions at different graphite pastes, significantly. Swofford and Carman (18) were first to realize the need for a paste electrode with appreciable mechanical strength to be used as a rotating disk. They used epoxy resin as a binding agent. Pungor and Szepsvary (19,20) described a new type of electrode based on silicone rubber as a binder.

The success attained in using electrochemical detectors in flow systems (21) encouraged the electrochemists to develop more reliable "universal" electrochemical detectors. Those made of carbon or graphite are more practical than other electrode materials because of their availability, working potential range, and price. Two forms of graphite are commonly used, glassy carbon and graphite paste electrodes. Neither of these is ideal for all applications. For surface renewability, availability, price, and ease of fabrication, paste electrodes are more attractive. Glassy carbon electrodes are more useful for use in a wide range of solvents and are mechanically more stable.

The efforts to develop of more reliable graphite electrodes resulted in the construction of a new generation of electrodes that display some of the advantages of glassy carbon and graphite paste. They utilize solid matrices as binders instead of the organic liquids used with the classical paste electrodes. Klatt et al. evaluated Teflon as a binding agent (22). Anderson et al investigated the usefulness of Kel-F as a binding material (23). Armentrout

et al. used polyethylene as a binding agent (24). Stulik et al. introduced poly(vinylchloride), chloroprene rubber, and alkylphenol resins as binders species (25). Anderson et al. (26,27) and Mclean (28) employed these electrodes as sensing elements in flow systems with electrochemical detectors. Difficulties associated with electrode fabrication, shaping, and surface renewal have limited the popularity of these electrodes. Despite their shortcomings, graphite electrodes, as already mentioned, are better for amperometric sensors because of their low background current and working potential range. Their level of utility is enhanced significantly by modifying their surfaces by the attachment of some chemical species.

Chemical Modification of Carbon Paste with Ferroin/Ferriin Couple

Electrodes that have foreign molecules on their surfaces are called "surface-modified electrodes". The modification process is employed to impart specific chemical or electrochemical properties to the plain electrodes. Such possibility may be employed to customize the electrode surfaces to eliminate drawbacks that limit usability of graphite electrodes, for example, and enhance their sensitivity.

Iron complexes with 1,10-phenanthroline, particularly tris(1,10-phenanthroline)iron(II), ferroin, and di-u-hydroxy-bis[bis(1,10-phenanthroline)iron(III)], the

binuclear reduced form of ferroin, have been chosen as modifying species in this study. These two complexes are known for their usage (especially ferroin) as redox indicators. An attractive feature of these species is that oxidation or reduction can be accomplished merely by changing the oxidation state of the central metal ion without affecting the organic moiety. This can be achieved chemically as well as electrochemically. It has been found recently that solutions of these species can be used as chemical probes for the determination of SO_2 (29) and NO_2 (30) in air samples. Immobilizing these reagents on graphite electrode surfaces is not expected to change their chemical or electrochemical behaviors. The modification process should increase the sensitivity and minimize surface poisoning of graphite electrodes as well as reduce reagents consumption.

The foregoing discussion is intended to introduce the rationale behind the idea of selecting graphite as electrode material and the iron complexes of 1,10-phenanthroline as chemical modifiers as the electrochemical sensors for determination of pollutants having redox characteristics.

This thesis reports the following:

1. The work done in the area of chemically modified electrodes is critically reviewed in chapter IV. Obviously it is not intended to be an exhaustive survey of surface-modified electrodes; rather, it is restricted to cases in

which the modifying species is covalently attached to electrode surfaces, including graphite.

2. Chapter II is aimed to contribute to the knowledge of the behavior of iron complexes of 1,10-phenanthroline. These complexes are used to modify graphite electrode surfaces and as probes for monitoring the activity of nitrogen dioxide and sulfur dioxide in air samples. Conclusions about these complexes are built on results obtained from cyclic voltammetry. The construction of the instrument designed and used for cyclic voltammetry is also discussed. The chapter includes discussion about utilizing a four-electrode cell arrangement. The cell offers many advantages over the conventional three-electrode cells:

a. Lower limits of detection can be approached since the measurements are carried out in the absence of electrochemical interferences other than the analyte species.

b. Introduction of a second indicator electrode for background suppression is expected to allow cyclic voltammetry to offer qualitative and quantitative information regardless of scan rates up to appreciable values.

c. The cell is an enhanced tool to study the kinetics and the mechanism of many electrochemical reactions.

3. Efforts concerned with the modification of the microstructure of graphite paste electrode surfaces, in

order to increase conductivity in electrochemical detection in continuous-flow system, are discussed in chapter III.

4. Chapter V describes the procedural steps used to modify graphite surfaces chemically by attaching tris(1,10-phenanthroline)iron(II), ferroin. Another modification approach based on physical incorporation of ferroin in wax-based graphite electrodes is also discussed. Characterization of the modified electrodes as well as preliminary results obtained with them are presented in the Chapter.

CHAPTER II

THE ELECTROCHEMICAL BEHAVIOR OF FERROIN/FERRIIN COUPLE

The iron complexes with 1,10-phenanthroline, particularly the tris(1,10-phenanthroline)iron(II) complex, known as ferroin, have found use in analytical chemistry as redox indicators as well as for the absorptiometric determination of iron (31). The iron(III) complexes can exist as mononuclear ones, known as ferriin, or binuclear ones. The binuclear form involves mixed-ligand complex formation (32,33). Basic electrochemical information regarding these redox couples in aqueous solutions is, however, rather scarce. Pantani and Ciantelli (34) studied the voltammetric behavior of these complexes at a platinum electrode using a cell allowing the periodic renewal of the diffusion layer. The ferroin/ferriin system, in 1.0 M H_2SO_4, was found to be reversible, involving a one-electron exchange, and exhibiting an $E_{1/2}$ equal to +0.844 V vs. the SCE. The potential of the cathodic wave was observed to shift to less positive potential values when the concentration of the acid was increased (e.g. to +0.695 V in 5 M H_2SO_4). The binuclear complex of iron(III), of yellow color and prepared by direct complexation in excess ligand

and in acidic medium of low ionic strength, was studied at a superficially reduced platinum electrode. The electron exchange process was quasi-reversible with anodic and cathodic waves separated by about 0.8 V (34).

Ogura et al. have reported on an electrochemical study of the oxidation of ferroin in aqueous sulfuric acid at a platinum electrode. They compared kinetic data to those for homogeneous systems (35) and presented the cyclic voltammogram of ferroin/ferriin in sulfuric acid (pH = 1.63) and 0.10 M Na_2SO_4 (platinum electrode, scan rate 1 $mV.s^{-1}$) (36). The cyclic voltammogram of ferroin solutions confirmed the reversibility of the electron exchange process (identical cathodic and anodic currents) with E_{pa} 0.89 V and E_{pc} 0.81 V.

Formal redox potentials in sulfuric acid solutions of different molarity are also available for the ferroin/ferriin couple (31).

The new experimental work reported in this chapter was aimed to contribute to the knowledge of the behavior of the iron complexes with 1,10-phenanthroline. Information about the iron complexes was derived by employing cyclic voltammetry as a diagnostic tool using both platinum and graphite paste electrodes. The instrument used to generate the driving potential for cyclic voltammetry as well as the reaction cell output modifier are also discussed.

Experimental

Reagents

1,10-Phenanthroline and 1,10-phenanthroline ferrous sulfate (0.25 M solution in water), ferroin, were obtained from G.F. Smith Chemicals (Columbus, Ohio). Ferric nitrate [$Fe(NO_3)_3.9H_2O$] was reagent grade from Fisher Scientific (Fairlawn, New Jersey). All salts used for supporting electrolyte purposes and all other chemicals used were of analytical reagent grade. All solutions were used immediately after preparation to avoid decomposition, especially of ferroin at low pH values. The water used for solution preparation was deionized and further purified by distillation in all-borosilicate glass still with a quartz immersion heater.

Preparation of Binuclear Species

The binuclear complexes were prepared by chemical and electrochemical methods. Chemical preparation consisted in placing 5.00 mL of a 1.00×10^{-2} M iron(III) nitrate solution containing 0.1982 g of 1,10-phenanthroline in a 200-mL volumetric flask containing the required amount of acid and filling the flask to the mark with supporting electrolyte. The final solution was 1.00×10^{-2} M in ligand and 5.00×10^{-4} M in iron(III).

Electrochemical oxidation was performed by mixing 2.00 mL of 2.50×10^{-2} M ferroin (stock solution) with 80 mL of

1.00 M KCl that contained a given amount of 1,10-phenanthroline in a 150 mL-beaker. The required amount of acid was added to adjust the pH and the volume increased to 95 mL. The solution then transferred to a 100-ml volumetric flask and the flask filled to the mark by adding 1.00 M KCl solution. The final solution was oxidized electrochemically by exposing the working electrode (cylindrical platinum gauze) to a potential of 1.20 V vs SCE in a conventional three-electrodes cell. The oxidation process can be monitored visually, as the solution color changes from red, to purple, to blue, then to yellow. The blue color is that of the ferriin and the purple color is a mixture of the red ferroin and the blue ferriin. The yellow is due to the binuclear complex of iron(III) with 1,10-phenanthroline. The rate by which the oxidation process proceeds is a function of pH as well as the amount of excess 1,10-phenanthroline present in the solution. For example, it took more than 72 hours for ferroin solution at pH 1.0 to be completely oxidized to the binuclear when 0.0493 g of 1,10-phenanthroline was added to the 100-mL flask containing the ferroin solution. At pH 4.0 the oxidation process is completed in about 1 h in a solution with the same amount of 1,10-phenanthroline. When the amount of the 1,10-phenanthroline was increased to 0.2980 g the oxidation process reached completion in about 30 min. at pH 2.0 or at higher pH values. At pH 1.0 it was still possible to increase the rate by which the ferroin was

converted to ferriin by increasing the amount of 1,10-phenantroline; however, it took more than 24 h to convert the ferroin completely to the binuclear complex.

Carbon Paste (Working) Electrodes

Graphite powder (UCP-1-M, from Ultracarbon Corp., Bay City, Michigan) was mixed with high-vacuum silicone grease (Dow Corning, Midland, Michigan) and hexadecane (Aldrich Chemical Co., Milwaukee, Wisconsin). Usually 1 g of carbon powder was mixed with the silicone grease, which had already been blended with the hexadecane to form a thick oily paste. Mixing, usually for 15 min, to produce a uniform paste, was done with a spatula covered with Teflon tubing. This paste was pressed into the well of the electrode and its surface smoothed against a clean computer card. The paste was in direct contact with a copper wire to provide electrical contact with the measurement circuit. As will be discussed later, the body of the electrode was made of Teflon and the electrode surface was easily renewed by screwing the thick copper wire (3 mm o.d.). The copper wire was fitted inside the Teflon holder used for electrical contact. The geometric area of the electrode exposed to solution was 0.21 cm^2; the electrochemical area calculated from the slope of charge-vs-$t^{1/2}$ plots obtained from chronocoulometric measurement (37) was 0.244 ± 0.002 cm^2. The procedure used for the electrochemical area measurements is detailed in Chapter 4.

Paste Composition

Several alternatives were considered in preparing the carbon paste electrodes used in these studies. Mixtures of carbon powder with silicone grease, hexadecane, and a mixture of hexadecane and silicone grease were used and evaluated. A general trend was observed with respect to background current; it was larger the greater the percentage of silicone grease used. The silicone grease, however, was needed to provide desirable consistency to the paste. A satisfactory compromise was observed with the following percent composition in weight: 50 parts of carbon, 25 parts of hexadecane, and 25 parts of silicone grease; this was used throughout this work. Figure 1 shows the background current observed with different paste compositions.

Apparatus

The triangular wave generator and potentiostat used for cyclic voltammetry measurements are described below. The potential between the working electrode(s) and the reference electrode (SCE) was monitored with a Hewlett Packard multi meter (HP3468A) and a platinum wire was used as a counter electrode to complete the three-electrode and the four-electrode cells used in these studies.

The four-electrode electrochemical cell was used to study the behavior of the ferroin/ferriin couple without interferences from the background current. Voltammograms were recorded with a Houston Instruments X-Y recorder (model

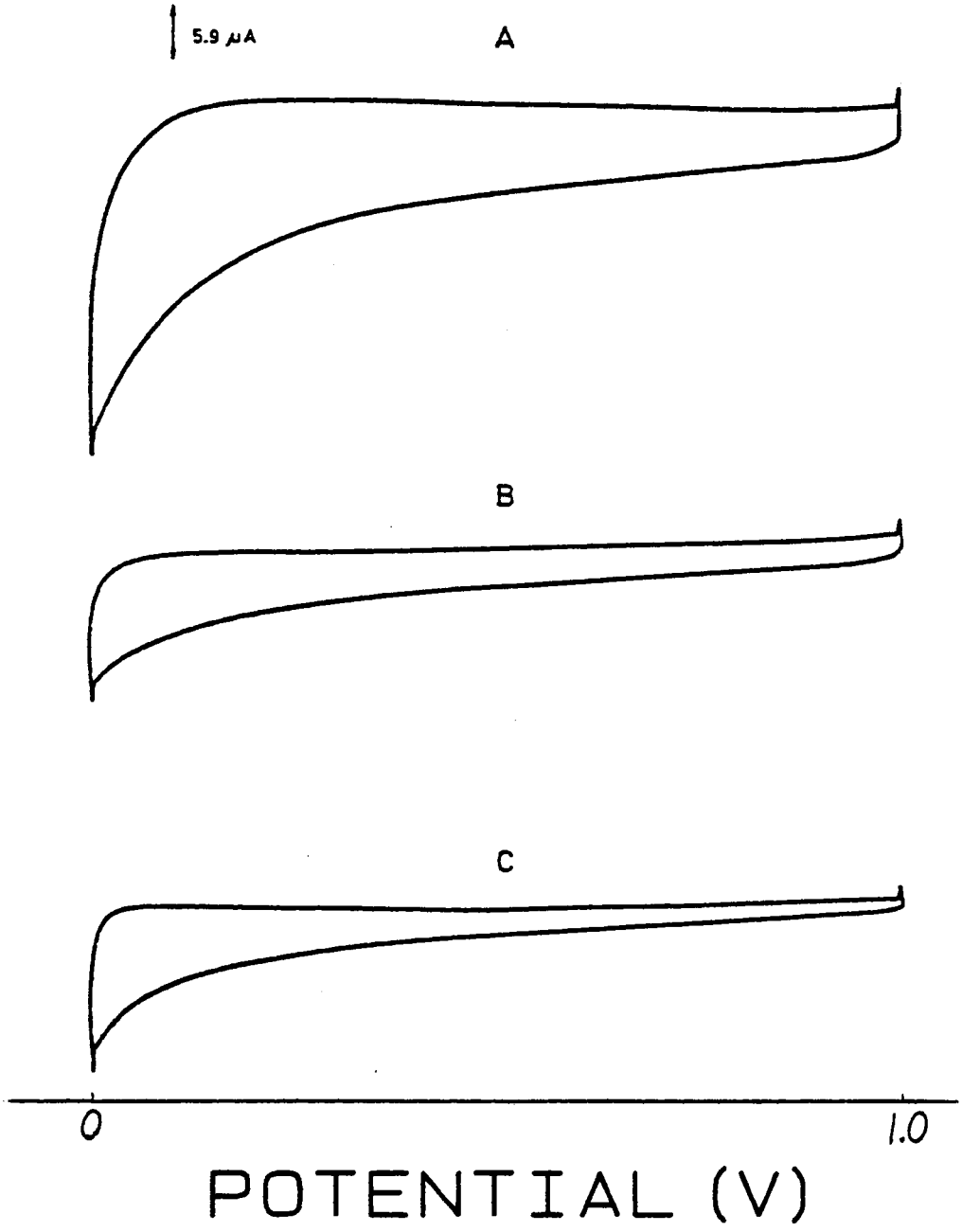

Figure 1. Background current of paste electrodes observed in 1.00 M KCl. Electrode composition; (A) 50% silicone grease and 50% graphite; (B) 25% hexadecane, 25% silicone grease, and 50% graphite; (C) 50% hexadecane and 50% graphite.

2000). Chronocoulometric experiments were performed with the aid of a BAS-100 electrochemical analyzer (Bioanalytical Systems Inc., West Lafayette, Indiana). All pH measurements were made with a Model 601A Orion digital pH meter equipped with a combination electrode (Sensorex, Westminster, California). An MP-1026 power supply (McKee-Pedrson Inst., Daville, California) working in the potentiostatic mode was used to electrolytically convert ferroin into the binuclear complex.

Circuit-Related Considerations

An advantage of cyclic voltammetry lies in its ability to offer information about the oxidized as well as the reduced form of the same species in a single experiment. This can be accomplished by applying a single cathodic sweep of voltage followed by an anodic return at the same rate to the starting point. The cathodic voltage ramp followed by the anodic one is simply a triangular-wave potential. This form of potential can be generated by the function generator described below.

Trianglular-Wave Generator. Figure 2 gives the diagram for the signal generator. Switches S_1 and S_2 permit choosing a multicycle operation (free run) or a single-cycle operation (single shot). Switching S_1 and S_2 to the midway position disables push button switch PS and connects the noninverting input of the multivibrator, OA1, directly to the output of the integrator, OA2, setting conditions for a

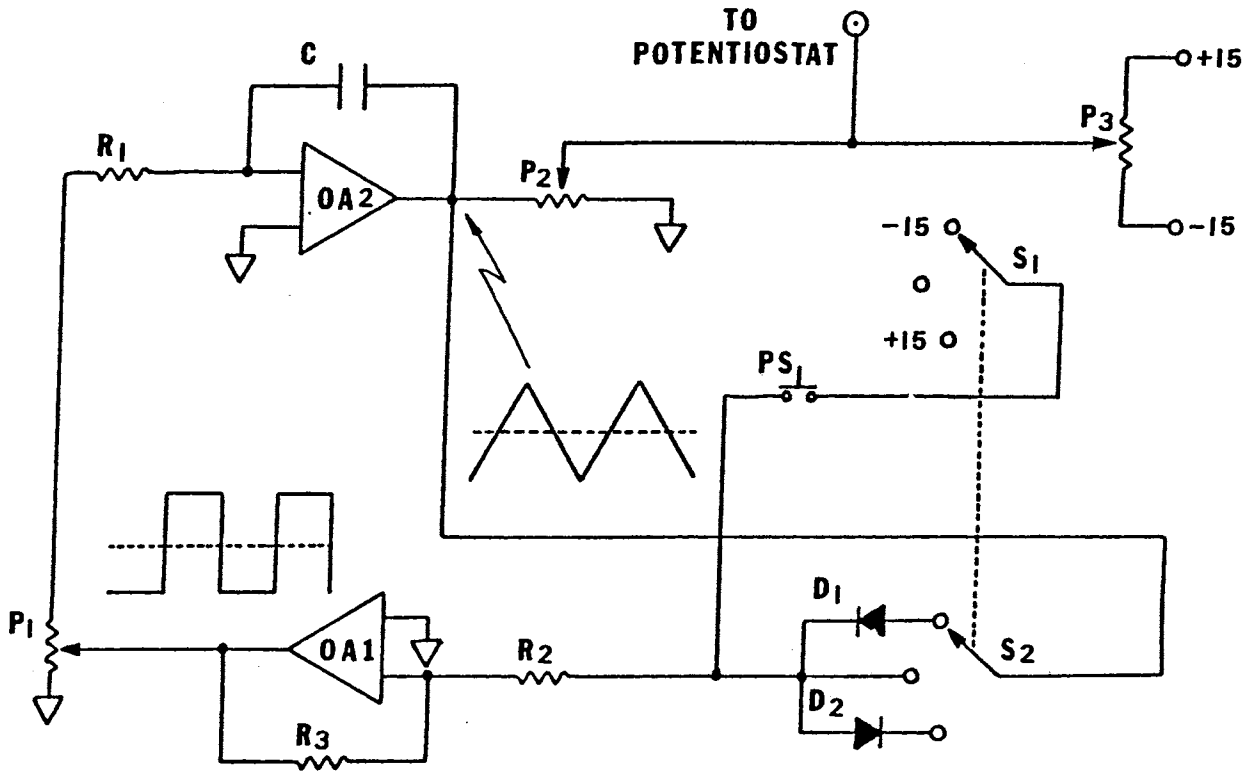

Figure 2. Circuit diagram of the triangular-wave generator used for cyclic voltammetry experiment. (See text for definition of symbols).

free run operation. The multivibrator has two metastable states at +13 and -13 V, and the amplifier is continuously switching between these limits generating a square-wave output of 26 V amplitude. Such potential is supplied by the integrator operating at frequencies dictated by the selection of resistor R_1 and capacitor C. When OA1 has just switched to its +13 V output, OA2 will integrate the portion of voltage passing through potentiometer P_1. Since OA2 has a negative feedback and the signal applied to its inverting input is positive, the result is a negatively increasing (down) signal ramp. This signal will be the output of the generator circuit until the output potential reaches the selected minimum limit. At such a moment, OA1 will switch to its -13 V output. The portion of the negative voltage passing now through P_1 will be integrated by OA2 and the result will be a positively increasing (up) signal until the output of the integrator reaches its maximum potential when the multivibrator will switch again back to the -13 V output. This alternation will continue as long as the power is on.

Switching S_1 and S_2 to the up or down position permits the selection of a single triangular output (single-shot operation). Having both switches in up position (as shown in Fig. 2) causes diode D_1 to allow only a positive signal to pass through and the multivibrator will show positive saturation. The output of the integrator will decay down until it reaches its minimum potential value, when it will

latch at this potential. The level of the minimum potential is dictated mainly by the setting of potentiometer P_3 but it is also affected by that potentiometer P_2. Potentiometer P_2 should be set first to select the amplitude of the triangle; then P_3 can be used to shift the triangle up and down in the voltage scale. Final adjustment using P_2 may be needed. In the single-shot mode, momentary closing of push button PS will apply a negative potential to the vibrator noninverting input, changing its output to -13 V. The integrator will integrate the negative applied signal until its maximum allowable output is reached. Then D_1 will open again allowing the positive-going signal to pass to OA1 and its output will be a negative going signal until it reaches the original potential. With both switches in the down position the operation is similar, with diode D_2 open only to negative-going signals.

Potentiostat. Figure 3 illustrates the circuit used to maintain the potential between the working electrode and the reference electrode constant. The potential is furnished by an external circuit through OA3 acting as a controller. It supplies the current necessary to compensate for the current produced by the electrochemical reaction at the surface of the working electrode. The output current from the working electrode is converted into a measurable voltage by OA5. The reference electrode is connected through a unit-gain voltage follower, OA4, to isolate the electrode and minimize the current flow through it.

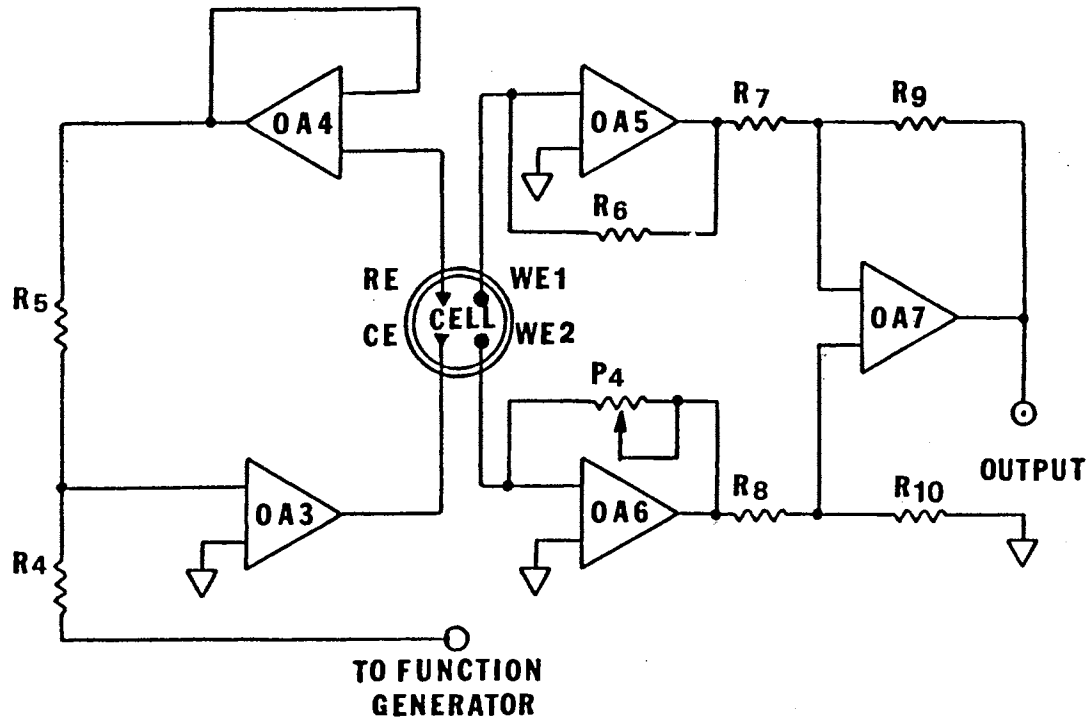

Figure 3. Circuit didgram for the potentiostat, the four-electrode cell, and the instrumentation amplifier. (See text for part description)

Instrumentation Amplifier. A combination of two current followers with gain and a difference amplifier was used to assemble a differential-mode amplifier with high input impedance acting as instrumentation amplifier (Fig. 2). The two inverting inputs of OA5 and OA6 were connected to the two working electrodes of the four-electrode cell described later. The two input signals are amplified by the current followers and their difference is amplified by amplifier OA7.

Circuit Performance

Satisfactory symmetry of the triangular signal was observed. The ratio of areas under the two halves of the triangular signal was always between 0.98 and 1.00. The system proved to be stable for long period of operation. Well characterized systems [e.g. $Fe(CN)_6^{-3}/Fe(CN)_6^{-4}$ and Cu(I)/Cu(II)] were experimentally tested and the generated cyclic voltammogram data and characteristics reproduced the available information in the literature.

The Four-Electrode Cell

Figure 4 shows details of the four-electrode cell centered around a 30-mL beaker. Two holes (2 mm in diameter) were made directly across from each other about 25 mm from the bottom of the beaker. Two Teflon blocks, machined to fit the circumference of the beaker, were attached (by using paraffin) across the holes in the sides

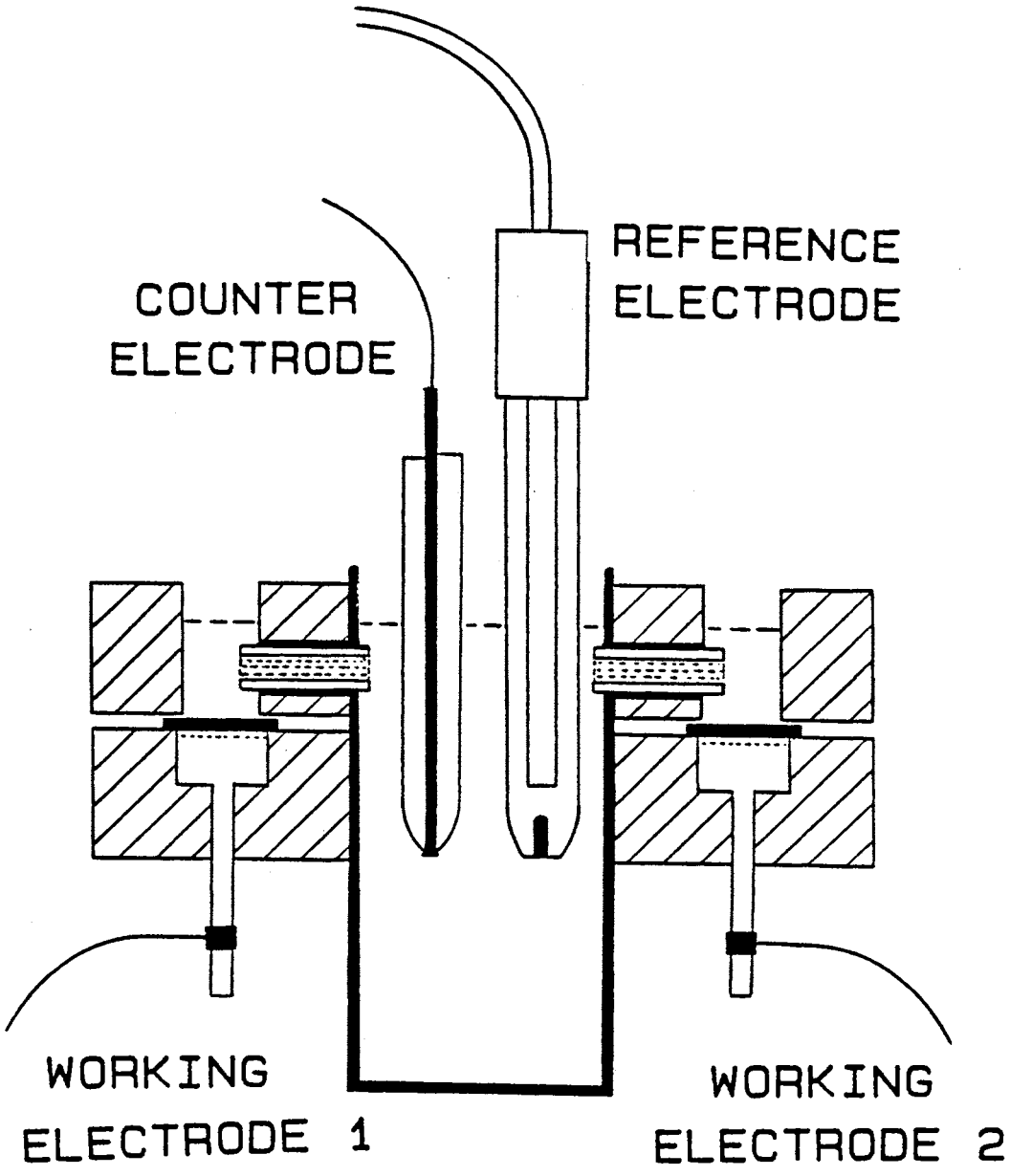

Figure 4. Schematic diagram of the four-electrode cell.

of the beaker, each block about 2 x 2 x 2 cm in dimensions and each cut into halves. The upper half of the block was pierced with a central hole of 0.5-cm^2 area. A corresponding hole of the same area but only 6 mm in depth was cut in the lower part of the block. As shown in Figure 4, these openings permit the assembly of the working electrodes, each made of a copper sheet connected to the circuit via a copper wire. On top of the copper sheet a few drops of mercury provided a closer contact between the copper sheet and a platinum foil (the actual working surface) of about 0.5 cm^2 in area. The upper part of the Teflon block was fastened with screws to the lower part, sandwiching the platinum foil-Hg-Cu electrode assembly. Contact between the content of the beaker and each reservoir (of about 300 μL in volume) was provided by a perforation in the reservoir that was aligned with one of the holes in the beaker wall. To minimize the diffusion of solution between the working electrode compartments and the central container (beaker), small Teflon tubes filled with glass wool were inserted in the channels connecting them. The glass wool was cleaned by boiling in concentrated HCl for about 15 min and washing thoroughly with distilled water until a negative acid test of the washings was obtained.

Performance of the Four-Electrode Cell

As stated earlier, the four-electrode cell is particularly useful for the elimination of interfering

background current(s). To illustrate such a situation the redox system comprised by the redox couple tris(1,10-phenanthroline)iron(II)/tris(1,10-phenanthroline) iron(III), the ferroin/ferriin system, in 1.00 M KCl + 1.00 M H_2SO_4 as supporting electrolyte was chosen. Figure 5 shows the cyclic voltammogram of the supporting electrolyte solution with a three-electrode cell. The background current is the result of the current-potential curve for platinum in H_2SO_4. Measurements were carried out here under static conditions because the method of cyclic voltammetry is not suitable under hydrodynamic conditions. Figure 5 also shows the current-potential curve when the four-electrode cell is used; the minimization of the background current is clearly seen. Figure 6 shows the voltammogram for the ferroin/ferriin system with the three- and with the four-electrode systems. The solution used for these experiments was freed of oxygen by bubbling nitrogen gas through it for about 15 min and then kept air-free during the measurements by flowing nitrogen gas inside a 2-L capped polyethylene bottle with the bottom cut off and with a lateral hole for nitrogen introduction. This bottle covered the entire cell assembly. As can be seen in Figure 6, the use of a four-electrode cell minimized the background contribution and enhanced the details of the voltammogram for the electrochemical species of interest.

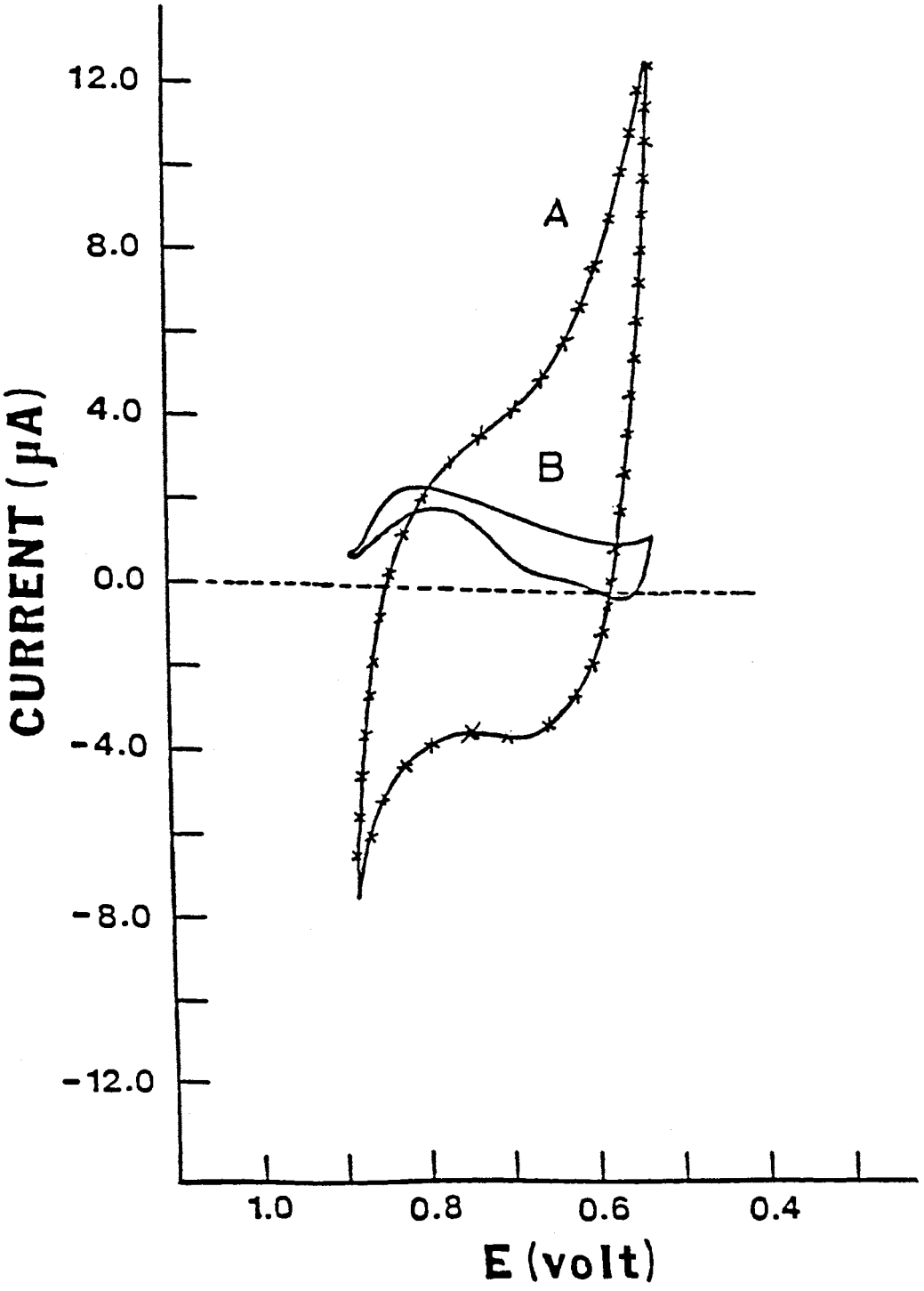

Figure 5. Cyclic voltammogram of 1.00 M KCl (supporting electrolyte) observed with (a) three-electrode cell and (b) with four electrode-cell. Sweep rate 20 $mV.s^{-1}$.

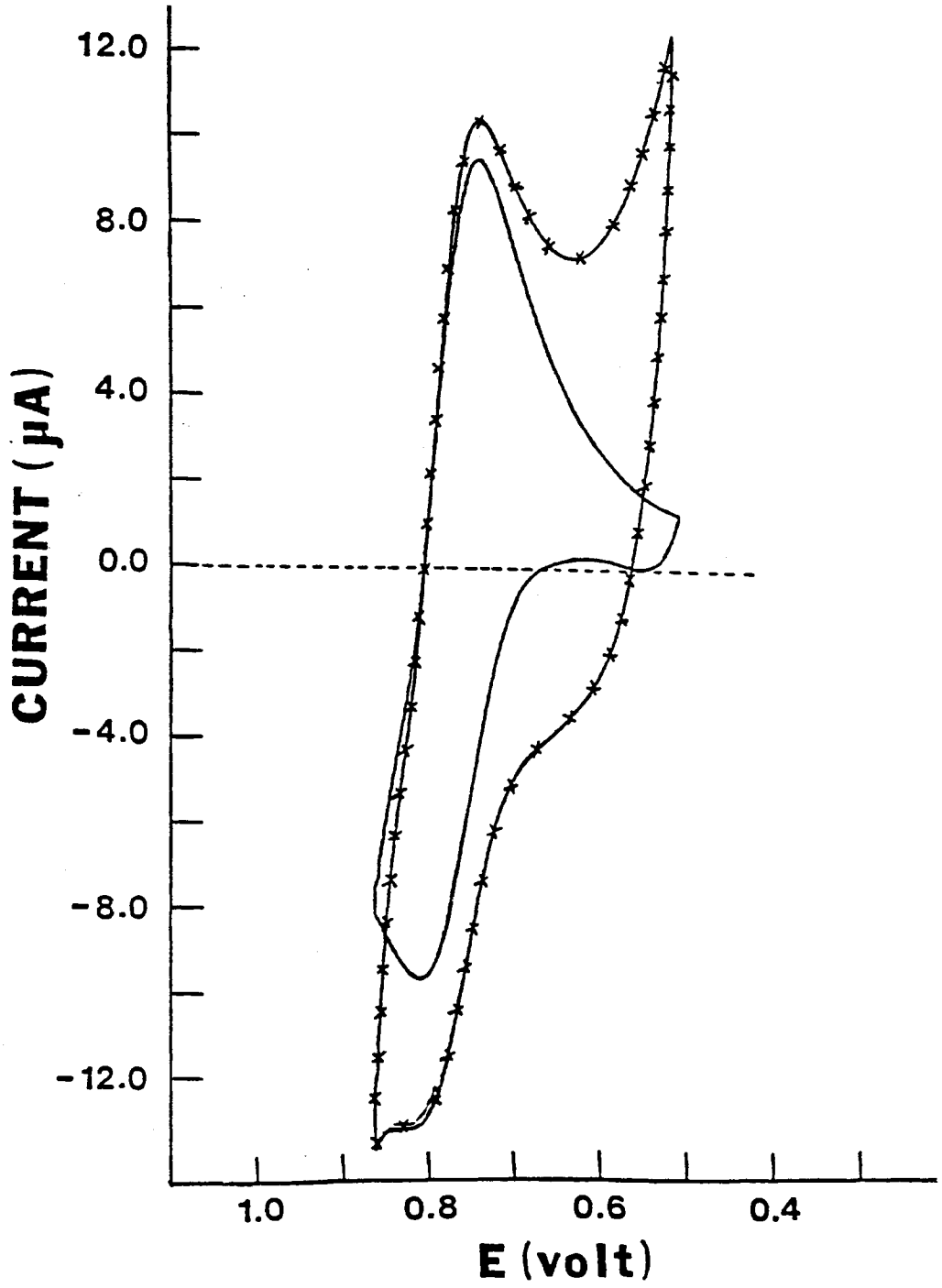

Figure 6. Cyclic voltammogram for a 1.25×10^{-4} M solution of ferroin in 1.00 M KCl + 1.0 M H_2SO_4 solution. (A) Voltammogram obtained with a four-electrode cell, (B) voltammogram obtained with a three-electrode cell. Sweep rate 20 $mV.s^{-1}$.

Electrochemical Behavior of Ferroin Solutions

The effects of hydrogen ion concentration and the type of supporting electrolyte used were studied concurrently. The pH of solutions of supporting electrolytes--potassium chloride, sodium sulfate, and potassium nitrate--was adjusted, as needed, by addition of the corresponding acid. Exceptions to this were solutions containing nitrate, which were acidified with sulfuric acid. The use of nitric acid was avoided because of its oxidizing nature. The pH range studied was between 0 and 5. Parallel studies were carried out using buffered solutions. No changes were observed between pH 3 and pH 5 with buffered or unbuffered solutions. Below pH 3, the presence of competing ligands from the buffer components introduces some additional peaks. In phthalate buffers, for instance, a small peak appears at +0.95 V. Since the need for buffering is not critical below pH 3 and in order to keep the overall picture within boundaries of complexity, all results and interpretations presented here are for solutions containing no competing ligands other than OH- and the anion of the supporting electrolyte.

Voltammograms of solutions of pH higher than 2 and for all supporting electrolytes were very reproducible even 24 h or more after preparation. Interesting trends were observed, however, in solutions of pH below 2 in about 10 h after preparation. Figure 7 shows the typical voltammogram obtained at pH values 3 to 5 in chloride solutions,

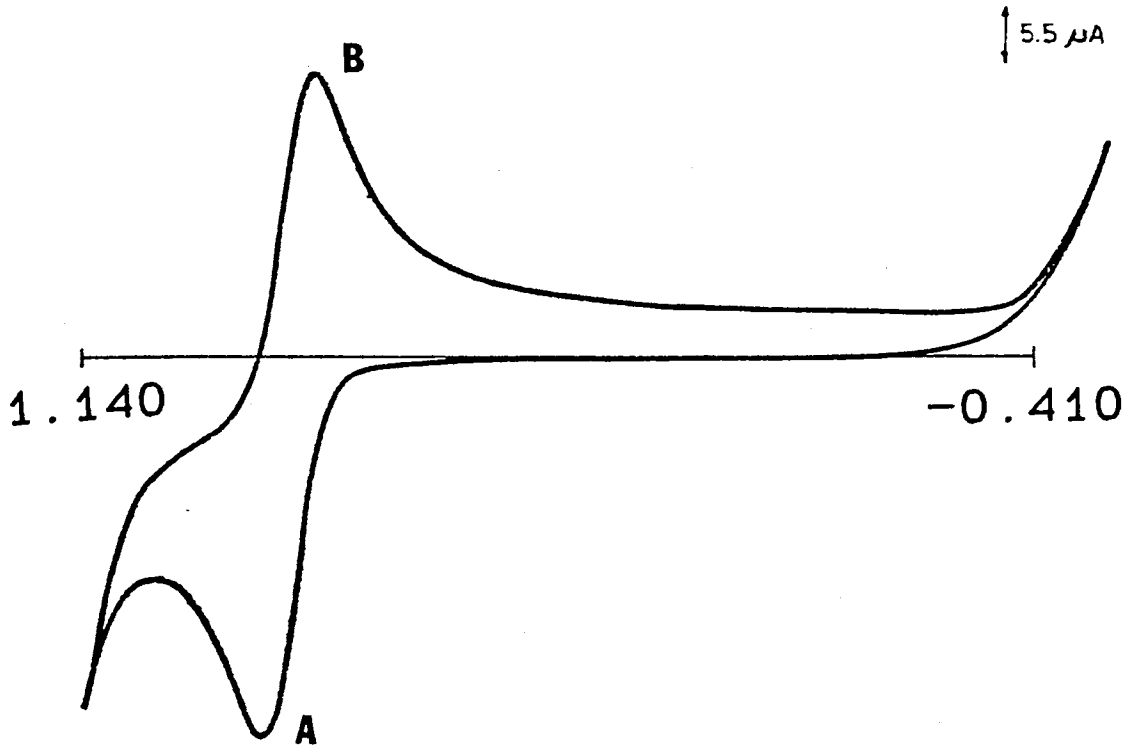

Figure 7. Typical cyclic voltammogram for a 2.50 x 10^{-4} M ferroin in 1.00 M KCl at pH 5.00. (A) Oxidation of ferroin to ferriin, (B) reduction of ferriin to ferroin. Scan rate 400 $mV.s^{-1}$.

including the cathodic and anodic peaks corresponding to the iron(III) and iron(II) complexes. The process is reversible at scan rates in the range of 100 to about 1000 $mV.s^{-1}$ (E_p = 56 to 66 mV). As expected, peak separation increases slightly as the scan rate increases; typical values are shown in Table 2. The dependence of peak current on the square root of scan rate (100 to 10,000 $mV.s^{-1}$) can be represented by the following equations valid at pH 5.0:

$$i_{pa} = 0.234 + 0.106v^{1/2} \quad (1)$$

$$i_{pc} = 0.0363 + 0.0900v^{1/2} \quad (2)$$

and at pH 2.0:

$$i_{pa} = 0.208 + 0.100v^{1/2} \quad (3)$$

$$i_{pc} = 0.0505 + 0.0830v^{1/2} \quad (4)$$

where i_{pa} is the anodic peak current
i_{pc} is the cathodic peak current
v is the scan rate

with correlation coefficients better than 0.999 for all equations. In sulfate solutions the reversibility trend is the same but peak heights are about 20% lower. No difference in peak height was observed between chloride and nitrate solutions. From the collected data a formal potential in chloride solutions of pH 2.0 and 5.0 for the ferroin/ferriin couple of 0.823 V vs. SCE (1.065 V vs NHE) was estimated. The following equation was used to calculate the formal potential:

$$E_{formal} = (E_a + E_c) / 2 \quad (5)$$

where E_a is the potential of the anodic peak

TABLE II

DEPENDENCE OF PEAK SEPARATION, $\Delta E_p = E_{pa} - E_{pc}$, ON SCAN RATE

SCAN RATE	ΔE_p (mV)	
$mV.s^{-1}$	pH = 2.00	pH = 5.00
100	56	57
200	58	58
300	60	62
400	62	62
500	63	64
600	64	64
700	64	63
800	62	65
900	64	67
1005	66	66
2007	73	72
5120	86	86
10240	92	93

E_c is the potential of the cathodic peak

Values ranging from 1.141 to 0.76 V have been reported in sulfuric acid solutions in the 0 to 8.0 M concentration range (31).

Increasing hydrogen ion concentration (pH below 2) brought about changes in the cyclic voltammograms with time. Figure 8 compares trends observed at pH = 0 in solutions of chloride and nitrate as supporting electrolytes and at different times. A slow decomposition of the iron complexes at such high hydrogen ion concentration was observed in both media. The chloride medium showed complete disappearance of the ferriin reduction wave after 24 h but some still remained in the nitrate and sulfate medium. In the chloride medium redox processes of the iron(II)-iron(III) moieties responsible for the waves observed at the extremes of the potential range swept seem to be more readily reversible than the corresponding ones in the nitrate-sulfate solution. It is known that reaction of the iron(III)-iron(II) complexes show different degrees of quasi electrochemical irreversibility depending on the background solution (39).

In solutions of low ionic strength (0.10 to 0.50 M, at pH 2 and pH 5 and with potassium chloride as supporting electrolyte) poor reproducibility was observed. Comparable and reproducible cyclic voltammograms were obtained at ionic strengths of 0.50 and up to 3.0 M.

At ferroin concentrations in the 1.0×10^{-6} M and 2.5×10^{-3} M range, linear dependence was observed between the

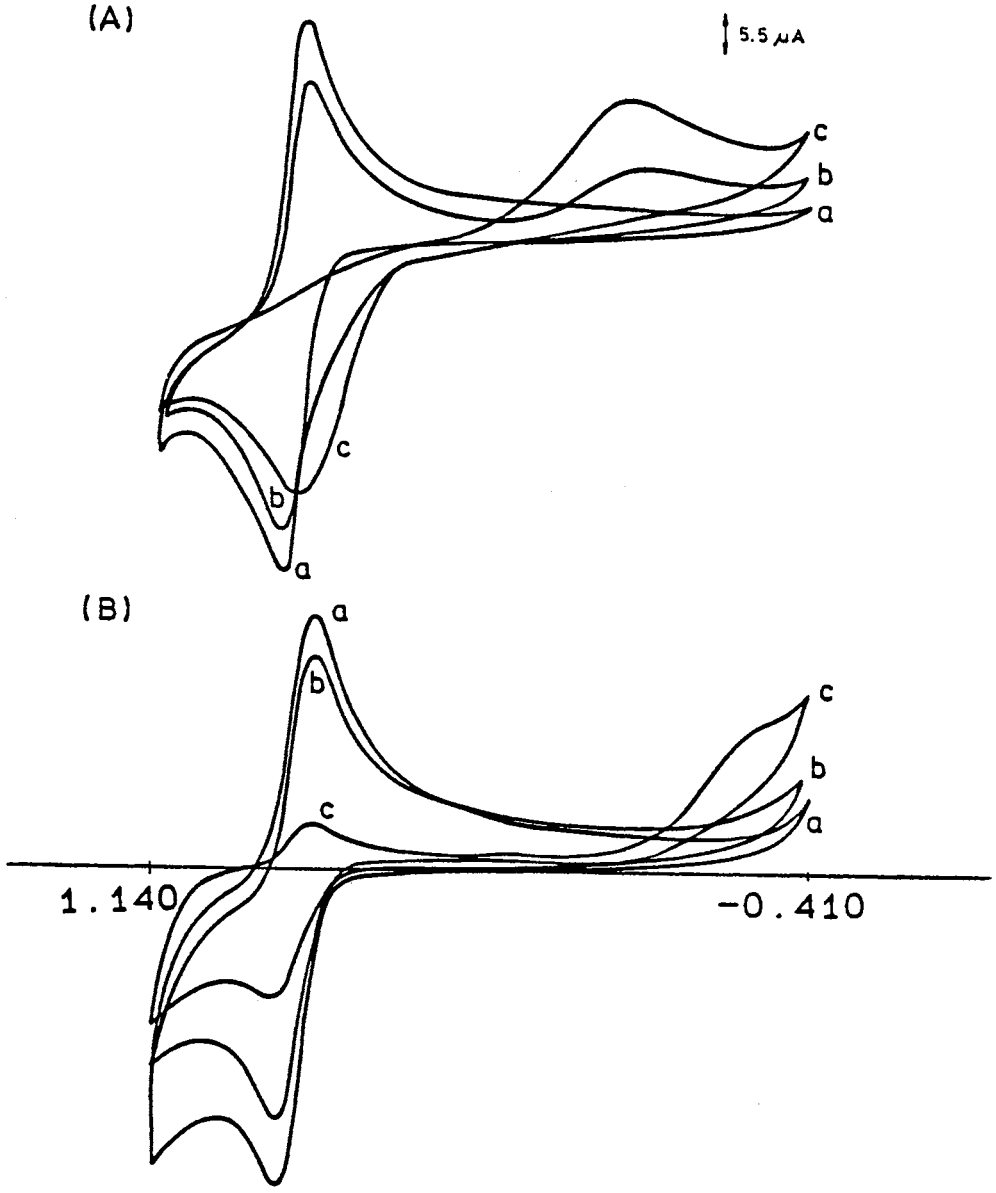

Figure 8. Comparative cyclic voltammograms at pH 0 taken at different times after preparation in solution of chloride (A) and nitrate + sulfate, (B). ferroin concentration: 2.50×10^{-4} M; scan rate: 125 $mV.s^{-1}$. (a) Freshly prepared solution, (b) 1 hour old solution, and (c) 24 hour old solution.

anodic peak heights and the ferroin concentration, both at pH 2.0 and at pH 5.0 (1.0 M KCl). The straight lines representing this behavior are described by equations:

$$i_{pa}(\text{in } \mu A) = 0.533 + 3.32 \times 10^{+4}[\text{ferroin}], \text{ at pH} = 2.0, \quad (6)$$

and

$$i_{pa}(\text{in } \mu A) = 0.922 + 3.38 \times 10^{+4}[\text{ferroin}], \text{ at pH} = 5.0 \quad (7)$$

Stabilization of these solutions can be obtained by addition of excess ligand. The relative concentrations (ligand/complex) needed for stabilization are 4:0 at pH = 0.0, 3:1 at pH = 1.0, and 1.5:1 at pH = 2.0. The excess ligand is needed to repress the dissociation of the complex by upsetting the competition of protons for the nitrogen-coordinating sites of the 1,10-phenanthroline.

Electrochemical Behavior of Iron(III) Complexes

As already iron(III) complexes with 1,10-phenanthroline can exist, depending on experimental conditions, as mononuclear species (ferriin) or as binuclear (32,33). Because of instability and restricted use of the mononuclear species (1) it was not studied.

The binuclear iron(III) complex with 1,10-phenanthroline in solution was prepared by two different routes. As discussed earlier, one of the methods consisted in direct electrochemical oxidation of ferroin solutions containing an excess of ligand. The other route involved direct mixing of Fe(III), as nitrate, and ferroin resulting

in solutions with ratios of [ligand]/[metal] in excess of the stoichiometric one. Since different voltammetric behaviors of solutions prepared by these two method were observed in exploratory studies, a sequential reporting of data is given here.

Figure 9 shows a series of voltammograms obtained with solutions prepared by mixing iron(III) with 1,10-phenanthroline and covering the pH range 0 to 5. Voltammograms from 9a to 9f represent a gradual increase in pH. Voltammogram 9a, at zero pH, shows two peaks which, considering the high chloride concentration, the low [OH^-], and the relatively low concentration of unprotonated ligand, are ascribed to a binuclear mixed-ligand complex with chloride and 1,10-phenanthroline as ligands. The system is irreversible, with $\triangle E_p$ = 350 mV at scan rates of 125 $mV.s^{-1}$. Since iron(III) in the chloride medium used here and at the same scan rate shows poorly developed peaks and marked irreversible electrochemical behavior, peaks 1 and 2 cannot be assigned to the solvated and chloro-complexed cation. It is of interest to note that since all iron present is iron(III), if the first scan is initiated at a potential of +0.322 V vs. SCE and conducted in the direction of increasing positive potential, no anodic peak is observed in the first scan. In the second scan, however, the oxidation peak appears.

In voltammogram 9b (pH = 1.0) five peaks can be seen, Peaks 1 and 2 are considered to results from the same

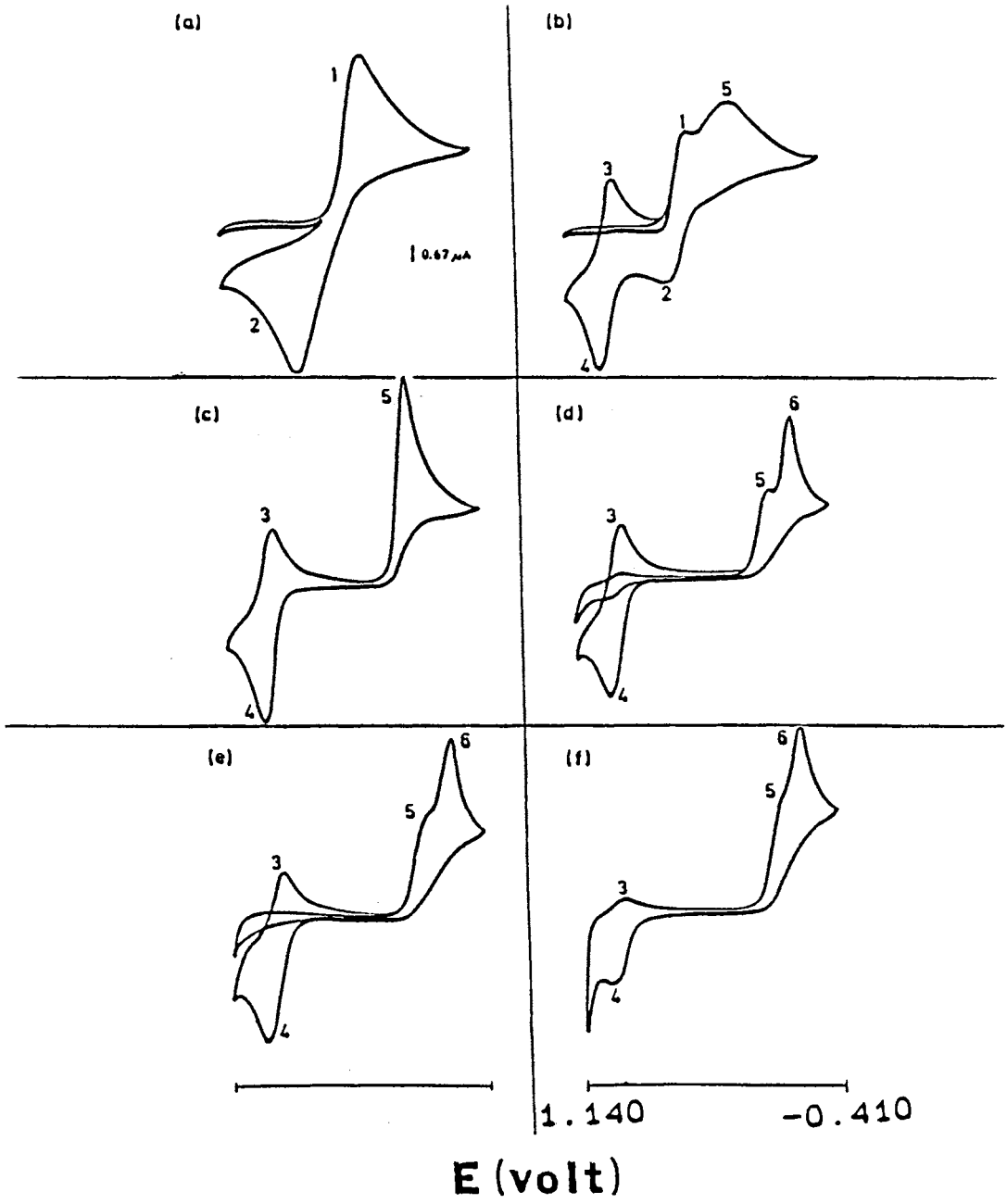

Figure 9. Cyclic voltammogram of iron-1,10-phenanthroline in excess of the stoichiometric ratio; iron(III): 5.01×10^{-4} M as nitrate; 1,10-phenanthroline: 1.00×10^{-2} M in 1.00 M KCl at different pH's; (a) pH 0.00; (b) pH 1.00; (c) pH 2.00; (d) pH 3.00; (e) pH 4.00; (f) pH 5.00. Scan rate 125 $mV.s^{-1}$. For interpretation of voltammograms see text.

complexes that gave 1 and 2 in 9a. The change in pH brings about less electrochemical irreversibility in these electrode processes (ΔE_p = 103 mV). Peaks 3 and 4 correspond to the reversible oxidation-reduction process of the mononuclear species known as ferroin and ferriin. Peak 5 seems to correspond to a new binuclear species in which the number of 1,10-phenanthroline ligands is higher than in the species responsible for peaks 1 and 2. This binuclear complex shows a corresponding oxidized form in the voltage range scanned here; no corresponding oxidation peak appears in the voltammogram. Initiating the scan at a potential of +0.352 V vs SCE and in the direction of increasing positive potential does not produce peaks 2, 3, and 4 which appear during the second cycle of voltage sweep.

A substantially simplified voltammogram is observed at pH 2.0 (voltammogram 9c). Peaks 3 and 4, as before, correspond to the reversible ferroin/ferriin couple and peak 5 to the binuclear complex considered to be stable at this pH and represented as $[Fe_2(phen)_4(OH)_2]^{+4}$.

Voltammograms 9d, 9e, and 9f show two trends. A new peak, peak 6, of increasing current as the pH increases from 3.0 to 5.0 appears. Correspondingly the height of peak 5 decreases as the pH increases. This is interpreted to signify the formation of a new mixed-ligand complex with replacement of the 1,10-phenanthroline in the coordination sphere of the binuclear iron core (see Fig. 11). This complex is chemically at equilibrium with

$[Fe_2(phen)_4(OH)_2]^{+4}$. The second trend is observed in the decrease of height of peak 3. The system seems to evolve to an irreversible redox pair constituted by the binuclear complex with higher OH^- content and the ferroin mononuclear species (peaks 6 and 4). As before, peaks 3 and 4 do not appear in the first positive-going scan.

Voltammograms obtained with solutions prepared by electrolysis of ferroin with excess 1,10-phenanthroline are shown in Fig. 10. Voltammograms 10a and 10f correspond to the same pH values as 9a to 9f; the numbering of peaks also corresponds to the peak assignments in Fig. 9. Electrolysis at very high hydrogen ion concentration (pH's 0.0 and 1.0) generates the mononuclear species ferriin. This is evidenced by the blue color observed at pH zero and the purple tint at pH 1. On the other hand the solutions of pH 2 to 5 are yellow as a result of the formation of binuclear complexes. At very low pH, electrochemical conversion is not as easy as at pH's 2 or above. The conversion to the yellow color at pH = 0.0, for instance, requires days of electrolysis while at pH value of 2.0 the yellow binuclear species is obtained after just 30 min of electrolysis.

A change in the chemical composition of the supporting electrolyte only slightly modifies the trends observed in Figs. 9 and 10. Table 3 gives a summary of observations collected by replacing chloride by nitrate and sulfate in the supporting electrolyte. At very low pH. electrochemical

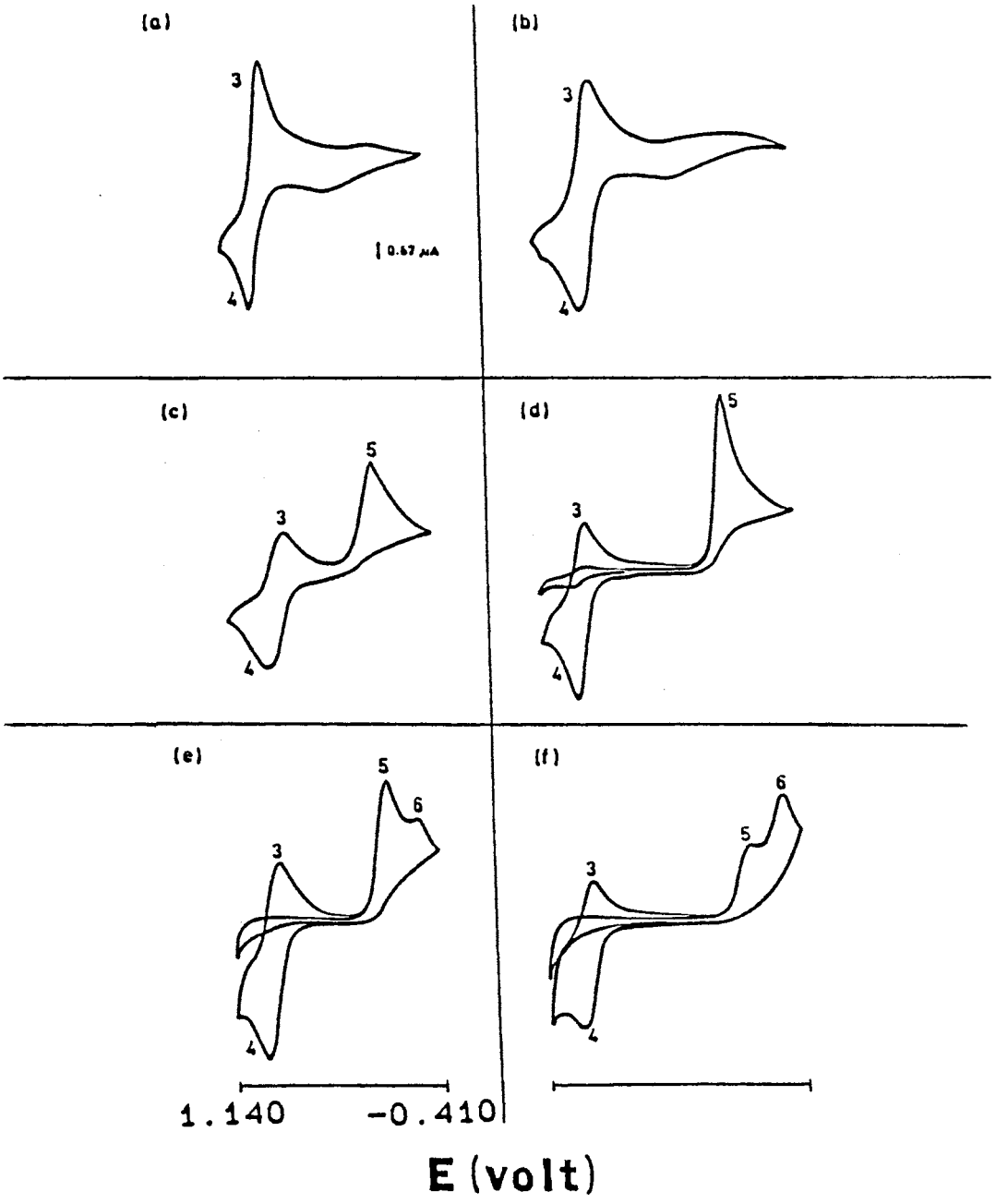

Figure 10. Cyclic voltammograms of iron-1,10-phenanthroline species. Original solutions prepared by electrolysis of ferroin in excess of 1,10-phenanthroline at different pH's. Ferroin was 5.03 x 10^{-4} M and 1,10-phenanthroline was 8.50 x 10^{-4} M in 1.00 M KCl. (a) pH 0.00; (b) pH 1.00; (c) pH 2.00; (d) pH 3.00; (e) pH 4.00; (f) pH 5.00. Scan rate 125 $mV.s^{-1}$.

TABLE III

ELECTROCHEMICAL BEHAVIOR OF THE IRON(III)/1,10-PHENANTHROLINE COMPLEXES IN NITRATE AND SULFATE MEDIA

pH	NITRATE MEDIUM		SULFATE MEDIUM	
	Direct Mixing	Electrolysis	Direct Mixing	Electrolysis
0	Irreversible anodic and cathodic peaks at -0.028 and 0.966 V, respectively	Voltammogram like that obtained in chloride medium	Irreversible anidic and cathodic peaks at 0.010 V and 0.950 V, respectively	Typical voltammograms of ferroin solutions. Reversible peaks of ferroin/ferriin couple. A cathodic peak at -0.048 V
1.00	Peaks 1, 2, 3, 4 and 5 (Fig. 9b). Peaks 1 and 2 not so well defind	Same as at pH 0	Same as in Fig. 9b. Peak 3 relatively small	Same as for direct mixing but peak 3 well defined
2.00	Voltammograms identical to that in Fig. 9c	Well defind peaks 3 and 4 (Fig. 9c) Peak 5 slightly developed	Peaks 1, 3, 4, and 5 (Fig. 9b)	Peaks 1, 3, and 4 (Fig. 9b). Peak 5 strongly suppresed
3.00	Same as in 9c	Same as in 9c	Same as in 9c. Cathodic peak close to peak 5 in potential but considerably broader	Same as for direct mixing
4.00	Same as in 9c	Similar to that in 9e	Same as above	Same as above
5.00	Same as in 9c	Similar to that in 9e	Same as above	Same as above

reversibility of the waves follows the trend chloride, sulfate, nitrate. The formation of the commonly assigned binuclear form of ferriin, $[Fe_2(phen)_4(OH_2]^{4+}$, and its electrochemical behavior at a carbon paste electrode, are given in voltammogram 9c at the corresponding experimental conditions. The features of this voltammogram appear in nitrate solutions even at high pH but not in sulfate solutions.

Voltammograms obtained at different times after preparation of the iron(III) complex(es) did not show any change in the number of peaks or the potentials at which they appear in Fig. 10.

A series of experiments were performed in which the molar ratio of metal to ligand was varied in the sequence 2:1, 1:1, 1:2, 1:3, 1:4, 1:5, 1:6, and 1:7. The solutions were prepared by direct reaction of iron(III) with 1,10-phenanthroline in 1.0 M KCl. For comparative purposes two pH values were chosen: pH 2.0 and pH 4.0. The final analytical concentration of iron in these solutions was 5.03 x 10^{-4} M at pH 4.0 and 2.01 x 10-4 M at pH 2.0. Table 4 gives a summary of the observations. These were qualitatively reproduced with solutions prepared by electrochemical generation of the binuclear species at ratios of metal to ligand 1:2 or smaller. Of interest to note is the absence of peak 3 at relatively high ratios of metal to ligand and the appearance of peak 6 at pH 4.0 and high ligand-to-metal ratios. Evidently the high ligand

TABLE IV

CHARACTERISTICS OF CYCLIC VOLTAMMOGRAMS FOR SOLUTIONS CONTAINING DIFFERENT METAL/LIGAND MOLAR RATIOS

$C_{Fe}/C_{1,10\text{-phen}}$	pH = 2.00	pH = 4.00
2:1	Peaks 1, 2, 4, and 5. Peak 3 noticeably absent. Peaks 1 and 2 comparatively small.	Same as at pH 2.00.
1:1	Same as at ratio 2:1.	Peak 3 starts to appear; otherwise same as at ratio 2:1.
1:2	Same as at ratio 2:1.	Peaks 1, 2, 3, 4, and 5. Peak 3 very well developed. Peaks 1 and 2 decreased in size, particularly peak 1.
1:3	Same as at ratio 2:1. Peaks 1 an 2 well developed. Peak 3 starts to appear.	Peaks 3, 4, and 5 only.
1:4	Same as at ratio 1:3.	Peaks 3, 4, 5, and 6 which appears as a slight shoulder.
1:5	Same as at ratio 1:3.	Same as at ratio 1:4.
1:6	Same as at ratio 1:3.	Same as at ratio 1:4.
1:7	Same as at ratio 1:3.	

C stands for total (analytical) concentration

Concentration of iron: pH 2.00, 2.01×10^{-4} M: pH 4.00, 5.03×10^{-4} M. All solutions 1.00 M in KCl. Temperature 25 °C.

concentration stabilizes the ferroin/ferriin couple responsible for peaks 3 and 4. At pH 2.0, the relatively higher Cl^- (than OH^-) concentration favors the presence of peaks 1 and 2, which appear in all voltammograms at this pH and were observed at even lower pH in the voltammograms of Fig. 9 (9a and 9b). It was also observed that with time the relative peak heights of peaks 5 and 6 (particularly noticeable with peak 6) decrease and increase, respectively, in the solutions of pH 4.0 and 1:5 and 1:6 metal/ligand ratio.

All the results described in the foregoing considerations indicate the presence of at least six species in the several solutions. Some predominate at low pH, some at high, and some when the Cl^- is relatively high or when the ligand/metal ratio is relatively high; the scheme in Fig. 11 summarizes these observations.

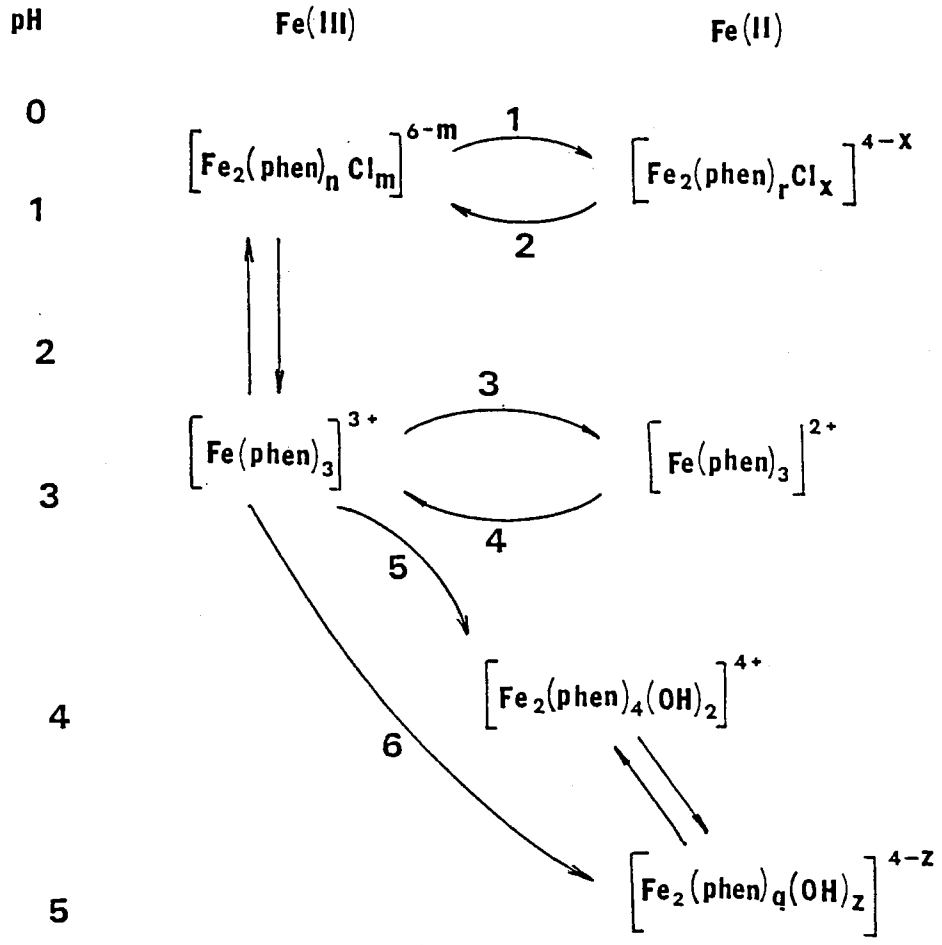

Figure 11. Schematic representation of chemical species postulated to be involved in the electrochemical behavior of iron and/or 1,10-phenanthroline complexes in aqueous chloride solutions. Numbering on arrows identifies peaks as numbered in Figs. 9 and 10.

CHAPTER III

IMPROVED RESPONSE OF CARBON-PASTE BY TREATMENT WITH SURFACTANT

Carbon paste electrodes are commonly considered to display very low residual currents (40). It is actually possible to change the paste composition to the point where there is no current passing at all. This resistance, which can be considered to be located at the carbon paste/solution interface, hinders the electron transfer process at the working electrode and limits performance of paste electrodes in flow systems. The small background current of paste electrodes is considered advantageous, however, for achieving low limits of detection in liquid chromatography with electrochemical detection (41). It should be noted, though, that working at fixed potential (e.g. in amperometry or coulometry) usually results in a defined background that can be suppressed electronically or by using a reference signal from a second working electrode sensing the background solution (42). This points to the possibility of achieving low limits of detection and improved sensitivity even with relatively high background signals (the typical case with metallic electrodes such as platinum or mercury). Inasmuch as paste electrodes are easy to prepare and their

surfaces also easy to renew, enhancement of their surface conductivity is of interest in flow systems allowing their use in place of metallic electrodes, which offer a more limited voltage region for study. Rice et al. (14) have studied the effect of different pasting liquids on the electrode background current and reactivity. They found that the residual current of dry graphite powder is very high, but decreases with increasing oil content in the paste. Dry graphite electrodes display impedances comparable to those of metal electrodes. Dry graphite electrodes are difficult to use, however, particularly under flow conditions.

The work reported here concerns further efforts to alter such microstructure in order to increase conductivity in electrochemical detection in continuous-flow systems. It involved six different paste compositions (three commercially available and three locally made) and the use of surfactant solutions for surface modification. Cyclic voltammetry, double-potential-step chronocoulometry, and Osteryoung square-wave voltammetry were used for electrochemical evaluation. Electrochemical probes used were hexacyanoferrate(II), tris[1,10-phenanthroline]iron(II), sulfite ion, and the reduced form of nicotinamide adenine dinucleotide (NADH).

Experimental

Apparatus

A conventional three electrode cell was used with a saturated calomel electrode, SCE, as reference and a platinum wire as counter (auxiliary) electrode. Monitoring of cell output was accomplished with a BAS-100 electrochemical analyzer (Bioanalytical Systems, West Lafayette, IN). The output of data was plotted with the aid of a Houston Instrument DMP-40 digital plotter (Houston Instruments, Austin, TX).

A block diagram of the flow injection system is shown in Figure 12. This system was used for the determination of sulfite and hexacyanoferrate(II) under flow conditions. The carrier solution was 1.00 M KCl. The flow of the carrier in the system was propelled by gravity and fixed at a rate of 3.00 mL/min. The analytes were introduced into the carrier by use of a four-way rotary valve (Rheodyne Inc., Cotati, California). Figure 13 shows the electrochemical cell used with the flow system. A saturated calomel electrode was used as a reference electrode and a platinum disk as a counter electrode. A graphite paste electrode was used as working electrode. The cell potential was controlled by a home made potentiostat and the cell output was recorded on a Hewlett-Packard model 7128A strip-chart recorder.

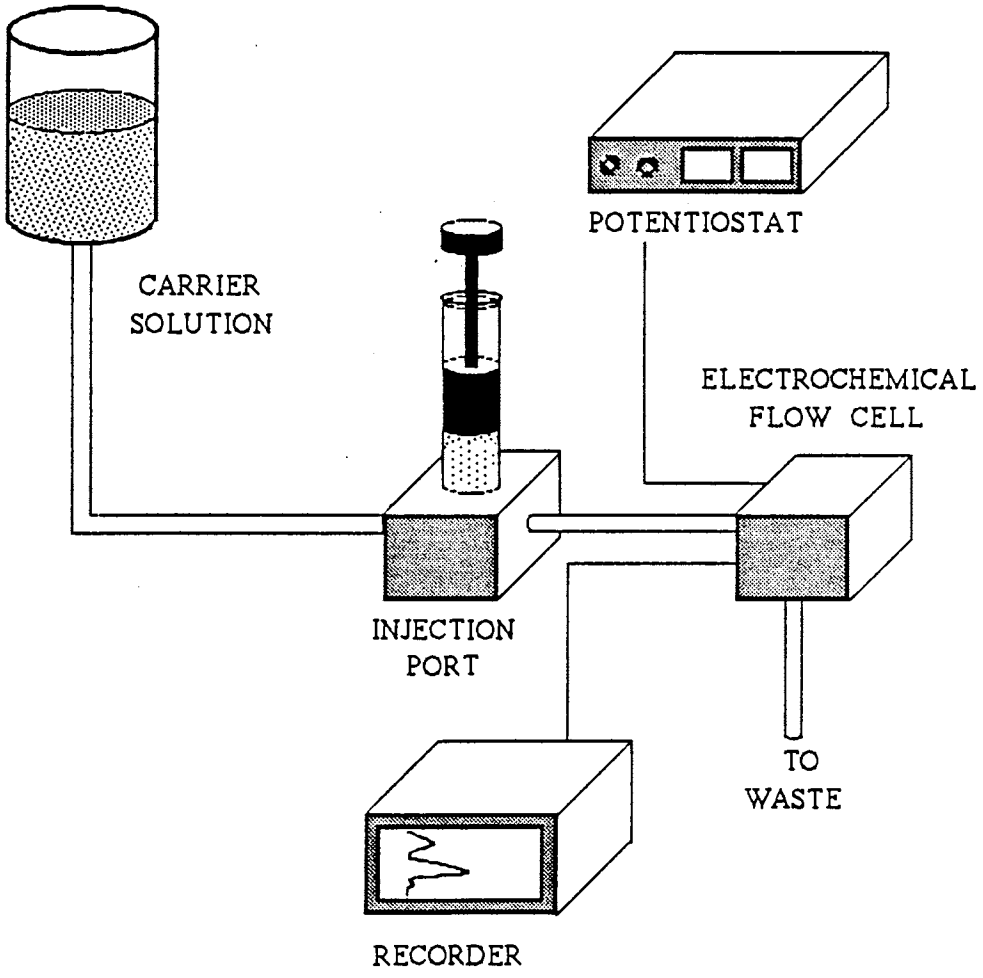

Figure 12. Block digram of the flow injection system setup.

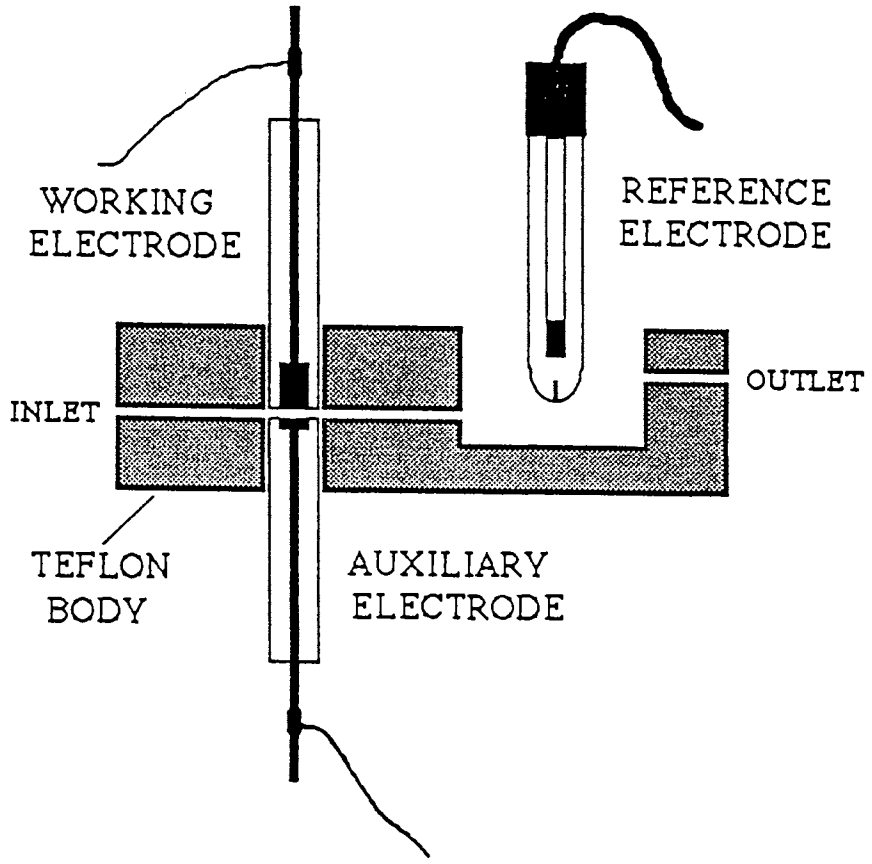

Figure 13. Cross-sectional view of the flow cell used with the flow injection system shown on Figure 12.

Reagents and Solutions

All reagents used were of AR grade. 1,10-Phenanthroline and tris[1,10-phenanthroline]iron(II) sulfate (ferroin solution, 0.025 M) were obtained from G. F. Smith Chemicals (Columbus, OH). ∝-Nicotinamide Adenine Dinucleotide (reduced form) was from Sigma Chemical Co. (St. Louis, MO). Surfactants used were Brij-35 [n-$C_{12}H_{25}(OCH_2CH_2)_{23}OH$] from Aldrich; Triton X-100 [$RC_6H_4(OCH_2CH_2)_nOH$] from Rohm and Haas (Philadelphia, PA); and sodium dodecylbenzenesulfonate from K & K Laboratories (Plainview, NY).

All solutions used were freshly prepared in deionized-distilled (all-glass still with quartz heater) water. Solutions of the surfactants were 0.10% w/v in water. Portions of about 40 mL were used for electrode treatment.

All measurements were carried out at 25 ± 0.5 °C after the solutions were deoxygenated by bubbling nitrogen gas through them for at least 15 min and allowing the nitrogen to cover the test solution during measurement.

Paste Materials

Three pastes were purchased from Bionalytical Systems, Inc. (West Lafayette, IN). These pastes were: CP-O (graphite with paraffin oil as binder), CP-S (graphite with silicone grease as binder, and CP-W (graphite with ceresin wax as binder). Neither the ratio of graphite/binder nor the type of graphite used was identified by the

manufacturers. Three other paste preparations were locally made by mixing graphite powder UCP-1-M from Ultra Carbon (Bay City, MI) with the required amount of pasting ingredient. The CP-O1 paste was prepared by mixing 5.0 g of graphite with 3.0 g of light mineral oil (laboratory grade, from Sargent-Welch Scientific Co., Skokie, IL); the CP-Sl paste was prepared by mixing 2.0 g of graphite with 2.0 g of high-vacuum grease (Dow Corning Corp., Midland, MI); and the CP-H paste was prepared by mixing 2.0 g of graphite with 2.0 g of hexadecane (Aldrich Chemical Co., Milwaukee, WI). Mixing was carried out with the aid of a spatula covered with Teflon tubing.

The work reported here required a large number of surface renewals. To simplify this procedure, the electrode used (Figure 14) was constructed so as to facilitate surface renewal. In its design the paste was in direct contact with a disk made of brass which was attached to a copper wire of about 3 mm o.d. providing electrical contact to the measuring circuit. The body of the electrode was machined out of Teflon and provided a screw system to slide the brass disk in and out which thus pushed the paste out of the electrode body for surface renewal.

Results and Discussion

In order to evaluate the effect of pasting liquid or wax used in preparing carbon-paste electrodes on the conductivity (resistance), measurements were performed with

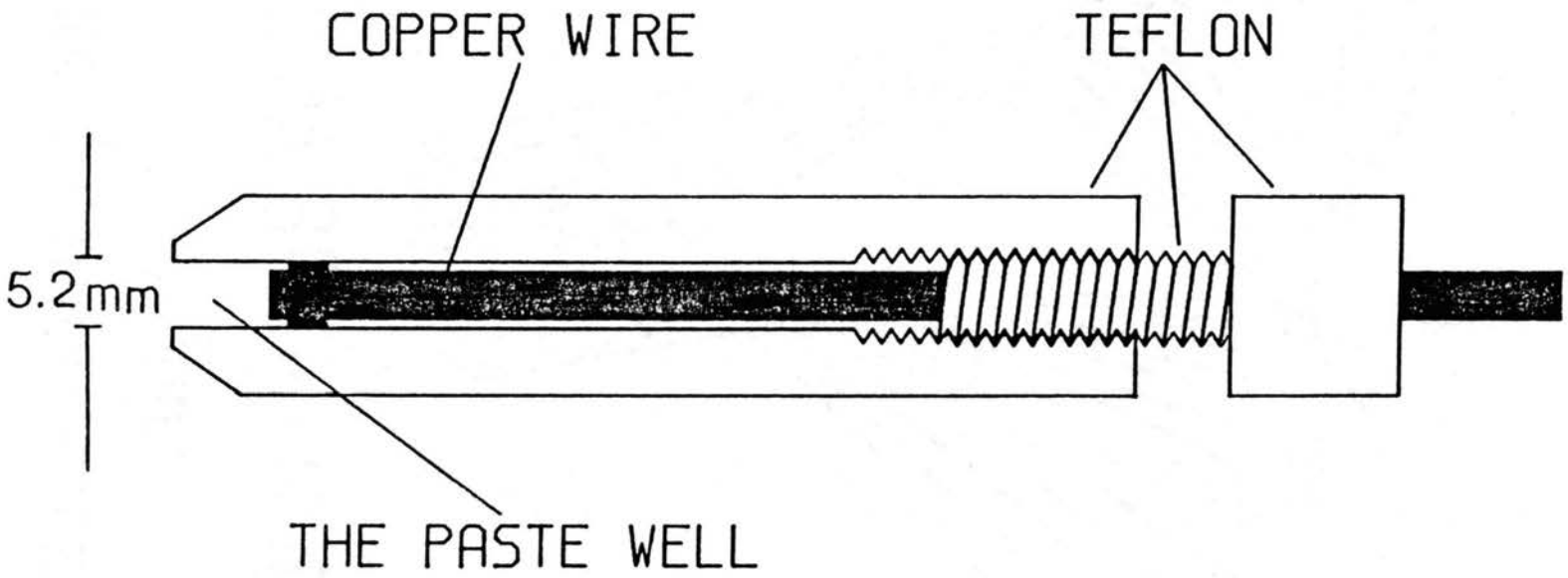

Figure 14. A cross-sectional view of the paste electrode holder.

a highly conducting supporting electrolyte (1.00 M KCl). Such measurements were directly made by the BAS-100 system by applying pulses of 50 mV in amplitude and in the vicinity of one of the test potentials (44). The test potential is selected in a region where electrolysis is not significant. Theoretically as a result of the potential pulse applied, the output current is given by

$$i = (\Delta E_{appl}/R_u)\ \exp\ (-t/R_u C_{dl}) \qquad (8)$$

where i is the cell current
ΔE_{appl} is the applied pulse amplitude(50 mV)
R_u is the cell uncompensated resistance
C_{dl} is the double-layer capacitance

At $t = 0$, $i = i_o$ and $R_u = (E_{appl}/i_o)$. The BAS-100 calculates i_o by selecting the current output at two different time intervals and extrapolating to $t = 0$ on the current vs. time plot. Then R_u is calculated and displayed as the cell resistance. Table 5 lists the measured cell resistances of the six paste types studied. Values marked as "too high" were reported by the instrument for conditions which are beyond its capabilities and may represent values anywhere between a few kiloohms and infinity.

If there is formation of an insulating layer, during the smoothing process of carbon-paste electrodes, with localization at the electrode/solution interface, the iR drop of the cell is mainly due to the uncompensated resistance at such interface. The rationalization for this is based on: a) the resistance through the paste body was found to be 25 to 50 ohms, in agreement with previous observations (45), and b) replacing the paste electrode by a

TABLE V

CELL RESISTANCE USING UNTREATED AND SURFACTANT-TREATED CARBON-PASTE SURFACES

Paste Type	Cell Resistance, ohms[a]	
	Untreated Surfaces	Treated Surfaces[b]
CP-O	272 ± 2	12 ± 1
CP-S	TOO HIGH	15 ± 3
CP-W	TOO HIGH	25 ± 1
CP-O1	3650 ± 18	15 ± 1
CP-S1	TOO HIGH	15 ± 1
CP-H	3155 ± 70	43 ± 4

[a] Results are average of four independent measurements

[b] Surfaces treated for 10 min with a 0.10% w/v aqueous solution of Brij-35.

platinum electrode in the same configuration a resistance value for the solution of only 10 ohms. These observations invite ruling out both the paste body and the cell solution as sources of the high resistance observed in carbon-paste electrodes. Hence, removing (or decreasing) the surface oily layer should enhance cell conductivity to levels close to those of metallic electrodes. Washing the electrode surfaces with acetone or ethanol, for instance, decreased cell resistance as much as two orders of magnitude (except for CP-S and CP-Sl preparations) with a parallel increase in currents for electrochemical processes at the electrode surface. A decrease in resistance was also observed by incorporating KCl or KBr on the surface of the electrode during the smoothing process. Both of these procedures, however, lacked reproducibility at surfaces of the same preparation (the background current was not the same in repeated trials). Exposing the surface to wetting agents (surfactants), on the other hand, decreased the value of the resistance in the same extent but with good reproducibility and lasting effect. Of the three surfactants used, two were of nonionic nature (Triton X-100 and Brij-35) and one anionic (sodium dodecylbenzenesulfonate). The decrease in resistance was found to be independent of the surfactant employed; the three lowered it to about the same levels. This surfactant treatment is very simple; it involves merely immersing the smoothed surface in a stirred solution of 0.10% w/v of the surfactant in water for about 10 min. The

electrode is then removed and thoroughly rinsed with distilled water before use. No difference was observed when this treatment was prolonged for 20 to 30 min. Most of the results reported here, however, were obtained using Brij-35. The reproducibility of voltammograms obtained with untreated and treated surfaces was comparable, but currents with treated surfaces were considerably larger. The effect of lowering the resistance is quite lasting; even 12 h after treatment the low values were reproduced, as well as voltammograms and current values.

Figure 15 shows current-potential curves for CP-H electrodes in cells containing 1.00 M KCl as supporting electrolyte. It can be seen that these curves are essentially the same except for the current amplitudes, and point to an increase in surface wettability as a result of surfactant treatment. This wettability should in principle increase the microscopic surface area and make the conducting surface more accessible to electroactive species. Figure 16 shows cyclic voltammogram of 10 mM solution of hexacyanoferrate(II) in 1.00 M KCl. When untreated CP-W is used, peaks due to the redox process are hardly seen but the voltammograms for the same surface after surfatant treatment are well defined and comparable to those obtained with metallic electrodes. For quanitative comparision square wave voltammetry is preffered over cyclic voltammetry. The method involves measuring the sum of the absolute currents from the oxidation process and the

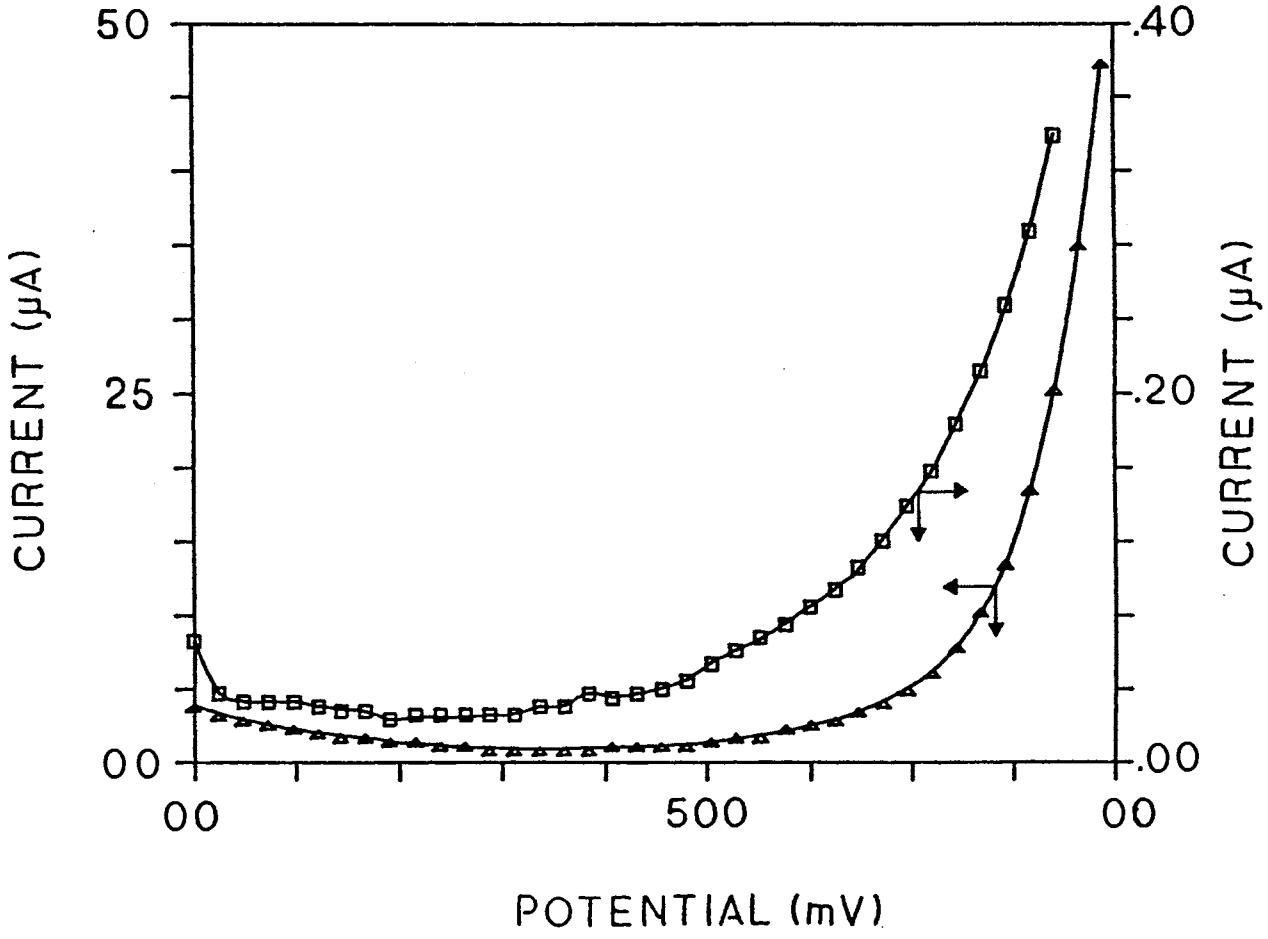

Figure 15. Background current observed with CP-H paste electrodes; (□) regular paste surface, (▲) after treatment with surfactant.

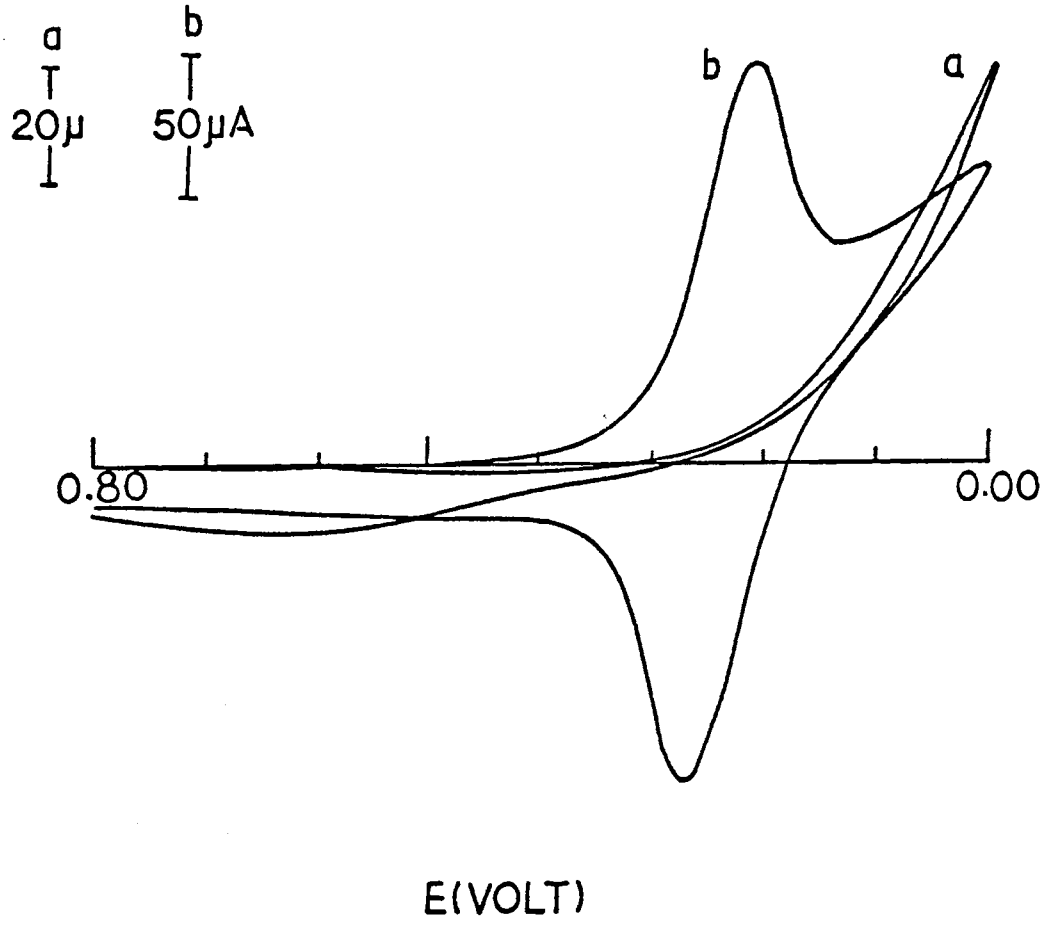

Figure 16. Cyclic voltammogram of a 0.010 M solution of hexacyanoferrate(III) obtained with CP-W paste; (a) untreated surfaces, (b) surfactant-treated surfaces. Scan rate 25 $mV.s^{-1}$.

reduction process. This can be achieved by continuously switching the potential of the electrode between two selected limits. Figure 17 shows typical results obtained with Osteryoung square wave voltammetry.

Carbon paste electrodes prepared with CP-01 pastes exhibited voltammograms showing the redox peaks even with untreated surfaces; peak currents, however, were substantially larger with treated ones. Peak separation, ΔE_p, with untreated surfaces was about 500 mV; after treatment the separation was 44 mV and similar to that observed with treated CP-W surfaces. This points to an increase in the rate of electron exchange in treated surfaces.

Peaks obtained with treated surfaces are symmetrical around the current axis with peak separation less than 59 mV (theoretical value). This behavior is expected because the redox couple is reported to show adsorption on the graphite used in this work. The effect of adsorption using tris[1,10-phenanthroline]iron(II) and hexacyanoferrate(III) as electrochemical probes can be seen in the data of Table 6. This Table also clearly shows the significant increase in peak currents (except for paste CP-S and tris[1,10-phenanthroline]iron(II) as probe). A noticable decrease in peak separation is also observed. Peak separation for tris[1,10-phenanthroline]iron(II) is less than what it should be expected for one-electron exchange process and is indicative of adsorption. Peak separation in the case of

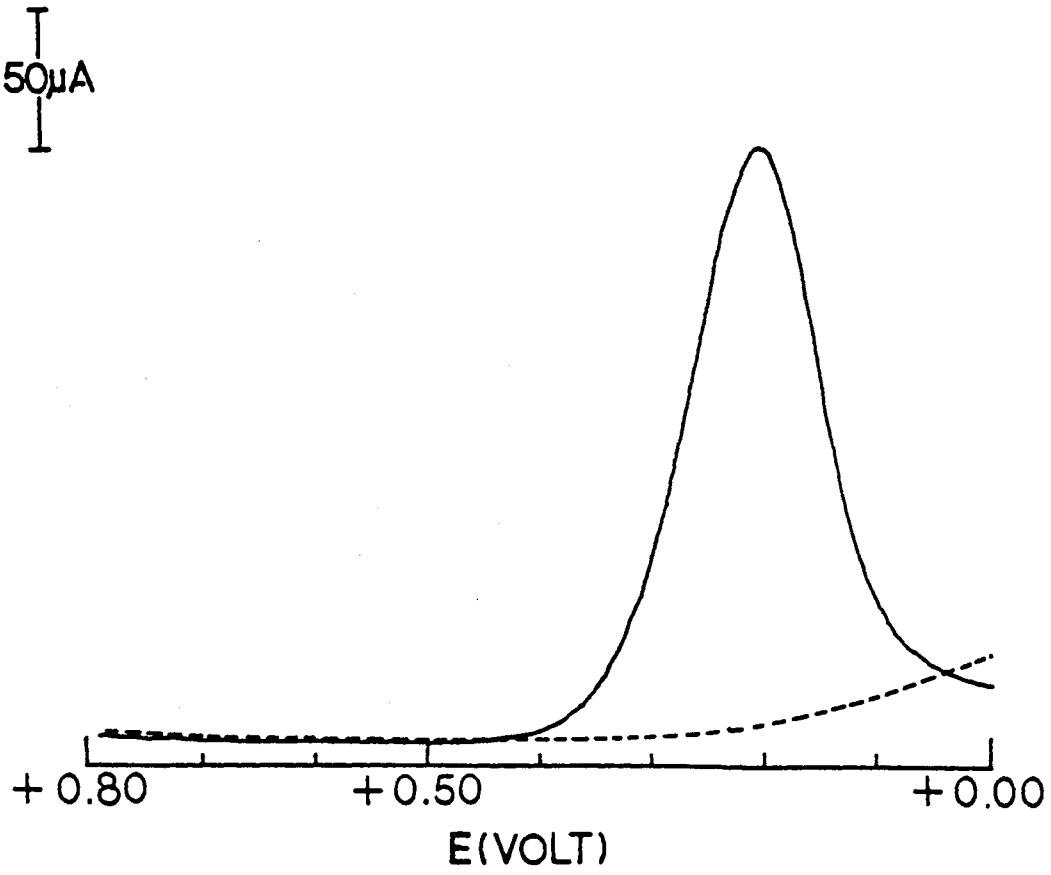

Figure 17. Square-wave voltammogram for solution of 10 mM $K_4Fe(CN)_6$ in 1.00 M KCl. Dashed line observed with regular paste CP-W electrode. Solid line observed with surfactant-treated CP-W electrode. Square-wave amplitude: 25 mV; pulse frequency: 15 Hz; potential step: 4 mV.

TABLE VI

CURRENT AND VOLTAGE DATA ILLUSTRATING THE CYCLIC VOLTAMMOGRAMIC BEHAVIOR OF DIFFERENT TREATED AND UNTREATED SURFACES WITH HEXACYANOFERRATE(III) TRIS(1,10-PHENANTHROLINE)IRON(II) AS ELECTROCHEMICAL PROPES.

Paste Type	Anodic Current ($A \times 10^5$)	Anodic Peak Potential (mV)	Cathodic Current ($A \times 10^5$)	Cathodic peak potential (mV)	ΔE_p (mV)
		UNTREATED SURFACES			
CP-O	2.313	849	1.565	749	65
CP-S	1.128	848	0.845	790	58
CP-W	1.143	854	0.837	788	66
CP-O1	2.015	849	1.602	792	57
CP-S1	3.025	846	1.384	803	43
CP-H	1.236	849	0.888	791	58
		SURFACTANT-TREATED SURFACES			
CP-O	4.084	840	1.942	813	27
CP-S	1.143	847	0.853	790	57
CP-W	2.969	842	1.236	812	30
CP-O1	10.31	844	2.165	832	12
CP-S1	7.466	836	3.047	821	15
CP-H	4.310	836			

Test solution: 2.5×10^{-4} M tris(1,10-phenanthroline)iron(II) in 1.00 M KCl. Potential scanned from 0.500 to 1.00 V. Scan rate was 100 mV/s.

TABLE VI (Continued)

Paste Type	Anodic Current (A x 10^4)	Anodic Peak Potential (mV)	Cathodic Current (A x 10^4)	Cathodic Peak Potential, MV	ΔE_p, mV
		UNTREATED SURFACES			
CP-O	1.745	353	3.101	108	249
CP-S		PEAKS ARE NOT WELL DEFINED			
CP-W		PEAKS ARE NOT WELL DEFINED			
CP-O1	1.658	356	3.137	106	250
CP-S1	1.901	375	2.340	86	290
CP-H		PEAKS ARE NOT WELL DEFINED			
		SURFACTANT-TREATED SURFACES			
CP-O	13.99	293	16.46	150	113
CP-S	0.342	528			
CP-W	6.618	289	8.440	170	119
CP-O1	10.53	287	12.18	168	109
CP-S1	3.493	282	4.820	181	101
CP-H	2.116	372	6.805	102	270

Test solution: 0.0010 M hexacynoferrate(III) in 1.00 M KCl. Potential scanned from 0.800 to -0.200 V. Scan rate was 100 mV/s.

hexacynoferrate(II) and -(III) also decreases with treatment but values are still larger than the expected value of 59 mV, probably as a result of high scan rates. Adsorption is also observed with this probe and peak separations are comparable to those reported with similar electrode materials (14). Confirmation of adsorption was obtained by removing the electrodes from the test solution, rinsing with distilled water, and testing them again in a cell containing supporting electrolyte only. The presence of the adsorbed species was evident from peaks with currents of about 20% those observed with the test solutions; these decreased with time. Under flow conditions, the same electrochemical probes show linear calibration curves (peak current vs. concentration of injected probe) for both treated and untreated surfaces with correlation coefficients of 0.9996 and 0.9995, respectively. The slope for the treated surface was 1.44 times as large in the case of tris(1,10-phenanthroline)iron(II) and 1.81 times as large for hexacyanoferrate(III). Evidently the continuous-flow operation and the temporary nature of the adsorption result in a combined effect beneficial for the use of treated surfaces in continuous-flow detection. Hydrogen sulfite ions, HSO_3^-, injected under conditions assuring a pH of 3.01 and a total electrolyte concentration 1.00 M in KCl (sensing potential 0.750 V vs. SCE) showed calibration curves with slopes for treated surfaces twice the value obtained under same conditions with untreated surfaces.

Voltammetric measurements with NADH, a chemical species for which adsorption behavior was not observed, showed peak currents 2.3 times as large for treated surfaces as for untreated ones at pH 6.80. The peak potential for untreated surfaces appeared at 0.676 V vs. SCE and the one for treated surfaces at 0.648 V (Fig. 18).

Figure 19 shows a comparison of treated CP-W surfaces with a platinum surface of comparable geometric area and experimental conditions. Peak heights and cathodic and anodic peak potentials are comparable for these surfaces.

Electrochemical Area Measurements

We have assumed earlier that the surfactant removes some of the pasting liquid from the elctrode surfaces and leaves more graphite sites available for the electrochemical reaction. If this assumption is valid, the electrochemical area of the treated surfaces should increase accordingly compared to the untreated surfaces.

Chronocoulometry was employed for area measurements. The technique involves applying a potential pulse to the electrochemical cell and integrating the ouput current over the time period of the pulse (the total charge transferred). The relation between the total charge and the pulse width (time) derived from the Cottrell equation is:

$$Q_d = 2nFAD^{1/2}Ct^{1/2} / \pi^{1/2} \qquad (9)$$

where Q_d = charge transferred
n = equiv/mole
F = the Faraday constant

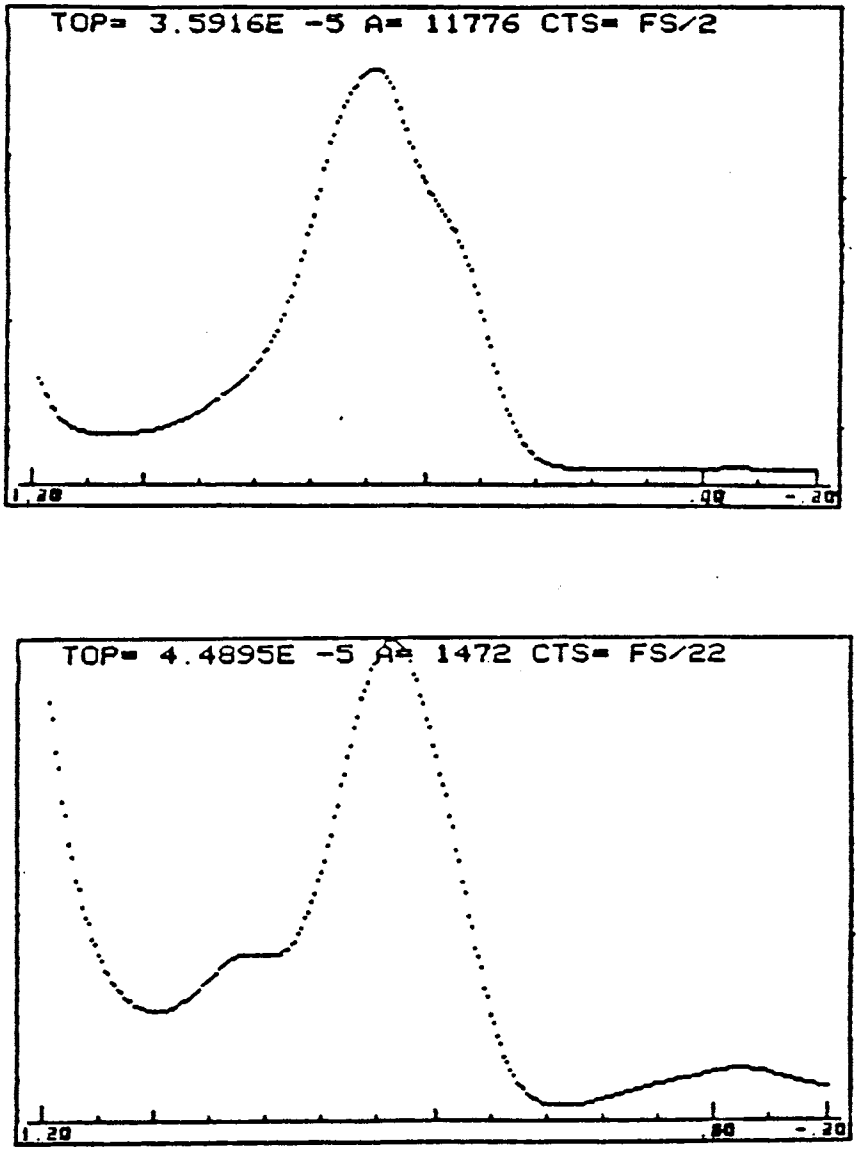

Figure 18. Electrochemical oxidation of NADH on plain paste electrode (top) and on surfactant-treated electrode surfaces (bottom).

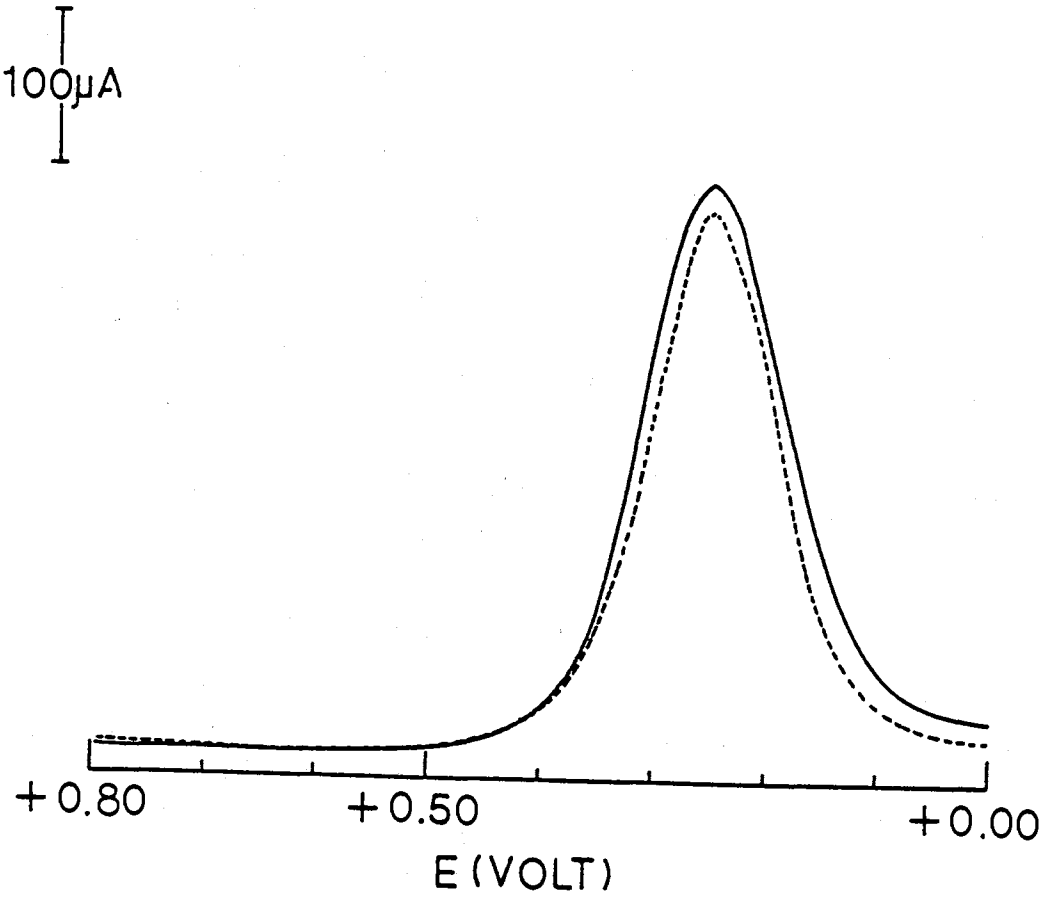

Figure 19. Square-wave voltammogram of 0.01 M solution of hexacyanoferrate(III) obtained with (———) a surfactant-treated CP-W carbon paste electrode and (-----) a platinum electrode of comparable geometric area; initial potential: 0.0 vs SCE; square-wave amplitude: 25 mV; pulse frequency: 15 Hz; potential step: 4 mV.

A = electrode area, cm^2
D = diffusion coefficient, cm/sec
C = bulk concentration, mole/cm
t = time, s

Plotting Q_d vs $t^{1/2}$ should give a straight line. The slope of the line is $2nFAD^{1/2}C/\pi^{1/2}$. From the bulk concentration and the analyte diffusion coefficient, the area can be readily calculated.

Factors such as pulse width, initial potential, and final potential of the pulse can affect significantly the accuracy of area measurements. These factors were evaluated using a 4 mM solution of $K_4Fe(CN)_6$ in 1.00 M KCl in a conventional three-electrode cell with platinum as indicator electrode.

Selecting the Initial Potential. the final potential of the applied pulse was selected at 0.240 V vs SCE, which is the potential at which hexacyanoferrate(II) is oxidized to hexacyanoferrate(III). The potential region between -0.200 V and +0.200 V vs SCE was screened to find the optimum initial pulse potential. The finding of this experiment is shown in Figure 20. The slope is constant for the region between -0.200 to +0.125 V and drops sharply thereafter. As will be discussed later pulse width of 250 ms was selected for these measurements.

Selecting the Final Potential. with an initial potential of 0.00 V, the final potential was measured between 0.125 V and 0.500 V. Figure 21 indicates that a final potential of 0.350 V or higher is sufficient to cause

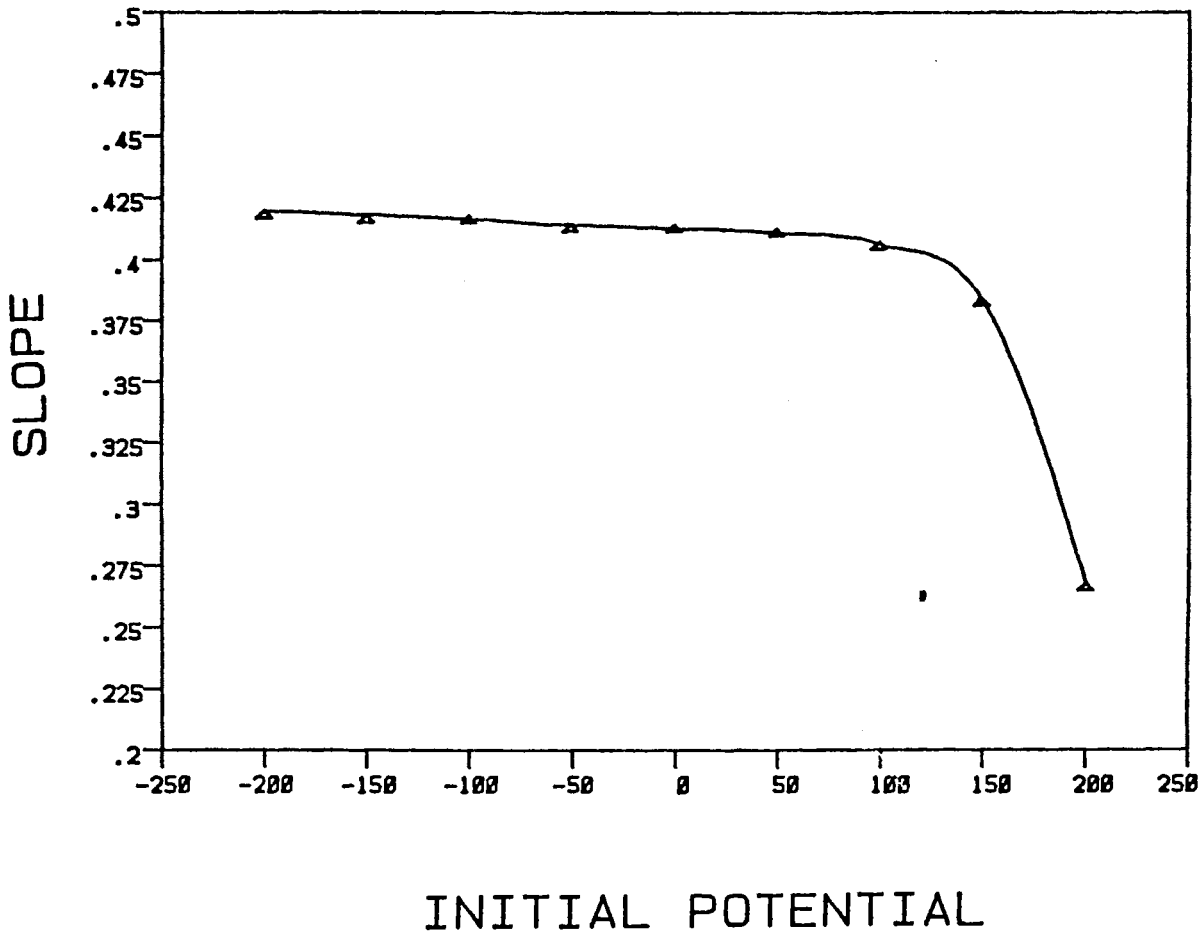

Figure 20. Effect of the initial potential applied in chronocoulometry experiment on the slope obtained from Anson plot (plot of charge vis $t^{1/2}$).

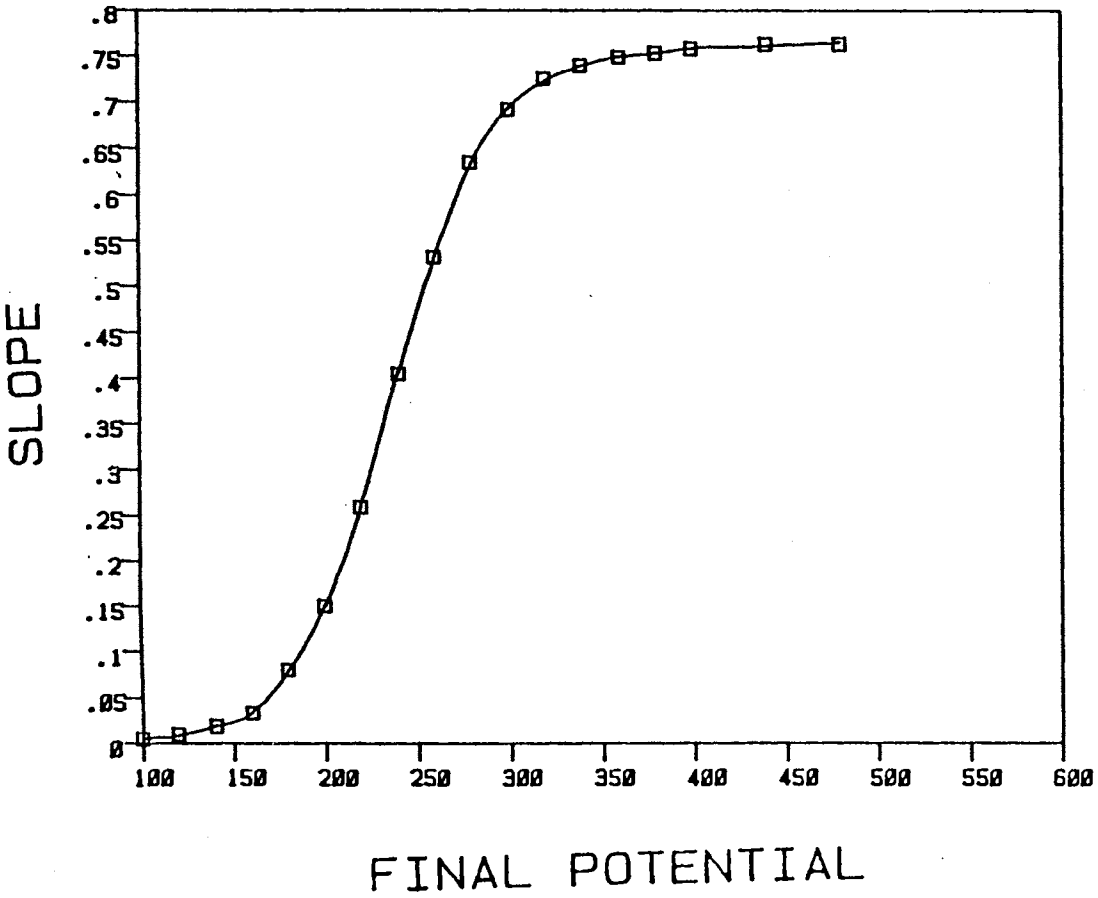

Figure 21. Effect of the final potential applied in chronocoloumetry experiment on the slope obtained from Anson plot.

complete oxidation of the hexacyanoferrate(II).

Effect of the Pulse Width. pulse widths between 10 ms and 1000 ms were examined with an initial potential of 0.00 V and a final potential of 0.480 V. Figure 22 shows that the slope is not sensative to pulse width larger than 100 ms. The data points on the figure represent the average of 10 measurements. The reproducibility of the measurements is significantly enhanced by pretreating the electrode before each measurement. The pretreatment steps are given in Table 7.

Electrochemical areas of CP-O1 surfaces before and after treatment were measured from the slope of plots of charge vs. $t^{1/2}$ from data obtained by double-potential-step chronocoulometry and 4.00 mM hexacyanoferrate(II) as test solution in 1.00 M KCl. For untreated surfaces the initial potential was 0.00 V vs. SCE (negative enough to insure negligible oxidation) and the final potential 0.740 V, sufficient to insure oxidation of the analyte. For treated surfaces the initial potential was also 0.00 V vs. SCE and the final potential 0.270 V. Oxidation peaks, determined by Osteryoung square wave voltammetry, were observed at 0.540 V and 0.264 V for untreated and treated surfaces, respectively. In the case of treated surfaces, the output currents at potentials larger than 0.270 V are too large for the capabilities of the BAS-100 system but not enough to reach the diffusion limiting current. Data for higher potentials were estimated by an indirect procedure. Using a

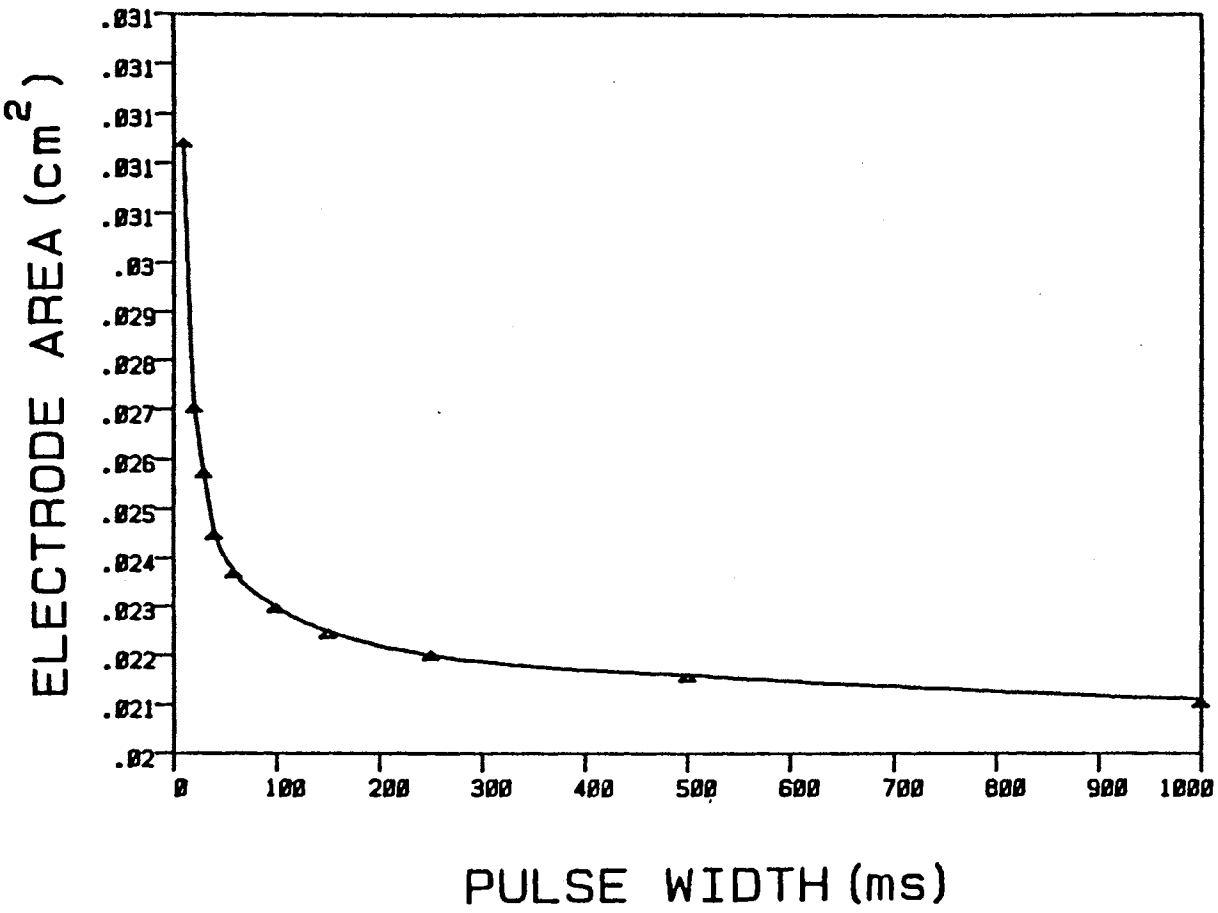

Figure 22. Effect of the width of the potential pulse applied in chronocoloumetry on the slope obtained from Anson plot.

TABLE VII

PLATINUM ELECTRODE PRETREATMENT STEPS

Step	Procedure
1.	Cleaning the electrode with distilled water.
2.	Polishing the electrode surface with polishing fabric (from BAS company).
3.	Cleaning the electrode with distilled water.
4.	Use the electrode in a three-electrode cell and as a working electrode and switch its potential between two defind limits.
5.	The control commands, available on the BAS instrument, to carry out the pretreatment were as follows: Initial potential (mV) = 0.0 High potential (mV) = 1200 Low potential (mV) = -300 Initial potential polarity = Negative Pulse width (mSec.) = 1000 Number of cycles applied = 10

small platinum electrode (geometrical area about 0.020 cm^2) a sequence of potential pulses was applied by increasing the previous pulse by 20 mV and using the same initial potential in each case. The charge transferred during each pulse was used to construct Q vs. $t^{1/2}$ plots (Anson's plots). The slopes from these plots were then plotted vs. each pulse potential and an S-shaped curve with inflection point at 0.236V was obtained. This curve was symmetrical with respect to the line parallel to the x-axis and passing through the inflection point. This symmetry permits extrapolation of the plot after the inflection point from the data collected up to the inflection point, and the data obtained with the platinum probe confirmed this (Figure 23). This approach was also repeated with an untreated CP-O1 surface and the calculated data again agreed with the data experimentally obtained. Using the surfactant-treated CP-O1 surface, points up to a pulse potential of 0.270 V could be obtained experimentally. Such a potential is high enough to construct the plot up to the inflection point (0.264 V as determined by Osteryoung square wave voltammetry). The second half of the S-shaped plot was estimated as explained above. The slopes for the plateau region of the plot corresponding to pulse potentials of 0.408, 0.428, and 0.468 V were used to calculate an average electrochemical area using the Cottrell equation. To avoid interferences from adsorption, the potential pulse width was 250 ms. Extending the pulse duration up to 1 s did not significantly change

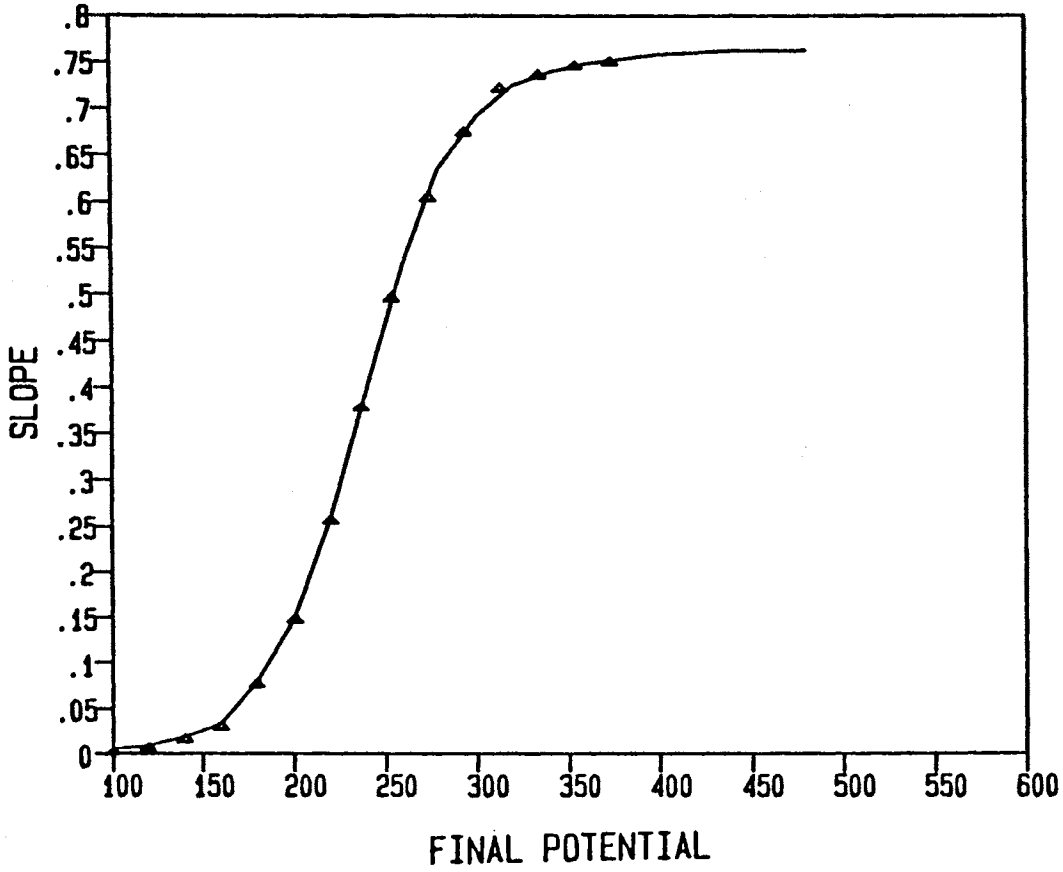

Figure 23. Comparison of slope-final potential plots from; (a) experimental data (solid line), and (b) data points estimated above the inflection point from experimental data below the inflection point (triangles).

the slope values, however. In calculating the slope of Anson's plots, the BAS-100 ignores the first 20% of collected data and the slope measurement is then carried out in a time window where the effect of adsorption on the determination of the electrochemical area is of no consequence (46). Correlation coefficients were between 0.9970 and 0.9999. By using the approach just outlined, an untreated CP-01 surface showed an electrochemical area of 0.10 ± 0.01 cm^2 (0.21 cm^2 geometrical area) compared with an electrochemical area of 0.43 ± 0.01 cm^2 after surfactant treatment. The removal of the film of pasting ingredient seems to increase the number of carbon centers available for electron exchange at the surface of the electrode. Increases in electrochemical area have been observed when polished electrodes based on Kel-F as inert ingredient were roughened and when the ratio of graphite to Kel-F was increased in the paste composition (47).

CHAPTER IV

A LITERATURE REVIEW OF CHEMICALLY MODIFIED ELECTRODES OF THE IMMOBILIZED AND ADMIXED TYPES

An overview of two methods used to modify electrode surfaces will be presented in this chapter. The first method is based on the modification by covalent attachment of the modifier to the electrode surfaces. The second method involves physical incorporation of the modifier (admixing) in the electrode body. The discussion will reflect the relative popularity of the two methods as they appeared in the literature. Covalent attachment is the more used and its practice is well advanced. Electrode modification by physical incorporation is less known and has serious limitations. This chapter discusses these modification types separately and in detail.

Chemically Modified Electrodes with Immobilized Modifier

The discussion will cover the type of electrodes used, the procedures followed to attach the modifier, and the type of modifiers used. To present a better view of the modification processes, a classification based on the ways the modifiers have been covalently attached to the surfaces, instead of using electrode types or kind of modifier as a

base for the classification, will be followed. This can be justified by the following; (a) modification has been conducted on many electrode surfaces and classification on this basis is tedious, (b) a large number of species have been used to modify electrode surfaces and a classification on this basis will make the subject confusing, (c) the attachment step is the most critical step in the modification process, and (d) each method of attachment is common to many electrode surfaces.

The chapter also will review studies performed on the surface layers of modified electrodes. Such studies are directed to determine the amount of modifier attached to the electrode surfaces, the electrochemical behavior of the modifier, and the physical and chemical properties of the modified surfaces. Techniques employed to accomplish such studies include electrochemical, spectroscopic, and conductometric methods. Areas where modified electrodes have potential applications as well as a conclusion extracted from this review will be presented.

Electrode Modification

One of the ultimate goals of immobilizing chemical species on electrode surfaces is that, in general, the electrode displays the chemical, electrochemical, and optical properties of the modifying species. This has extended the use of electrochemical methods to other areas of interest, not only to the analytical chemist, but to the

physicist, biologist, and others. Such popularity was expected since the immobilization process can be conducted on almost all electrodes which have hydroxyl or amine functionalities on their surfaces.

One of the approaches to the modification process is to attach the modifier covalently to the electrode surface. In this approach, the modifiers can be bound directly to the electrode surface or via a mediator. Silanes and cyanuric chloride are the only chemical species reported to have successfully served as mediators or bridgs. Other mediators such as silicon tetrachloride ($SiCl_4$) and basic chromium complexes ($Cr(OH)Cl_2$) have also been used but have not moved effective. Electrode surfaces modified with $SiCl_4$ showed complicated chemistry (48) and polymer formation by (Cr-O-Cr) bridging resulted when a chromium complex was used (49). These two mediators will not be discussed further since they have shown little usefulness.

Modification via Organosilanes

In line with their high sensitivity to water, organic silanes have been attached successfully to hydroxyl groups on carbon, metal, and semiconductor electrodes (50).

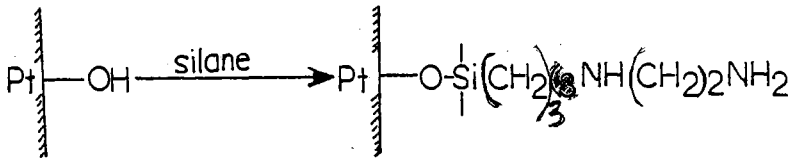

(10)

The new surfaces have been characterized and found to

be very stable under normal conditions. The reactivity of these surfaces depends on the availability of free amino groups. These amino groups can be coupled easily to other chemical species with hydroxylic acid functionalities via amide bond formation. The coupling procedure has shown best results when carried out in dry solvents and in the presence of a dehydrating reagent such as dicyclohexylcarbodiimide (DCC). The latter removes water as it forms in the coupling reaction (51):

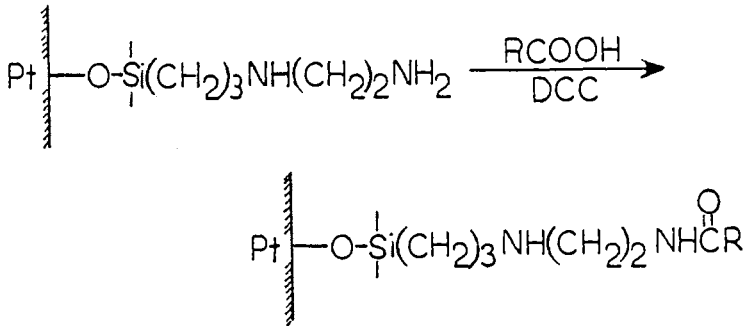

(11)

In addition to their reactivity towards hydroxylic acid groups, the amino terminal groups can undergo protonation or metal coordination when the modified electrodes are exposed to solutions containing these species.

Carbon Electrodes

Electrode Pretreatments. Glassy carbon (GC) electrodes are smoothed with silicon carbide paper to a mirror shine and these further polished with 1-μm diamond paste. The polishing components are washed off with water, then ethanol, and finally hot benzene. Spectroscopic

graghite (SG) electrodes are usually polished with sand-paper. Such electrode surfaces can be silylated without a pre-oxidation step.

Attachment of Organoxilane. electrodes with GC and SG electrode surfaces are treated with 1-2% solutions of -(aminopropyl)triethoxysilane (H_2NPr-silane) in refluxing benzene. The benzene is previously dried by distillation in presence of sodium and stored over molecular sieves under a nitrogen atmosphere. Following the treatment, the benzene solution is decanted and the electrodes vigorously shaken with ethanol followed by air drying. The electrodes are then treated with methanol in a Soxhlet apparatus for several hours and dried in an oven for 1 h. During all the steps above, care must be taken to prevent electrode exposure to atmospheric moisture. 3-(Chloropropyl)trichlorosilane (ClPr-silane) has also been attached to GC and SG electrodes by using this procedure.

Elliott and Murray (52) have reported the preparation of silylated surfaces with surface coverage of a monolayer or submonolayer by the above method. Dry reagents were used and the excess (unbound) silane washed from the electrode surfaces before introducing them to the outside atmosphere. The validity of the above statement was checked by boiling the silylated surfaces with toluene or 1% HCl in ethanol. This treatment did not change the surface population of silane on the GC electrode surfaces, suggesting that the silane formed a monolayer or submonolayer on the surface.

Spectroscopic measurements were used to verify the attachment of the silane on the electrode surfaces.

In an attempt to find another method for silane attachment, the electrodes were allowed to react with the organo-silane at 100 °C for several hours in a sealed tube (52). X-Ray photoelectron spectroscopy (ESCA) studies indicated that the formed layer had different binding energies for both N 1s and Si 2p bands and exhibited different chemical properties from those for silylated surfaces by the first method. Characterization of these surfaces after boiling with 10 M KOH or briefly polishing with 1-um diamond paste still indicated the presence of the Si 2p band. From these observations it was concluded that the organosilane had permeated the upper layer of the electrode surface, which was supposed to have poor porosity. This of course is not recommended for surface modification.

Reactivity of the Silylated Surfaces

Reaction With Metal Ions. The chemical reactivity of GC electrodes modified with H_2NPr-silane towards metal ions was tested by exposing these electrodes to a solution of $Cu(NO_3)_2$. After removal from the reaction vessel, the adsorbed Cu(II) was removed from the electrode surfaces by extracting with slightly acidic (0.40 mM HNO_3) ethanol. Copper(II), scavenged by the amino group, should not be affected by the above treatment. ESCA measurements conducted on the modified surfaces showed the presence of

the Cu 2P band. Similar results were obtained when the procedure was carried out on SG electrode surfaces.

Reaction with 8-Hydroxyquinoline. A method initially proposed to attach 8-hydroxyquinoline to controlled-pore glass via an organosilane (53) was used to bind 8-hydroxyquinoline to carbon electrodes modified with H2NPr-silane. The new surfaces were able to remove Cu(II) from acetone solution readily. The presence of the Cu(II) on the electrode surface was also verified by ESCA measurements. To test the effect of the silane group on the overall attachment process, unsilylated carbon electrodes were allowed to react first with 8-hydroxyquinoline and then with Cu(II). ESCA measurements showed a very small signal due to the metal ions. This signal was attributed to Cu(II) that had been retained by the adsorbed 8-hydroxyquinoline.

Metal Oxide Electrodes

Surface Oxidation. Formation of an oxide film on platinum electrode surfaces can be accomplished electrochemically by applying an appropriate potential under acidic conditions for a short time. Recent work on the subject has shown that the thickness of a PtO/OH layer so produced depends on the applied anodic potential as well as on the reaction time. Bonzel et al. (54) studied extensively this oxidation of platinum surfaces. Figure 24 shows a schematic representation of the chemical state of

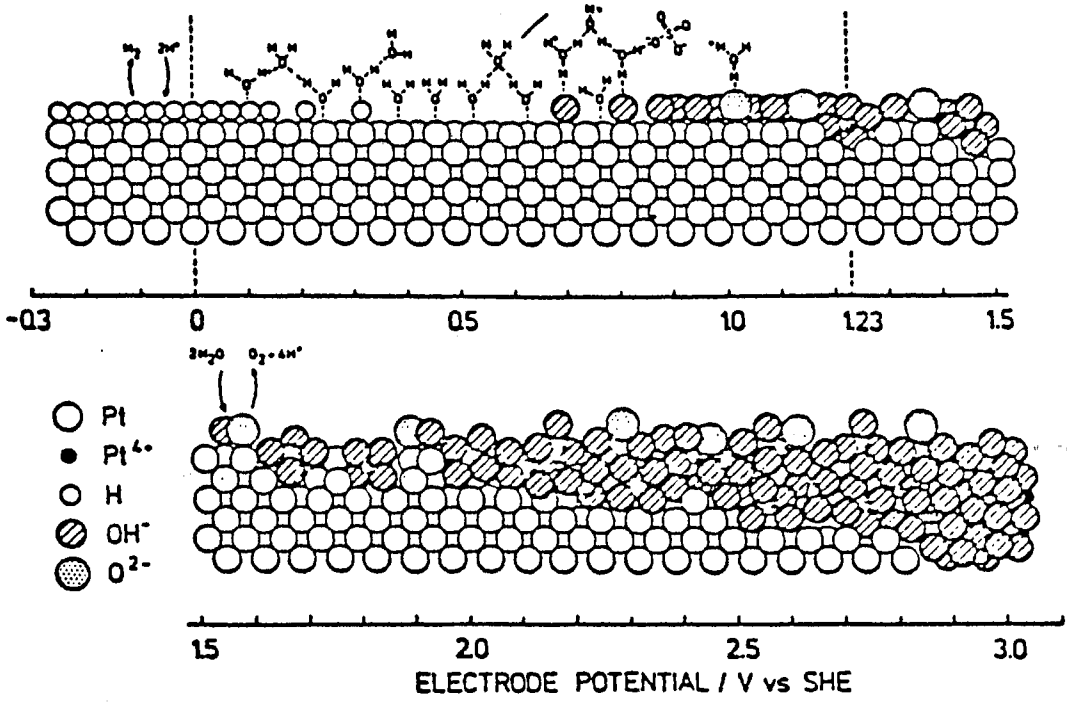

Figure 24. Model for surface composition of platinum electrode in acid electrolyte as a function of applied potential (from reference # 54).

the platinum surfaces oxidized at different potentials in 0.5 M H_2SO_4. The postulated mechanism is based on ESCA measurements which revealed the presence of a Pt(IV) peak at 74.4 eV. This shows that the surface is either populated by $Pt(OH)_4$ or by $PtO_2.H_2O$. This uncertainty was resolved by locating the oxygen 1s peak at 531.5 eV with a half width of 2.5 eV. These values are typical for hydroxides of transition metals. It seems that such treatment leads to the formation of a platinum hydroxide film rather than oxide and the reaction is expected to be:

$$Pt + H_2O \longrightarrow PtOH + H^+ + e^- \qquad (12)$$

Peuckert (55) tried to repeat the above investigation using an alkaline solution (0.10 N NaOH) instead of the acidic medium. ESCA studies showed that the location of the oxygen 1s band was shifted to the lower binding-energy region (530.9 eV) which implies that the oxidized surfaces may bear both, oxide and hydroxide species. The appearance of two reduction peaks on the cyclic voltammogram supported this assumption about the presence of two different oxides. The formula assigned to the new film is $PtO(OH)_2$, platinum-oxide dihydroxide. The mechanism for the growth of this layer may be written as:

$$Pt + OH^- \longrightarrow PtOH_{ads} + e^- \qquad (13)$$

$$PtOH_{ads} + OH^- \longrightarrow Pt(OH)_{2,ads} + e^- \qquad (14)$$

$$Pt(OH)_{2,ads} + 2OH^- \longrightarrow PtO(OH)_2 + H_2O + 2e^- \qquad (15)$$

Even though the first treatment is very efficient for surface hydroxyl formation, electrodes are usually pretreated at 1.9 V vs SCE for a few minutes in 0.5 M H_2SO_4. The potential of the electrode is then cycled betwee O_2 and H_2 evolution in the same acidic medium until the voltammograms become constant. The electrodes are then oxidized at 1.1 V vs SCE until the current decreases to background levels (56-59). By comparing results from the above treatment with those of Fig. 1, it can be concluded that the latter is capable of generating a monolayer of platinum hydroxide film.

Surfaces of gold electrodes are cleaned by dipping them into concentrated HNO_3 for 5 min at room temperature. The electrodes are then mounted in an electrochemical cell and the potential is held at 1.9 V vs SCE for 15 s in aqueous acid solution (0.5 M H_2SO_4). The potential of the electrode is then cycled between 0.0 and 1.0 V vs SCE for 15 s. This electrochemical treatment is usually followed by washing with water and then with acetone and finally allowing the electrodes to dry in air (56).

The surface of titanium electrode is smoothed with very fine emery paper and polished to a mirror finish with a polishing wheel prior to oxidation. The clean metal is heated to 150 C and exposed at that temperature to vapor of tetraisopropyl orthotitanate. The latter is heated in a flask set in a water bath, and its vapor carried to the substrate by dry nitrogen. Thick films of TiO_2 exhibiting

good adherence properties are usually generated by this treatment (60).

Other metal oxide electrodes such as SnO_2 and GeO_2 electrodes are commercially available (PPG Industries, Pittsburgh, PA) as thick films on glass or quartz backing.

Organosilane Attachment. The most popular method for silane attachment to metal oxide electrode surfaces is the one originally described by Murray et al. (61). In this method, a solution of the selected silane in dry benzene is allowed to react with the metal oxide surface for 5 min at room temperature under a nitrogen. The silanized surface is washed either with CH_3CN or sequentially with CH_3CN, CH_3OH, and water (57). It has been shown that such a reaction forms a monolayer or submonolayer of the silane when the experiments are carried out under anhydrous reaction conditions. With slight variations, the foregoing procedure is a standard method for the silylation step. The variations involve the type of solvent used, the reaction time, and the concentration of the silane. The attachment of the silane to the metal oxide surface is usually verified by ESCA measurements which show the presence of N 1s and Si 1s bands.

Allred's group (62) had shown that it is possible to attach some trimethylsilyl to platinum oxide electrodes by electrochemical reduction of silane in acetonitrile:

$$Me_3SiCl \overset{e}{\longleftrightarrow} Me_3SiCl^{-} \longrightarrow Me_3Si\cdot + Cl^{-} \qquad (16)$$

The above reactions shows the formation of a radical intermediate which should attack the electrode surface. Electron spin resonance (ESR) (63) failed to show the presence of these radicals, but ESCA measurements revealed the presence of the Si 2s band on the modified surfaces with binding energies between those of pure silicon and silica.

Reactivity of the Silylated Surfaces. Reaction 1 produces a functionalized electrode surface which is suitable for further modification by aculating the nitrogen functionalities with carboxylic acid or acid chloride sites on other molecules. One of the earliest examples to show such behavior is the reaction of 3,5-dinitrobenzoyl chloride with platinum oxide electrodes silanized with an aminosilane (57). This reaction was carried out in CH_3CN that contained a few drops of 2,6-lutidine and was followed by sequential washing with CH_3CN, CH_3OH and water.

Metal oxides silanized with aminosilane also showed high reactivity with acid anhydrides (64), with sulfonyl chlorides (to form sulfonamides (65)), and with carboxylic acids (57). Schiff base formation also was reported with oxalyl, malonyl, succinyl, glutaryl, and sebacoyl chlorides (65,66). The general scheme for these reactions is represented in Figure 25.

Electrode surfaces silanized with pyridine silane showed further chemical modification by reaction with 2,2'-bipyridyl complexes of ruthenium and a n-alkyls (58,68).

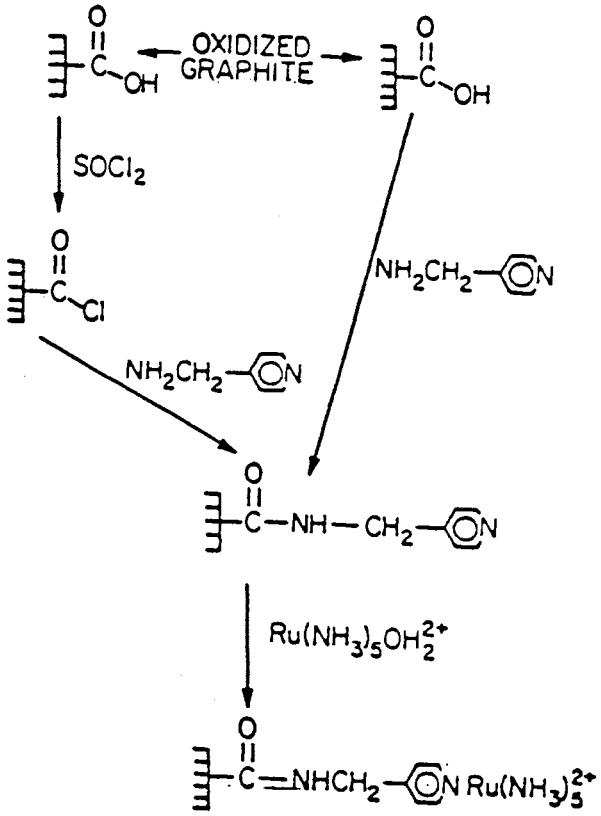

Figure 25. General scheme for the reaction of silylated surfaces with other functionalities (from reference # 76).

Advantages of Using Organosilanes as Mediators

In addition to their high sensitivity to surface hydroxyl groups, organosilane reagents display three distinctive advantages. First, the organosilyl groups are electrically insulating and background current due to these groups is not a limiting factor in their applications. Second, submonolayer coverage usually occrs in the silanization process. This means that the silane layer appears to be "porous" enough to allow the diffusion of electroactive species to the electrode surface. Third, silyl groups are available of sufficient molecular lengths to allow for chain folding. Such flexibility may permit the attached electroactive species to approach the electrode surfaces close enough for electron exchange to take place. However, such properties may prohibit the electron transfer process when the electroactive species are very large molecules (such as dyes) as will be discussed later.

Modification via Cyanuric Chlorides

Graphite Electrodes

Electrode Pretreatments. Electrode pretreatments are usually carried out on graphite electrodes to maximize oxygen-containing functional groups on the electrode surfaces. Kuwana et al. (68,69) were the first to report such treatment on pyrolytic graphite surfaces. Organic contaminants were first removed from the electrode surfaces

by extracting with methanol in a Soxhlet apparatus. The extracting methanol was removed and the electrodes dried under vacuum. The electrode surfaces were then etched by radio frequency treatment in an electrodeless-discharge plasma generator at a pressure of 150 mtorr:

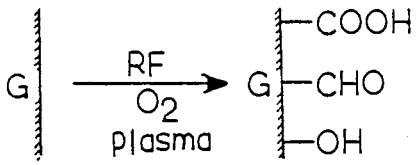

(17)

The oxygen was admitted to the plasma chamber via a needle valve. The oxidized surface was then methylated with a methanolic solution of dimethyl sulfate. The above O-alkylation process was promoted by a KOH solution at 0 °C. Following the addition of the base, the solution was allowed to warm up to room temperature and then refluxed for about an hour. The excess of methyl sulfate was hydrolyzed and washed out with water and the surfaces vacuum dried. A reduction process was also carried out in a refluxing anhydrous ether solution of lithium aluminum hydride (69). The latter increased the surface coverage of the modified electrodes. Furthermore, surface coverage was enhanced when the reduced surfaces were allowed to attain equilibrium with sodium hydroxide, presumably due to the formation of sodium salts (-O-Na) with surface hydroxyl groups.

Attachment of Cyanuric Chloride (CC). Attachment of CC

to the activated electrode surfaces was achieved by allowing the alkali-treated electrodes to react with a solution of CC in anhydrous benzene (5%). After completion of the above reaction, the electrodes were washed thoroughly with anhydrous acetone at 4 °C, then triply distilled water at the same temperature to remove NaCl, and then again with anhydrous acetone to remove residual water. Following the washing procedure, the electrodes were treated with anhydrous benzene for 14 h in a Soxhlet apparatus to remove unreacted CC.

Modifiers Attached via CC. An effective surface coupling may result when CC is attached to pyrolytic graphite electrodes. This is of particular interest when the modifying species contains amino or hydroxyl groups and a covalent attachment is desired. Figure 26 shows a general scheme for the attachment using CC. By utilizing this scheme, the following species were coupled successfully to pyrolytic graphite via CC:

(Hydroxymethyl)ferrocene (69,70). A few milligrams of (hydroxmethyl)ferrocene and sodium hydride were mixed and dissolved in 100 mL of benzene and the solution was allowed to react with electrodes previously treated with CC. Distilled water was used to wash the electrode, which was then extracted with anhydrous benzene in a Soxhlet apparatus to remove any adsorbed reactants. The modified electrodes were analyzed by X-ray photoelectron spectroscopy, cyclic

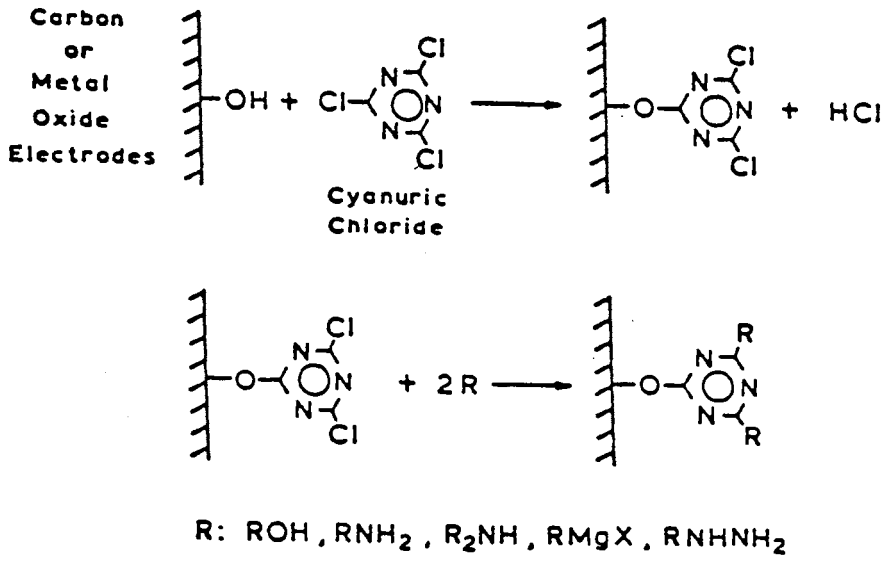

Figure 26. General reaction scheme employing cyanuric chloride as a linking agent for carbon or metal oxide electrodes (from reference 69).

voltammetry, and differential pulse voltammetry.

<u>o-Tolidine (OT)</u>. Kuwana et al. (71) coupled OT to pyrolytic graphite electrodes, previously modified with CC by treating these electrodes with a 20 mM solution of OT in boiling anhydrous benzene. The reaction was expected to proceed according to the following scheme:

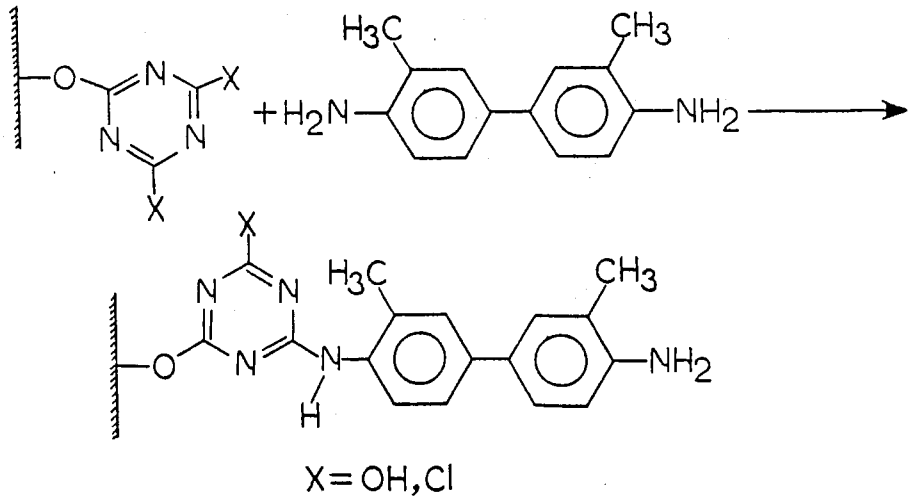

(18)

ESCA measurements supported the above suggested reaction scheme. Electrochemical studies have also been found to be consistent with the spectroscopic results.

<u>Enzymes.</u> Yacynch et al. (72) were able to immobilize glucose oxidase and L-amino acid oxidase on PG-CC electrodes according to:

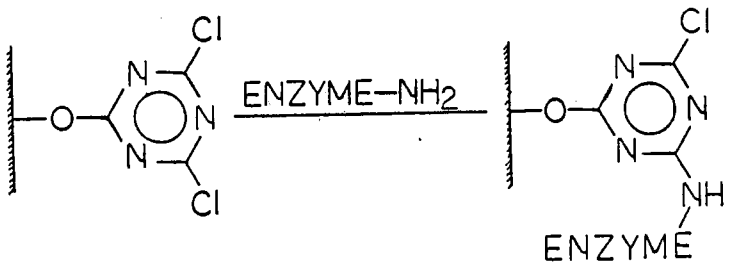

(19)

The above treatment generated electrode surfaces with high porosity and large surface areas. Therefore, these electrodes were used as amperometric sensors. Experimental results indicate that the above electrodes displayed a rapid response and extended the linear range for quantitative measurements compared to conventional enzyme electrodes.

Metal Oxide (SnO_2 and In_2O_3) Electrodes

Electrode Pretreatment. The surfaces of the electrodes (73) were washed in an ultrasonic bath with detergent, then with isopropyl alcohol and finally with triply distilled water. Oxidation of the surfaces was performed by sealing the electrodes in a saturated solution of NaOH for 17.5 h and washing thoroughly with distilled water to remove the unreacted base. Then the electrodes are oven dried to remove the water from the surfaces.

Attachment of Cyanuric Chloride (CC). Without allowing the dried electrodes (from step a) to react with moisture, they were transferred to a flask containing 13% (w/v) solution of CC in methylene chloride at room temperature and the whole shaken mechanically for 7 h. The unreacted CC was removed from the surface by rinsing with anhydrous acetone.

Species Attached via CC.

1.1'-Bis(hydroxymethyl)ferrocene (BHMF): The CC-modified electrodes were treated with 1% (W/V) solution of

BHMF in acetone. The adsorbed BHMF was removed from the surface by extraction with anhydrous benzene in a Soxhlet apparatus. Attachment of BHMF to the metal oxide electrodes was confirmed by electrochemical and by spectroscopic measurements.

Advantages of Using Cyanuric Chloride as a Mediator. Of the many available linkage reagents, CC is an attractive one for the attachment of many electroactive species to graphite and metal oxide surfaces. It has been indicated that the coupling reaction to the surface proceeds readily and through a predictable chemical route. Cyanuric chloride is available in relatively high purity at low cost. The CC is electrochemically inactive in the region of potential where the graphite or metal oxides are used and shows a good chemical stability.

Compared to organosilane linkage, CC offers a short binding between the electrode surface and the modifying species. Electron transfer is expected to progress readily over this short distance (i.e. such proximity will facilitate the electron exchange process).

Surface Modification by Acylation

Building surfaces with a variety of species can be accomplished by attaching the modifier directly to the desired electrodes. Miller at al. (43) were the first to consider such a possibility. Their work involved oxidation

of spectrographite (SG) electrode surfaces by baking in air to produce acidic groups on these surfaces followed by treatment with thionyl chloride in dry benzene. The oxidized electrodes bearing -COCl groups were then exposed to a solution of (S)(-)-phenylalanine methyl ester chloride. These electrodes were used to reduce 4-acetylpyridine to the corresponding alcohol. Similar electrodes were used by the same authors to reduce ethyl phenylglyoxylate to the alcohol. In each case the products were identified by NMR and by gas chromatography.

This acylation approach was carried out on glassy carbon (GC) electrode surfaces by Murray et al. (74). The GC surfaces were first polished to a shiny finish and then oxidized at 500°C. The electrodes were then treated with a solution of $SOCl_2$ in a Na-dried boiling toluene. After had been cleaned with fresh toluene and dried in air, the electrodes were allowed to react with a solution of tetra(R-aminophenyl)porphyrin in a mixture of toluene and methylene chloride. Further modification was accomplished by bringing the electrodes into contact with a refluxing solution of $CoCl_2$ in dimethylformamide. After these treatment, fresh solvent was used to wash the electrodes and remove any adsorbed $CoCl_2$ from the surface. Cyclic voltammetric studies of these modified surfaces produced symmetrically shaped waves. These voltammograms were independent of stirring rate and exhibited linear dependence of peak current on scan rates. The redox potentials of the

modified surfaces were in good agreement with those reported for the Co(II) complex with tetra(R-aminophenyl)porphyrin in solution. The presence of Co(II) on the electrode surfaces was confirmed by detecting the Co 2p band by ESCA measurements. Enhanced sensitivity of the modified surfaces was also demonstrated by differential pulse voltammetry.

Pyrolytic graphite (PG) electrode surfaces, oxidized in radio frequency plasma, were modified by Kuwana et al (75) by attachment of benzidine via amide linkage using N,N'-dicyclohexylcarbodiimide as a coupling agent. The modified electrodes were characterized by electrochemical methods and used to catalyze the oxidation of ascorbic acid.

Koval and Anson (76) have also attached pentaamminopyridene ruthenium(II) to graphite electrodes by amide formation. Two procedures have been used for the above attachment. First, thionyl chloride was used as reported earlier. Second, the electrodes bearing -COCl groupswere in a refluxing solution of benzene containing small amounts of 4-(aminomethyl)pyridine. This treatment was followed by Soxhlet extraction with benzene. The modified surfaces were then treated with $[Ru(NH_3)_5Cl]Cl_2$ in sodium trifluoroacetate. These reaction steps are summarized in Fig. 27. Both cyclic voltammetry and differential puls voltammetry indicated the presence of ruthenium on the electrode surfaces. The electrochemical behavior of the chemically modified electrodes was compared with those modified by irreversible adsorption of ruthenium

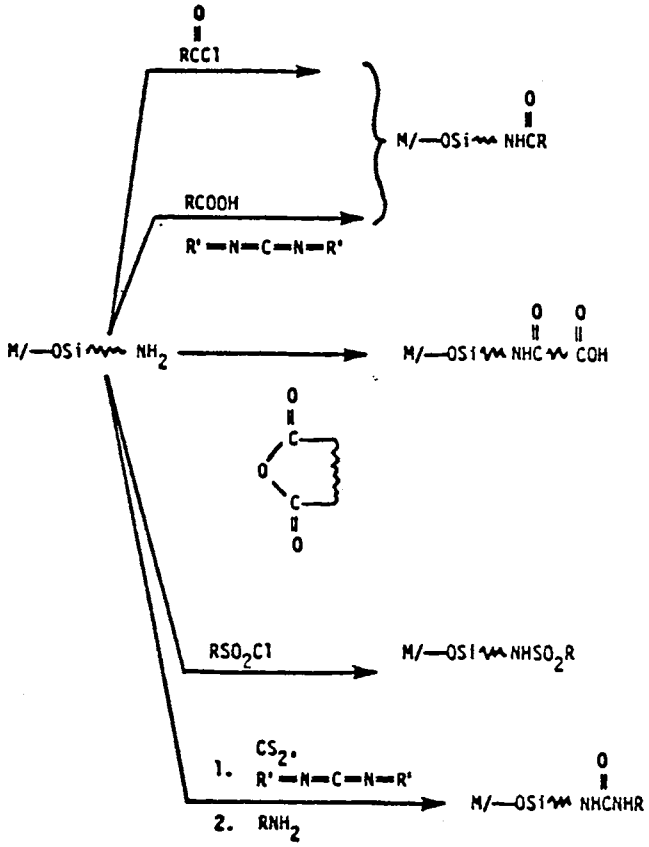

Figure 27. The likely surface chemistry involved in the attachment of $Ru(II)(NH_3)_5^{2+}$ to graphite electrode surfaces (from reference # 127).

complexes on graphite surfaces. Electrodes modified by the second method yielded larger quantities of complex on the electrode surfaces but covalent attachment was found to persist on the electrode surfaces for longer times when the first procedure was used.

Murray et al. (77) extended their work on metallation of immobilized tetra(R-aminophenyl)porphyrin on GC electrodes (74) to include manganese, iron, nickel, copper, and zinc. Thionyl chloride was tried as mediator for the attachment of tetra(R-aminophenyl)porphyrin to the electrode surfaces.

Metal ions were introduced to the above surfaces by subjecting the electrodes to a refluxing DMF solution of the metal(II) chloride (cobalt, nickel, copper, and zinc). Manganese(II) acetate was employed instead of the chloride salt. Iron(II) was inserted by heating the electrodes in a tetrahydrofuran solution of anhydrous $FeCl_2$.

Anson et al. (78) have also etched pyrolytic graphite surfaces in RF plasma and exposed the etched surfaces to ammonia, ethylenediamine, or diethylenetriamine in anhydrous methylene chloride which also contained nicotinic acid and DCC. Excess of reactant was removed from the surfaces by washing with anhydrous methylene chloride, methanol, and water. After drying under vacuum, the electrodes were treated with a stirred aqueous solution of $[Ru(NH_3)OH_2](PF_6)$ under an argon atmosphere. The amount of ruthenium complex attached to the surfaces was calculated

from the area under the voltammograms. A value of 6 x 10^{-10} mol cm^{-2} was reported for electrodes modified with ammonia, 7 x 10^{-10} mole cm^{-2} for ethylenediamine, and 15 x 10^{-10} mol cm^{-2} for ethylenetriamine.

Advantages of Ester Linkages

Chemical modification of electrodes via ester linkages showed its potential advantage when applied for photosensitization processes. Such behavior is expected since the photosensitizer is attached directly to the electrode surface. Experimental results have verified this advantage in comparison to preparations using silylation. However, electrochemical and ESCA studies showed that ester linkage formation is characterized by low surface coverage and less surface stability.

Surface Characterization

Electrochemical Methods

Because of their high sensitivity, electrochemical techniques are the methods of choice for the characterization of chemically modified electrode surfaces. The class of information revealed by electrochemical measurements is based on the current flow at the working electrode as a function of the applied potential (current-potential curves). Such information includes:

1. Electrode surface coverage as obtained by estimating the area under the current-potential

(time) curves.

2. Formal potential of the redox couple as determined by locating the potential at which the peaks appear.
3. Rate of electron transfer as evaluated by monitoring the separation of the anodic and the cathodic peaks and lack of symmetry in the wave shapes.

Electrochemical methods commonly used for surface characterization are cyclic voltammetry, differential pulse voltammetry, and alternating current voltammetry.

Cyclic voltammetry (CV). Cyclic voltammetry (79) is the most useful instrumental technique for the characterization of chemically modified electrodes, specifically where the electrode surface coverage is high and the background current is low. Figure 28 shows a typical current-potential curve for a cyclic voltammetry experiment. The important parameters of the voltammogram are peak potentials, peak heights, symmetry of the wave, and the peak widths at the half height. The wave shown in Fig. 28 is for an ideal reversible system involving one electron exchange. This wave shape can be described mathematically by:

$$i = \frac{-4i_p \exp(\phi)}{[1+\exp(\phi)]^2} \qquad (20)$$

where

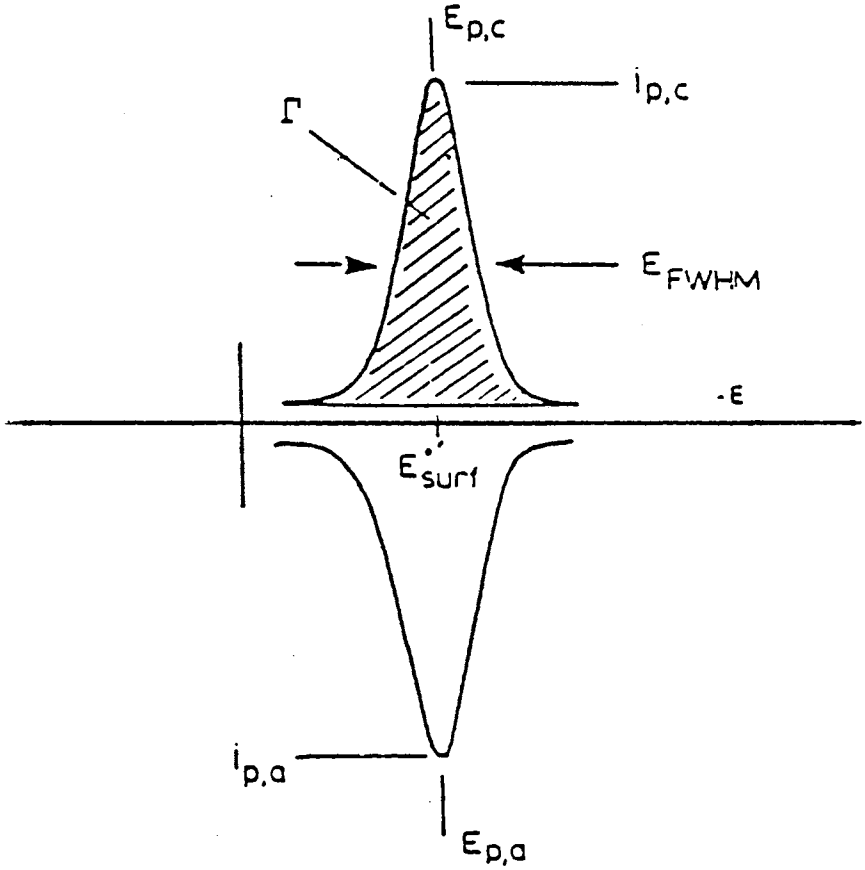

Figure 28. Schematic, reversible cyclic voltammogram for a monolayer of an immobilized redox species.

$$i_p = \frac{n^2 F^2 A \Gamma_t V}{4RT} \qquad 21)$$

and

$$\phi = \frac{nF(E-E_{surf})}{RT} \qquad (22)$$

and

n is the number of electrons involved in the oxidation or reduction,
A is the area of the working electrode
Γ_t is the total electrode coverage
v is the scanning rate for the applied potential
E is the formal potential of the attached couple.

Experimental results by Brown and Anson (80) indicate that Equation 20 produces qualitatively similar curves to those obtained experimentally, However, the two shapes showed lack of quantitative correspondence. Such differences are corrected by using the redox couple activities in Eq. 21 rather than concentrations. These differences are related to perturbing influences reflected by a given molecule of attached oxidant or reductant due to the presence of other attached oxidant or reductant molecules. These parameters are designated as r_{OO}, r_{OR}, r_{RR}, and r_{RO}. Introducing these parameters will change Eq. 20 to the following one:

$$i = \frac{4i_p \exp(p)}{[\{1+\exp(p)\}^2 - (r_O + r_R)\exp(p)\}} \qquad 23)$$

where

$$p = \phi + (r_O + r_R)\Gamma_O - r_R \Gamma_t \qquad 24)$$

$$\Gamma_o = \Gamma_t \frac{\exp(p)}{1+\exp(p)} \quad (25)$$

$$r_o = r_{oo} - r_{oR} \quad (26)$$

$$r_R = r_{RR} - r_{Ro} \quad (27)$$

Usually it is assumed that;

$$(r_o + r_R) / 2 = r \text{ and } r_o = r_R \quad (28)$$

Assuming a value of -2.67×10^{-11} mol^{-1} cm^{-1} for r_o and r_R, Brown and Anson were able to reproduce the experimental voltammograms by using Eq. 23. The introduction of the perturbing parameters have been found useful in defining the redox potential of the attached couple (81):

$$E_{peak} = \frac{E + RT(r_R - r_o)\Gamma_t}{2nF} \quad (29)$$

The deviation of E_{FWHM} value for modified electrodes from a theoretical value of 90 mV also can be accounted for by introducing r_o and r_R in the calculation:

$$E_{FWHM} = \frac{2RT}{nF} \{\ln(Q) - (r_o + r_R)\Gamma_t \left(\frac{Q-1}{2Q+2}\right)\} \quad (30)$$

where

$$Q = \frac{\{6-(r_o+r_R)\Gamma_R + (r_o+r_R)^2 \Gamma_t^2 - 12(r_o=r_R)\Gamma_t+22\}}{2} \quad (31)$$

Murray et al. (81) also investigated the validity of Eq. 30. Their work revealed the following: a) the product $r\Gamma_t$ is more characteristic of a particular surface species than r itself, c) E_{FWHM} is independent of Γ_t, and c) E_{FWHM} depends linearly on the product $r\Gamma_t$ (82).

The foregoing observations indicate that CV is a very useful technique to characterize the modified electrode surfaces. Indeed, CV is the most widely used electrochemical method for characterization purposed (83, 84).

Differential Pulse Voltammetry (DPV). Surface characterization of modified electrodes by CV is hampered in many cases by the high background due to the double layer charging current. Differential pulse voltammetry (85) is considered to be an ideal approach to overcome such a drawback. It is well suited for precise measurement of peak potential and for detection of small surface coverage. Surface coverage as low as 4.2×10^{-11} mol cm^{-2} of a pentaammineruthenium(II) complex on a PG electrode was easily detected by Brown and Anson (80). Yacynch et al. (86) used DPV to monitor the electrochemical behavior of glucose oxidase immobilized on a PG electrode. The attachment of (hydroxymethyl)ferrocene to the PG electrode was verified by Kuwana et al. (69) using DPV. The technique has also been used by many researchers in combination with CV (78).

Alternating Current Voltammetry (ACV). Chemically modified surfaces cannot be analyzed quantitatively by CV when the resulting voltammograms are poorly defined. The peak potential value and the concentration can only be approximated because of the high background current due to

double layer capacitance. As a result, it becomes difficult to detect the faradaic current, due to the redox behavior of the electroactive species, in the presence of a large charging current. The effect of such a current is significant at higher scan rates.

In addition to DPV, discussed earlier, ACV (87) has also been found to be useful under the above conditions. Diaz and Kanazawa (88) were able to determine the peak potential and electrode surface coverage of an SnO_2 electrode, modified by pyrazolines via silylation, using ACV. Murray and Lennox (89) recognized the high sensitivity of ACV in their work on a glassy carbon electrode which has been modified by tetra(R-aminophenyl)porphyrin and then with cobalt. The results of this work also revealed the presence of a residual, unmetallated tetra(R-aminophenyl)porphyrin. Such information was not obtainable by CV measurements.

Spectroscopic Methods

To gain more information on surface microscopic details, several surface and nonsurface spectroscopic methods have been applied in addition to the electrochemical methods. These methods include electron spectroscopy (ESCA and Auger), inelastic electron tunnelling spectroscopy, fluorescence spectroscopy, infrarred spectroscopy, and Raman spectroscopy.

ESCA. ESCA (90) is the most widely used spectroscopic method to study surface composition of modified electrodes.

The measurement involves excitation of chosen elemental tags on the immobilized reagent. Usually the excitation energy is selected at a region where the background signals due to the electrode backbone and other surface elements are minimum. The appearance of the elemental tag band on the ESCA spectrum is an indication of the success of the immobilization process. Information about surface layer content of a given element may be extracted by measuring the relative intensity of its band.

The work by Kuwana et al. (70, 71) is an attractive example for the critical information available via ESCA measurements. The authors tried to follow the building up of different functionalities on a pyrolytic graphite surface. The modification process involved the attachment of o-tolidine (OT) to PG via cyanuric chloride. The experimental steps for the complete attachment process are summarized in Table VIII. Surface analysis was carried out on the unmodified surface and also after each modification step.

Murray et al. (91) used the ESCA method to set the optimum conditions for immobilizing aminoalkylsilanes on metal oxide surfaces. The study was based on the relative intensities of the N 1s and Si 2p bands. The study also revealed that mono(alkylamino)silanes were fairly unreactive toward derivatization compared to di(aminoalkyl)silanes. The low reactivity of the former was attributed to the cyclic structure formation which could take place between

TABLE VIII

EXPERIMENTAL STEPS IN THE ATTACHMENT OF CC AND OT TO GRAPHITE

Step	Procedure
1.	Extraction with methanol to remove organic contaminants.
2.	Plasma treatment using 10 mTorr anhydrous oxygen plasma for 5 min to introduce oxygen functional groups.
3.	Reflux in ethereal $LiAlH_4$ solution for 3 h to maximize surface hydroxyl groups coverage; followed by washing with ether, 1 M aqueous HNO_3, and triply distilled water.
4.	Equilibration with 1 M aqueous NaOH to promote deprotonation of surface hydroxides.
5.	Oven drying (150 °C, 3 h) to remove residual water.
6.	Reflux in neat CC for 0.5 h to couple CC to surface oxides.
7.	Washing with (a) copious quantities of anhydrous acetone at 4°C, (b) triply distilled water at 4°C, and (c) anhydrous acetone at 4°C (to remove residul water); followed by extraction with anhydrous benzene for 12 h and drying in vacuum at room temperature.
8.	Reaction of OT with bound CC: 12 h reflux in 20 mM OT in anhydrous benzene, followed by overnight extraction with anhdrous bezene.

the amino group and the O-position and a SiOH function on the chain via hydrogen bonding. This assumption was verified by monitoring the increase in surface coverage of mono(aminoalkyl)silanes with the electrode kept in an anhydrous atmosphere. Such conditions are effective in inhibiting the hydrolysis of the dangling group and preventing the formation of a hydrogen-bonded cyclic structure. The capability of the ESCA method for electrode surface analysis has been widely recognized in the literature (92-95).

Auger Electron Spectroscopy (AES). AES (96) is a surface-sensitive technique that has been used to study modified electrode surfaces. Quantitative and qualitative information about these surfaces are obtained by analyzing the secondary electrons emitted from the specimen which has been irradiated with a medium-energy electron beam. The concentration of a particular elemental component in the modified surface layer determines the amplitude of the peak in the Auger spectrum. Changing the concentrations of a particular component can be followed precisely by measuring the growth or decay of the Auger peak. The energy at which a given peak appears on the spectrum is used to identify the specific element in the specimen.

AES measurements were conducted on a SnO_2 electrode silylated and then modified with α-naphthol to determine the depth of the modified surface layer by Kuwana et al. (97). The thickness of the silane layer was estimated to be 80-100

A. The conclusion on the depth profile was based on the decay of the carbon band and the growth of tin and oxygen bands until the stoichiometric Sn/O ratio of a "clean" tin dioxide surface was reached. The authors have also reported the usefulness of AES for further surface analysis, particularly if characterization is needed before and after electrochemical treatment.

Murray et al. (98) used AES to probe amine site spacing on a SnO_2 electrode using the following coupling reaction:

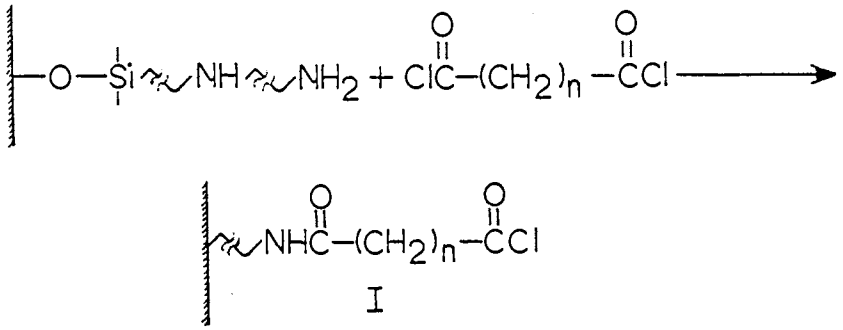

(32)

I

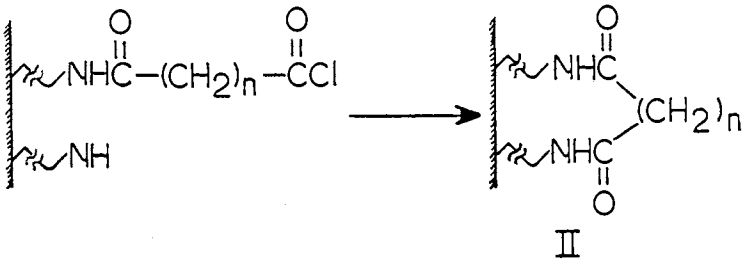

(33)

II

The relative population of the open chain (product I) and the closed chain (product II) determined as a function of n shows the bifunctional coupling (closed chain) is possible if n is such that the reagent can accommodate to an amine N-

N spacing of 4-8 ^{o}A.

It has to be stressed here that the information available by AES is similar to that obtained by the ESCA method except that some of the elemental tags are less sensitive to ESCA measurement than and they are to AES (e.g. sodium).

Inelastic Electron Tunneling Spectroscopy (IETS). Diaz et al. (99-101) used IETS (102) to study metal oxide electrode surfaces modified by silyl derivatives. The IETS technique is highly sensitive for studying bond vibrations in a given specimen sample that is too thin to be examined by conventional infrared spectroscopy. The authors used aluminum oxide (Al_2O_3) that had been silylated with triethoxyvinylsilane. The result of this work indicated the extensive removal of surface OH groups. The IETS spectrum also showed the presence of a series of bands that were related to the presence of $-OCH_2-CH_3$ groups on the surface. The origin of these bands was further investigated by repeating the experiment on similar electrodes with excess of the silane groups on the surface. The intensity of the bands previously related to $-OCH_2-CH_3$ was increased significantly. These results indicate that some of the ethoxy groups survived the silylation reaction and remained unreacted.

The above work confirms that IETS can offer on-site information about the modified layer of the surface. Such information cannot be verified by ESCA or AES.

Fluorescence Spectroscopy. In part of their effort to analyze the surface coverage of chemically modified electrodes, White and Murray (65) immobilized dansyl chloride on metal oxide electrodes. This was achieved by attaching the dansyl chloride to a surface modified with 3-(2-aminoethylamino)propyltrimethoxysilane according to the following reaction:

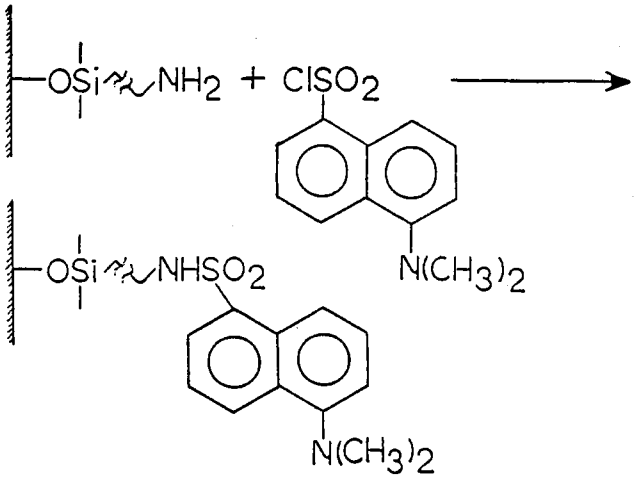

(34)

The success of the coupling procedure above was verified by the appearance of S 2p and Si 2p bands in the ESCA spectrum. The modified electrode was then immersed in a small volume of 0.1 N KOH in ethanol for 2 h to cleave the dansylamide from the surface:

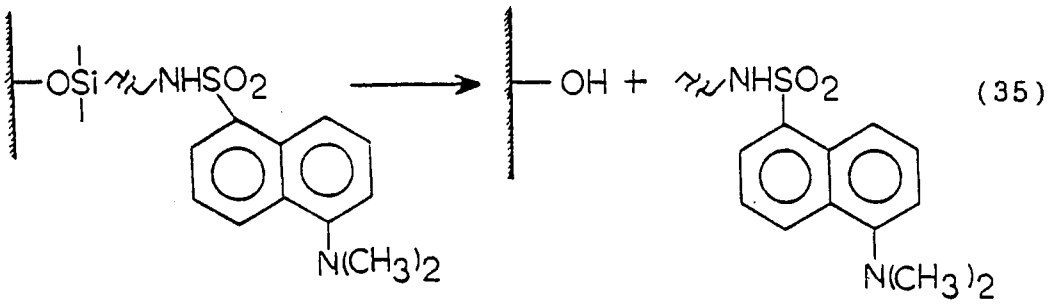

(35)

The solution was pipetted out of the reaction vessel and

analyzed with a fluorometer. The intensity of the fluorescence signal was related to the concentration of the dansylamide removed from the surface. Complete removal of the dansylamide was ascertained by the subsequent ESCA observation of Si 2s and 2p at background level.

Infrared Spectroscopy (IR). Finklea and Vithanage (103) were able to obtain an IR spectrum of TiO_2 powder modified by the attachment of methylsilanes in the gaseous phase. The success of the attachment of the silane groups to the surface is reflected by the appearance of new peaks in the IR spectrum. These new peaks are assigned to C-H stretches of the methyl groups on the silane. Likewise, peak intensities of surface O-H groups are attenuated. Proof of the covalent attachment to the TiO_2 surface is given by the thermal stability of the modified surfaces. Electrodes heated at 150 ^{o}C under vacuum showed no decrease in the intensities of the methyl C-H or Si-C bands.

The important results revealed by the above work are: a) the TiO_2 surface has two different kinds of O-H groups, terminal and bridging (the terminal groups are found to be more reactive than the bridging groups), and b) there is no indication of the presence of unreacted Si-X (X is Cl or OMe) bonds after the silylation process. However, results obtained by others (104) indicate the presence of such bonds after the modification procedure.

Raman Spectroscopy. Srinivasan and Lamb (105)

attempted to use Raman spectroscopy to study SnO_2 electrode surfaces modified by silylation with 3-(chloropropyl)trichlorosilane. The authors claimed that some of the Si-Cl was not involved in the silylation process. The results they presented were not clearly reflected in the spectrum provided.

Resistivity Method

Srinivasan and Lamb (105) tried to use an independent technique to confirm some observations reported by other groups about the modified surfaces, specifically the work by Murray et al. and Kuwana et al. (61,97). Both indicated that the electrode surfaces are not completely covered by the silylation processes. To test this, Srinivasan and Lamb used a four-point probe method to measure the resistivity of three different electrode surfaces. These electrodes were: (a) clean tin oxide electrode, (b) SnO_2 electrode modified with an organosilane, and (c) silylated electrode further modified by dye attachment. A survey of their data indicates that the surface coverage is not uniform and cannot be related to the electrode surface area.

The reported data, however, do show that the resistivity change is relatively small and the technique is not powerful enough to discriminate between modified and unmodified surfaces.

Applications

Electrocatalysis

Evans and Kuwana (75) used linear sweep voltammetry and chronocoulometry to study the rate of ascorbic acid oxidation on three electrode surfaces; (a) unmodified pyrolytic graphite (PG), (b) pyrolytic graphite etched by radio frequency plasma and exposed to oxygen atmosphere (PGO), and (c) PGO followed by subsequent attachment of benzidine (PGB). Linear sweep voltammetry studies of the modified electrode surfaces showed well-defined, irreversible oxidation waves for PGO and PGB electrodes upon reaction with ascorbic acid (AH_2). Wave B of Fig. 29, which is related to the PGO electrode, is unexpected and has a peak shape characteristic of a diffusion-limited wave for AH_2 oxidation:

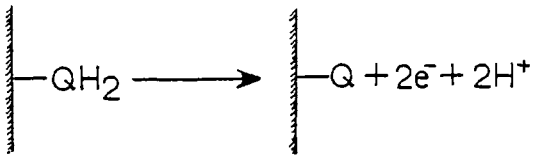

(36)

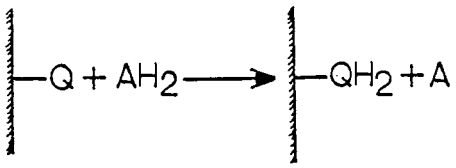

(37)

where QH_2 is hydroquinone residue and Q is the corresponding quinone. The hydroquinone functionalities are introduced to

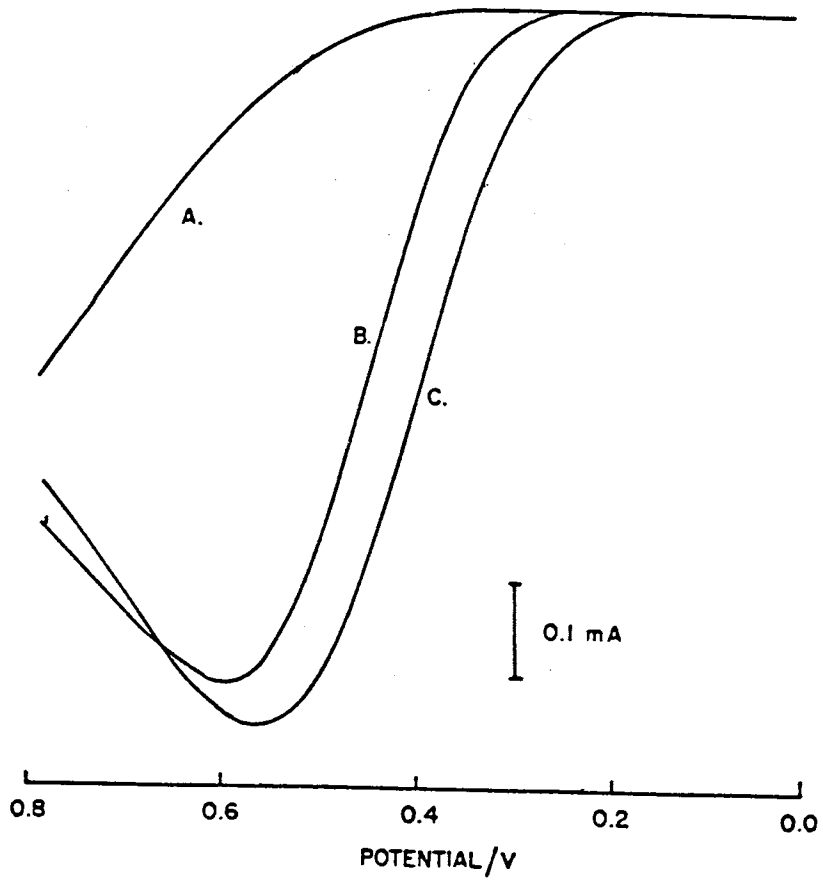

Figure 29. Linear sweep voltammetry of 2.11 mM AH2 pH = 2.50 glycine buffer at: A = PG; B = PT-PG; C = BZ-PG Which has been repeatedly cycled between 0.00 V and +0.70 V. Scan rate = 50 $mV.s^{-1}$, geometric electrode area = 1.82 cm^2 (from reference # 75).

the electrode surface by treatment with RF oxygen plasma (68).

The above reaction suggests that the ascorbic acid oxidation is coupled to the functional groups on the electrode surfaces (quinone/hydroquinone-like functionalities). On the other hand, wave C appeared because the benzidine acted as a "mediator" in the electron transfer process between the electrode and the ascorbic acid. The catalytic behavior of the modified surfaces has also been supported by chronocoulometric measurements. These measurements revealed that the slopes of the curves generated by plotting 'charge' vs 't' are much higher for the modified electrodes than for the unmodified electrodes. The slopes of these curves is a representation of the rate of ascorbic acid oxidation measured in charge/s.

Wosilait and Nason (106) proposed that some nonenzymatic reagents (e.g. orthohydroquinone) can oxidize NADH according to the following reaction:

$$R\text{-}Ph(=O)_2 + NAD + H^+ \longrightarrow R\text{-}Ph(-OH)_2 + NAD^+ \qquad (38)$$

where $-Ph(=O)_2$ is a quinone, $-Ph(-OH)_2$ is the reduced (dihydro) form, and R is some substituent group.

On the basis of the above observations Tse and Kuwana (107) tried to transfer catalytic properties of structures such as those of catechols, to electrode surfaces. To accomplish this, 3-hydroxytriamine (DA) and 3,4-dihydroxybanzylamine (3,4-DHBA) were attached to glassy

carbon electrodes. The modified surfaces generated well-defined cyclic voltammograms when present in phosphate buffer (pH = 7.0). Adding small amount of NADH changes the shape and height of current-potential (I/E) curves. This catalytic effect was clearly seen on the cyclic voltammograms of the electrode modified by DA. These voltammograms verify the validity of reaction scheme of Eq. 28. The equation suggests that the reaction is pH dependent. The result of the above experiment verified this; the rate constant decreased from 3.6×10^4 M^{-1} s^{-1} to 1.2×10^4 M^{-1} s^{-1} when the pH was increased from 6.5 to 8.5.

Ianniello and Yacynych (72) were able to covalently attach glucose oxidase and L-amino acid oxidase to graphite electrodes using cyanuric chloride as a mediator. Reaction between the enzymes and their respective substrates led to the formation of H_2O_2 in the presence of oxygen (107), e.g.

$$\beta\text{-D-glucose} + O_2 + H_2O \longrightarrow \text{gluconic acid} + H_2O_2. \quad (39)$$

The peroxide decomposed anodically on the electrode surfaces at the proper potential according to the following reaction:

$$H_2O_2 \longrightarrow 2H^+ + O_2 + 2e^-. \quad (40)$$

The current produced by the above reaction is related to the concentration of the substrates. Chemically modified electrodes causes current production by the same amount of substrate about two orders of magnitude as high as do conventional amperometric enzyme electrodes and response time is typically about half of that shown for conventional electrodes. Also, it has been reported that the chemically modified electrodes displayed an expanded linear response range and maintained their activities longer under proper storage conditions. The above properties make modified electrodes an ideal choice for electrochemical detection in HPLC and flow injection analysis (108). In later work, Yacynych et al. (86) showed that the glucose oxidase is covalently attached to the surface of the graphite electrodes. This conclusion was reached by monitoring the electrochemical response of the enzyme using differential pulse voltammetry, which resulted in a well-defined peak at a potential 100 mV more positive than that for the free enzyme.

Electrochemical Synthesis

Synthesizing organic species by electrochemical methods is a common practice in the field of electrochemistry. Using chemically modified electrodes to generate interfacial surfaces that can be used to perform specific and unique reactions is a valuable addition to the repertoire of synthetically useful techniques. Firth and Miller (110)

prepared optically active alcohols with a percentage yield of over 50% using chemically modified electrodes. To accomplish this, a spectroscopic-graphite rod was baked in air to generate acidic oxide on the surface. The prospective enzyme, (S)-(-)-phenylalanine methyl ester, was bound to the surface via thionyl chloride. The electrode was used to reduce 4-acetylpyridine to an optically active alcohol. Firth and Miller (110) also tried to generate chiral surfaces on SnO_2 and DSA (a mixture of Ta and Ir oxides) electrodes and attempted to use them for preparative asymmetric oxidations. The modified surfaces were prepared by attaching (-)-camphoric anhydride to the electrode surfaces via(3-aminopropyl)triethoxysilane. The anodic process chosen for the study was the conversion of aryl methyl sulfides to sulfoxides. Again, the product was optically active but with a low enantiomeric excess.

Photoelectrodes

Because of the world energy problems, attention has been directed to the use of sunlight to generate electrical energy by employing electrochemical photocells. One of the major difficulties with this approach is the low sensitivity of photoelectrodes during irradiation with visible light when they are present in aqueous solutions. These electrodes showed more sensitivity when irradiated in the ultraviolet region, but because of the earth's atmosphere, sufficient UV light from the sun cannot reach the photocells

on earth to make them useful. Extending the spectral response of the photoelectrode to longer wavelengths may be a feasible solution to the problem. The general strategy is to cover the photoelectrodes with reagents that are more easily oxidized by sunlight than the electrode itself. Highly colored dyes could be good candidates. Having the electrodes in a solution containing these dyes may sensitize them to the visible wavelength where the specific dye absorbs. However, a new problem may arise since most of the radiant energy is absorbed by the dye molecules in the solution rather than those at the electrode-solution interface. In 1975, Osa and Fujihira (111) tried to demonstrate that some of the dyes retain their catalytic activities after the attachment to electrode surfaces. The authors developed an electrochemical photocell with chemically modified electrodes. The modification involved a coupling of the carboxyl group of Rhodamine B (RhB) with (3-aminopropyl)triethoxysilane immobilized on SnO_2 and TiO_2 electrodes using dicyclohexylcarbodiimide (DCC) as a dehydrating agent. Results of this work indicated that the spectral dependence of the modified electrodes was quite close to that of the dye absorption spectrum and the anodic photocurrent was of the same order of magnitude as those observed at the unmodified electrodes. Later work by Fujihira et al. (112) confirmed that the anodic current they measured earlier was due to dye molecules attached to the electrode surface directly:

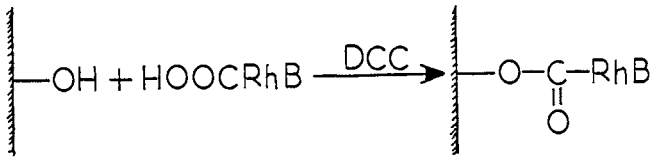

(41)

and not to those bonded to the electrode surfaces via the silane group. Coupling the dye directly to the electrode surfaces enhanced the photocurrent considerably. This enhancement may be attributed to two factors: a) the dye molecules are closer to the surface of the electrode when an ester linkage is used than those attached via a mediator, and (b) the silane is an insulating group and electrons will not tunnel through it. Kuwana et al. (113) tried to evaluate the efficiency of electrodes modified through ester linkages by calculating the quantum efficiency, ϕ, :

$$\phi = \frac{Ie}{Ih} \qquad (42)$$

where Ie is the number of photelectrons flowing (s^{-1}) and Ih is the number of photons "observed" by the surface-bound RhB to produce the excited-state RhB*. A value of 0.09 $\pm$ 0.03 was reported for light from 500 to 590 nm.

Hawn and Armstrong (114) tried to attach three xanthene systems, RhB, fluorescein, and erythrosin, to SnO_2 and TiO_2 electrode surfaces using an aminoalkylsilane as a mediator. Attachment of these dyes to the electrode surfaces was

verified by absorbance measurements in the visible region since these molecules have very high absorptivities. The authors compared the photoelectrochemical response of two SnO_2 electrodes, one modified by the attachment of erythrosin and the other immersed in the dye solution. These electrodes produced equivalent currents. However, the bound dye was much more stable than that in solution. The latter showed irreversible loss of the photocurrent activity for the same period of time.

Ferrocene derivative, (1,1'-ferrocenediyl)dichlorosilane, was attached to n-type silicon surfaces by Wrighton et al. (115,116). Characterization of the electrode by cyclic voltammetry revealed interesting results: (a) the electrodes are not passivated by build-up of a SiO_2 layer, (b) there are cyclic waves all the time (light or dark), (c) the oxidation current increases with irradiation intensity, (d) under illumination conditions, the peak current is linearly proportional to scan rate, (e) stirring the electrolyte solution does not affect the resulting voltammograms, and (f) the oxidation peak current appeared at a potential less positive than that for unmodified electrodes and the shift increased with light intensity. The modified electrodes showed good stability for several days. Bolts and Wrighton (116) repeated the experiment on n-type germanium surfaces. This gave the same results as for silicon surfaces.

Studying the Effect of Immobilized Groups Orientation on the Electron Transfer Process

Sharp (117) was interested in studying the effect of molecular orientation on the electrochemical behavior of molecules that are chemically bound to wax-impregnated graphite electrodes (WIGE). In that work 1-amino-9,10-anthraquinone and 2-amino-9,10-anthraquinone were attached to WIGE electrodes that were previously acylated by $SOCl_2$. Cyclic voltammograms of the two species indicated that 1-amino-9,10-anthraquinone is electrochemically active while the other isomer is not. Monitoring the redox behavior of the two isomers in solution indicated that both are electrochemically active and their oxidation-reduction current peaks are at similar potentials. By studying the molecular models of these isomers, Sharp found that rotation allows the 1-amino isomer to have the anthraquinone plane roughly parallel to the electrode surface and maximum electron interaction is expected between graphite and the quinone. Such favorable orientation is not available for the 2-amino isomer, and this may hinder the electron transfer.

Analyte Preconcentration

The approach of using chemically modified electrodes for preconcentration purposes is analogous to the technique of anodic stripping voltammetry, which has been used for the determination of analytes at very low concentrations (118).

The latter deposits the species of interest on the electrode surfaces electrochemically. In the case of the modified electrodes, accumulation of the analyte will be conducted by chemical reaction of the modified surfaces. Check and Nelson (119) were the first to report successful preconcentration of metal ions on chemically modified electrode surfaces. In that work, silver ions in aqueous solution were scavenged by the electrode modifiers. Using differential pulse voltammetry, the above workers were able to detect the presence of silver ions in a solution as low as 10^{-11} M in concentration. Detection at lower concentrations was limited by the purity of distilled water rather than by the sensitivity of the technique.

Conclusion

It follows from this review that the development of chemically modified electrode surfaces has opened a new degree of freedom in electrochemistry. The significance of the development can be related to the capability of the new surfaces in overcoming problems related to the slow electron transfer exhibited by many electroactive species. It has also expanded the usable potential range compared to that of unmodified surfaces. New electrode surfaces have extended the usefulness of electrochemical methods considerably and resulted in new applications as presented earlier in this review.

Of the three methods discussed to modify electrode

surfaces, attachment via an organosilane is the most popular approach. Such popularity is clearly reflected in the number of publications which have appeared on the subject compared to those dealing with cyanuric chloride or ester linkage. Table 9 shows a general comparison between the three attachment methods.

Among the many available organosilanes, 3-aminopropyltriethoxysilane and 3-(2-aminoethylamino)propyltrimethoxysilane appear to be the most useful reagents. Both reagents have been successfully bound to many electrode surfaces.

The modified surfaces are usually characterized by electrochemical and spectroscopic methods. The former can detect small quantities of the modifying species, while the latter offer information about the structure of the modifying layer. Cyclic voltammetry is the most popular electrochemical tool for such characterization. ESCA is the most widely used spectroscopic technique for the study of the modified surfaces. A general comparison between the electrochemical methods and the spectroscopic methods is presented in table 10.

Considering the fact that surface modification can be carried out easily on a variety of electrode materials using a vast number of chemical species, the use of modified electrodes should be extended to other research areas. It seems that chemically modified electrodes are promising analytical tools that can be used as sensors in flow systems

TABLE IX

COMPARISION OF THE THREE MODIFICATION ROUTES

	Ester Linkage	Cyanuric Chloride	Organosilane
Ease of the modification process	Can be conducted easily	Comparable to attachment via organosilane but more difficult than ester linkage	Similar to cyanuric chloride
Stability of the modifier on the surface	Poor	Good	Very good
Reported surface coverage	Very low	Fair	High
Attachment on different electrode surfaces	Good	Good	Excellent
Typical applications	Photosensitization Preconcentration Electrochemical synthesis	Catalysis	Catalysis Photosensitization
Approximate number of reports on the method	<10	<10	>25

TABLE X

COMPARISION OF ELECTROCHEMICAL AND SPECTROSCOPIC METHODS

USED FOR THE CHARACTERIZATION OF MODIFIED SURFACES

	Electrochemical Methods	Spectroscopic Methods
Potential applications	Determination of surface coverage	Provide information about the surface molecular structure
Detection limits	Chemical species that can be oxidized or reduced will be detected on the modified surfaces easly and at very low detection limit	Quantitative information may become available but at limits usually higher than that approached by electrochemical methods
Data handling and treatment	Data available through the voltammograms are easy to handle and does not need correction (except for background)	Data are hard to handle (usually computer used) and need to be corrected
Simplicity of the instruments	Electrochemical instruments are generally easy to operate and cheaper to maintain with less technical skill	Use highly advanced instruments, hard to maintain, and must be handled by skilled personal

such as high performance liquid chromatography (HPLC) and flow injection analysis. However, there are still many uncertainties in the techniques of chemical modification of electrodes that must be investigated before the full potential of the modified surfaces can be relized. Areas that need to be investigated include: (a) orientation of the modifier species with respect to the electrode surfaces, (b) the in sites structure of the modifier or the mediator, (c) factors disturbing the ideality of redox behavior of the modifier, and (d) enhancement of the catalytic behavior of the modified surfaces.

Modifier-Containing Carbon Paste Electrodes

In addition to covalent attachment, graphite paste electrodes can be modified by physical incorporation of the modifier into the electrode body. This procedure is called admixing. Ease of preparation and the flexibility in loading the electrode with the desired percentage of the modifier are the main advantages of admixing. The dissolution (leaching) of the modifier in the supporting electrolyte is the main shortcoming of this approach.

Modification of carbon paste electrodes by admixing is a simple and straightforward procedure. It usually involves mixing the desired weight of the modifier with graphite powder. A volatile liquid such as ether is added to the mixture to form a slurry. The mixture is then placed in an ultrasonic bath to evaporate the liquid and compact the residue. The pasting liquid is finally added to the dry graphite-modifier mixture. Hand mixing with the aid of mortar and pestle is used to bring the mixture to its final pasty form. This procedure was first reported by Check and Nelson (119) to modify graphite paste electrodes with organosilane, Z-6020. The organosilane contained ethylenediamine groups. The ethylenediamine was used as complexing agent for metal ions prior to voltammogramic determination. Currently the procedure above has been popularized by Baldwin and his co-workers to modify graphite paste electrodes with N,N,N',N'-tetramethyl-p-phenylenediamine (TMPD) (120) cobalt phthalocyanine (CoPC)

(121), and dimethylglyoxime (122).

Takeuchi and Murray (123) made their modified electrodes by dissolving the modifiers, iron and manganese tetraphenylporphyrin chlorides, in 1-nonanol. The nonanol solution then served as a pasting liquid.

Kutner et al. (124) loaded microparticle beads of a strong cation exchanger, Dowex 50Wx8, with an electrooxidant reagent, [Ru(II)(2,2',2"--terpyridine)(1,10-phenanthroline)(OH)]$^{+}$. The modified beads were incorporated into a classical carbon paste electrode.

Yao and Musha (125) modified graphite paste electrodes indirectly with nicotinamide adenine dinucleotide (NAD^{+}). Their procedure involved binding the coenzyme (NAD^{+}) to n-octanal. The coenzyme-octanal complex was physically incorporated into the paste electrode.

Carbon paste electrode modified by admixing found its application in the area of catalysis. Such modified graphite could be used to monitor species under flow and static conditions. Some of these species, as will be indicated later, have never been detected on plane graphite paste electrodes.

Electrodes modified with TMPD were used by Ravichandran and Baldwin (120) to catalyze the electrooxidation of ascorbic acid and nicotinamide. Cyclic voltammetry measurements showed enhanced quality of the oxidation peaks of the species monitored. The reproducibility of these measurements were within 5-10%. This points to the

possibility that the modifier was not uniformly mixed with electrode materials. Whether TMPD behaves purely as a catalyst is questionable. The authors indicated that the enhancement in voltammogramic peaks increased as the percentage of the modifier increased in the paste electrodes. This observation invites the assumption that the modifier behaves as a catalyst and may enhance the wettability of the paste electrodes. Thus is expected to make the redox species in the cell more accessible for the electron transfer process and hence to increase the current due to the oxidation process. Halbert and Baldwin (137) used electrodes modified by admixing of CoPC as sensing electrodes in amperometric detection following chromatographic separation. These electrodes catalyzed the electrooxidation of sulfhydryl-containing compounds such as glutathione, cysteine, homocysteine, and N-acetylcysteine. Similar electrodes used recently by Santos and Baldwin (121) for the determination of many carbohydrates in flow system. While plain paste electrode did not show any response to the carbohydrates, it was possible with modified ones to detect small injected quantities (in the range of 100-500 pmole) of glucose, maltose, fructose, and sucrose. These limits of detection are comparable to those reported with platinum and gold electrodes. The selectivity of the modified paste electrode, however, is better than that of metallic electrodes.

Check and Nelson (119) used their modified graphite

paste electrodes for the preconcentration of trace amounts of silver ions prior to voltammogramic determination. Silver ion concentrations as low as 10^{-9} M were easily determined. Similar approach was followed by Baldwin et al. (122) to preconcentrate nickel ions on paste electrode surfaces.

Electrodes modified with NAD^+ was used in the enzymatic oxidation of ethanol and L-lactic acid by their respective dehydrogenases. The NAD^+ was used as a coenzyme to consume protons generated during the oxidation process. The coenzyme regained its oxidized form by electrochemical oxidation. The oxidation current was found to be linearly related to the amount of substrate in the system (125).

Ravichandran and Baldwin (126) claimed that paste electrodes modified with phenanthreqinone catalyzed the electrooxidation of ascorbic acid and NADH. The catalytic behavior of the modified electrodes, however, was not clearly visible in the experimental results provided.

Paste electrodes loaded with modified micro-beads bearing ruthinum complex were used for the electrocatalytic oxidation of benzyl alcohol (124).

It seems from the above discussion that admixing is a proper way to modify graphite paste electrodes. To bring these electrodes to a higher level of utility several difficulties must be surmounted. In addition to the paste electrode problems discussed in chapter 1, the following problems need to be solved:

1. The dissolution of the modifier in the cell solution needs to be minimized (ideally the dissolution will be prevented completely).

2. Reproducibility of results reported for the modified electrodes is poor compared to electrodes modified by other techniques.

It should be noticed that the first problem is related to the nature of the modifier used and possibly can be minimized by using other forms or derivatives of the modifier.

The reproducibility problem is more difficult and its solution required overcoming several difficulties at the same time. The dissolution of the modifier is one of the problems. Nonuniform distribution of the modifier among the electrode materials and the consumption of the modifier by the electrooxidation process are also troublesome. Recently Santos and Baldwin (121) indicated that electrochemical treatment after each voltammogramic measurements restored the reactivity of some modified electrodes.

CHAPTER V

CHEMICAL MODIFICATION OF GRAPHITE ELECTRODES WITH FERROIN

This chapter describes two procedures followed in modifying graphite surfaces. The first method is based on attaching the modifier covalently to the graphite surfaces. The second method uses incorporation of the modifier in the electrode bodies. Methods used to characterize the modified surfaces are also discussed.

Experimental

Reagents and chemicals

The graphite used in this work was obtained from two sources, UCP-1-M from Ultra Carbon (Bay City, MI) and graphite powder grade #38 from Fisher Scientific (Fair Lawn, NJ). The binding agents were light mineral oil from Sargent-Welch (Skokie, Ill) and hexadecane from Aldrich Chemical Company (Milwaukee, WI). These two viscous organic liquids were used to prepare the graphite paste electrodes. Paraseal wax from W. & F. MFG. Company (Buffalo, NY) was used to prepare the wax-graphite electrodes. Oxidized polyethylene) was obtained from Aldrich Chemical Company, Inc. (Milwaukee, WI). Stearic

acid was obtained from Fisher Scientific Comp. (Fair Lawn, NJ). Potassium chloride used for IR measurements was obtained from Aldrich Chemical Company, Inc. All other chemicals are the same as those reported in chapters two and three.

Preparation of the Electrodes

Carbon paste electrodes were prepared by a procedure detailed in Chapter III. Wax-graphite electrodes were fabricated by melting the required amount of wax with the aid of a hot plate or a low-temperature oven. The required amount of graphite was added to the melted wax in a small beaker (50 mL). The materials were mixed very well while the wax was still in the liquid form. A spatula covered with Teflon was used for mixing. The mixing process took 15-30 min.. At room temperature the mixture solidified and preheating was required prior to loading of the material in the electrode holder shown in Fig. 14.

Modification of Graphite Surfaces by Chemical Attachment

The Attachment of the 5-amino-1,10-phenanthroline or the 5-amino derivative of ferroin to graphite surface was conducted according to the following procedural steps:

Oxidation of Graphite Surfaces. Experimental results by other workers (120,121) revealed the presence of a variety of oxygen-containing groups on the graphite

surfaces. These functionalities include hydroxyl, carboxyl, aldehydes, ketones, or quinones. The amounts of these functional groups depend on the source of the graphite and the kind of treatments it is exposed to. It is reported also that most of these functions can be converted to carboxylic acid groups by further oxidation (122,123). Classical oxidizing reagents such as potassium permanganate are expected to work well for this purpose. Experimental results (124), however, indicated that contamination of the graphite surfaces by the oxidizing reagents have limited their usage. To avoid the contamination problem we have used two other means of oxidation.

Using oxygen as oxidizing agent. Formation of carboxylic acid groups on the graphite surfaces by reacting with oxygen is expected to proceed as follows (125)

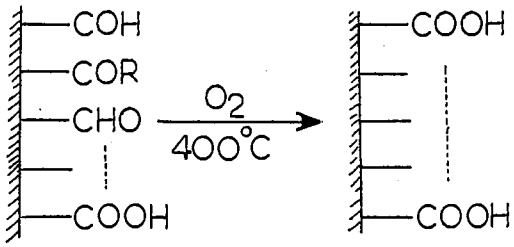

(43)

To achieve this, the graphite powder was heated in a tube furnace at 400 °C. Oxygen was allowed to flow over the heated graphite for 12 h. The oxidized graphite was stored in a desiccator for further modifications.

Using a mixture of concentrated sulfuric and nitric acid as oxidizing agent. The oxidation process was carried out using a procedure described by Cheek and Nelson (119). Graphite powder (10.0 g) was heated, in a hood, for 10 h in a mixture of 250 mL of concentrated H_2SO_4 and 250 mL of concentrated HNO_3. A double condenser apparatus was used to minimize the evolution of NO_2. After the refluxing period, the reaction vessel was cooled down in an ice bath. Cold distilled water (1 L) was then used to dilute the cold mixture in the vessel. The resulting acidic solution was filtered using a simple filtration apparatus. The graphite was washed continuously with distilled water until the washing water was free from acid. To insure complete removal of the acid, the graphite was washed further with 2.0 L of distilled water. The water content of the graphite was minimized by washing with 100 mL of ethanol and air drying for 30 min. Complete dryness was accomplished by leaving the graphite overnight at 90°C in an oven.

Formation of the Acid Chloride Functionalities. The same oxidized graphite (3 g) was heated in a 25% solution of thionyl chloride in sodium-dried benzene (5.0 mL of $SOCl_2$ and 15.0 mL of benzene). Evolution of hydrogen chloride was an indication of reaction between thionyl chloride and the acidic groups on the graphite surface. The reaction was expected to change the carboxylic acid groups into chloride groups according to the following scheme:

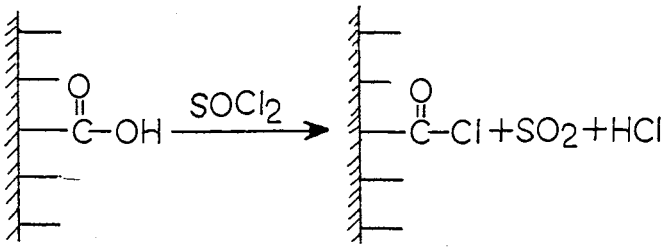

(44)

One of the evolved acidic gases, HCl, was trapped in a flask containing a solution of silver nitrate. The evolution of this gas stopped after about 15 min. indicating completion of the reaction. The mixture, however, was kept hot for another 15 min to insure completion. Dry nitrogen was allowed to flow over the reacting species to prevent any moisture from reaching the reaction vessel. Figure 30 shows the equipment set up used to carry out the reaction.

The excess of thionyl chloride and benzene was removed by aspirating with a water aspirator. A cold trapping flask was used to prevent water from flowing back to the reaction vessel and to collect the thionyl chloride and benzene at the same time. The graphite was dried further by using a vacuum pump. The thionyl chloride was prevented from reaching the vacuum pump by a trapping flask cooled with dry ice. After drying, nitrogen was allowed to flow in the system and to fill the flask containing the graphite.

Attachment of 5-Amino-1,10-phenanthroline and Tris(5-amino-1,10-phenanthroline)Iron(II). The 5-amino-1,10-phenanthroline was attached to the graphite surfaces as free ligand in one case (a) and as a complex with iron(II) in another case (b). These two attachment approaches were

accomplished by the following procedures.

a. Two grams of the modified graphite bearing acid chloride groups was allowed to react with 50 mL of dimethylformamide (DMF, HPLC grade) solution containing 0.500 g of 5-amino-1,10-phenanthroline. The equipment used was similar to that of Fig. 30. The completion of the reaction, again, was indicated by the cessation of HCl evolution according to the following scheme:

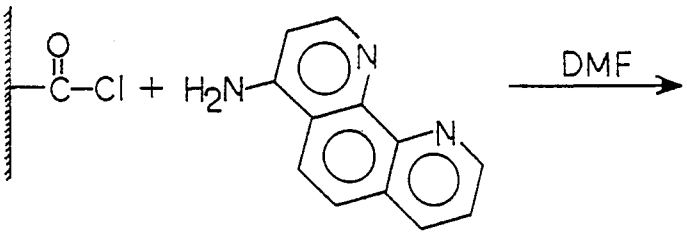

(45)

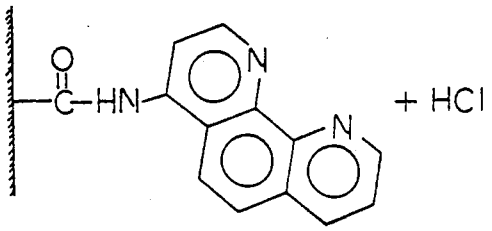

The DMF and excess 5-amino-1,10-phenanthroline were removed by filtration. The graphite was then washed first with petroleum ether to remove the DMF and then with ethanol to remove the petroleum ether and any unreacted amino compound. Distilled water was finally used to wash the graphite. After air drying, the graphite was allowed to react with 25 mL aqueous solution of iron(II) chloride (0.030 M) for 30 min. The iron(II) is expected to be complexed by one, two, or three immobilized ligands. The stability of the

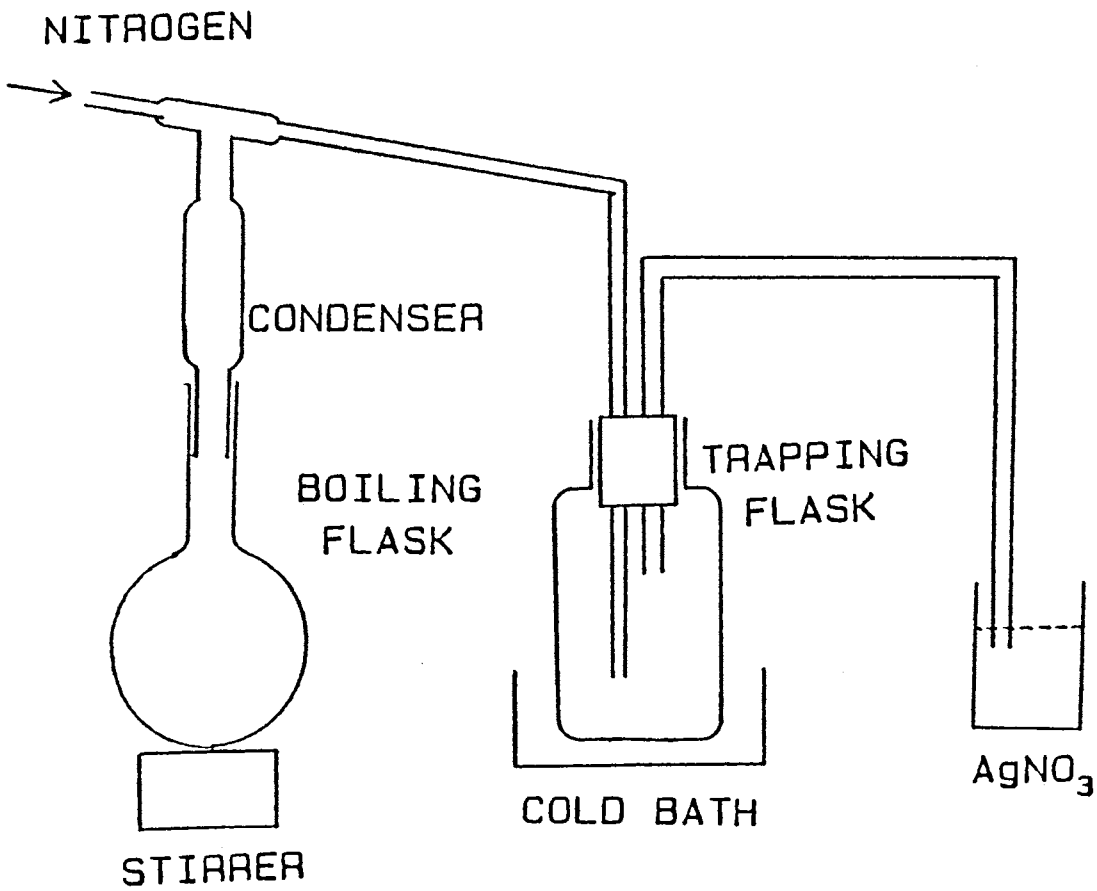

Figure 30. Experimental set-up used for the modification of graphite surfaces by covalent attachment of 5-amino-1,10-phenanthroline and tris(5-amino-1,10-phenanthroline)iron(II).

first two complexes is not known and presumed to be very low in solution. As will be discussed later only one peak appeared when the electrodes were examined electrochemically. This suggests that only one complex can form, probably the last one mentioned. The stability of the complex, however, will not be as high as that reported for the iron(II) and the ligand in solution. The instability of the complex may be related to the fact that the attached ligands will not be able to orient themselves freely to form a spherical shape of the complex. To remove such strain, 25 mL of an ethanolic solution of 1,10-phenanthroline (0.060 M) was added to the modified graphite. such addition will reform the complex in such a way that two 1,10-phenanthroline units from the solution and one unit from those on the surface of the electrode will be used. The iron(II) and the 1,10-phenanthroline that had not reacted with the graphite were removed as free reagent or as ferroin by washing with distilled water.

b. Another batch of graphite from step 2 was heated with a solution of the 5-aminoderivative of ferroin (the complex of iron and three 5-amino-1,10-phenanthroline groups). The complex solution was prepared by dissolving 0.025 mole of iron(II) chloride in 350 mL distilled water and adding 0.075 mole of 5-amino-1,10-phenanthroline. The required amount of ethanol (about 650 mL) was added to the solution and the volume completed to the mark in a 1.0-L volumetric flask. A red solution was obtained, which is the typical

color of ferroin and its derivatives. The ethanol/water mixture was dried out and the precipitate was dissolved in 500 mL of DMF. A 100-mL portion of this solution was then allowed to react with the graphite. The reaction is expected to follow equation 45 except that the complex is used rather than the free ligand. Completion of the reaction was again considered when evolution of HCL(g) ceased from the reaction vessel as described earlier.

Modification of Graphite Surfaces by Admixing

This approach involves mixing the modifying species physically with the electrode materials. To achieve homogeneous mixing, the modifying species (ferroin), in its perchlorate form, was dissolved in a small amount of absolute ethanol. The graphite powder was then added to the ethanolic solution and mixing was carried out in an ultrasonic bath. The ethanol was evaporated during this step and the ferroin was assumed to be uniformly distributed among the graphite grains. The final electrode material was obtained by mixing the graphite-ferroin mixture with the conventional pasting liquid or with melted wax.

Characterization of the Modified Surfaces

It is of interest to evaluate the success of the modification process. Since the attachment of the modifier to the graphite surfaces involved many experimental steps, surface examination was carried out after each treatment

step. Two methods were employed for the characterization purposes, spectroscopic and electrochemical.

Spectroscopic Methods

Graphite from experimental step 1 was examined by infrared absorption spectroscopy (IR). The IR pellet was prepared by mixing the oxidized graphite with KBr. Ratios of the graphite to the KBr was varied between 10-20%. Higher ratios of graphite resulted in a very dark pellet which can not be used for IR measurements as the transmittance dropped to less than 10%. Ratios less than 20% resulted in about 40% transmittance. Bands due to carboxylic acid groups, however, were not positively identified.

The same graphite was examined by FTIR (Fourier Transform Infrared) spectroscopy. Again, the results did not indicate of the presence of carboxylic acid groups.

IR spectroscopy was also used in an attempt to characterize graphite surfaces modified by attachment of ferroin. Peaks due to the carboxamide linkage were not identified, however. At this point it was determined that the spectroscopic methods employed lacked sensitivity enough to distinguish between modified and unmodified surfaces.

Electrochemical Methods

Electrochemical methods are more sensitive to show changes on the graphite surfaces. The surfaces were

characterized after each modification step. Cyclic voltammetry and square wave voltammetry were used for these characterization purposes.

Graphite paste electrodes prepared using both types of untreated graphite powders were first evaluated. UCP-1-M graphite electrodes did not show any detectable peak in the potential region examined between -0.200 V and 1.100 V vs. SCE when 1.00 M KCl was used as supporting electrolyte. Examination of electrodes prepared from untreated graphite powder #38 by cyclic voltammetry showed two well-defined peaks around 0.5 V vs. SCE. These two peaks were attributed to the presence of iron as a contaminating species in the graphite. The intensity of the peaks increased as the pH of the supporting electrolyte decreased. This observation suggests that the acid dissolved some iron to form iron(II) which can be detected electrochemically. These observations suggested that graphite powder #38 must be freed from iron before further usage.

Graphite (10.0 g) was washed with 500 mL of warm solution of concentrated hydrochloric acid (50% v/v) for 2 h. The washing process was carried out in a boiling flask equipped with two condensers to minimize the evolution of HCl gas. Gentle heating was applied during the washing period. The color of the solution changed from colorless to yellow. After the 2 h, the solution was cooled down and diluted further with 1.0 L of distilled water. The acidic solution was filtered and the graphite rinsed continuously

with distilled water for about 1 h. The washing step was repeated with the same amount of acid and continued overnight with gentle heating. The color of the solution changed only very slightly. The washing step was again followed by filtration and rinsing with distilled water.

Paste electrodes made from the washed graphite did not show any redox peaks in the potential region examined. It was assumed that the metal content of the graphite was below the sensitivity of the instrument.

Paste electrodes prepared after treating the graphite with oxygen as usual were examined by cyclic voltammetry. The voltammogram did not show any redox peaks. The oxygen treatment, however, increased the level of the background current significantly. Similar results were obtained for paste electrodes prepared after experimental steps 2 (after treatment with $SOCl_2$). The increase in background current may be attributed to the enhanced wettability of the surfaces.

Electrodes prepared from graphite bearing -COCl groups by treatment with 5-amino-1,10-phenanthroline showed a small redox peak around 0.95 V vs. SCE. The appearance of this peak was not expected since the amino compound without the presence of iron is not active electrochemically in that region. Because a Teflon-coated magnetic bar was used to stir the solution during steps 2 and 3, it was suspected that the stirrer was the source of the iron. It seemed likely that iron leached out of the bar and reacted with

1,10-phenanthroline on the surface of the graphite. The color of the magnetic bar also changed to a red-brown after treatment with 1,10-phenanthroline. This observation supported the assumption made regarding the source of iron. This problem was completely eliminated by replacing the Teflon-coated magnetic bar with a glass coated one.

Electrodes modified with 5-amino-1,10-phenanthroline showed two peaks when a small amount of iron(II) chloride was added to the cell. The first peak was related to the free iron(II) in the system since it appeared around 0.5 V vs. SCE. The second peak appeared around 0.9 V vs. SCE and was related to the complex of the added iron(II) with the 5-amino-1,10-phenanthroline immobilized on the electrode. The intensity of the peaks increased significantly when the electrode was exposed to a 0.1% (w/v) surfactant solution for 15 min before the characterization. The effect of surfactant on electrode surfaces is discussed in Chapter III. Figure 31 shows the two peaks after the surfactant treatment. The appearance of the peak around 0.9 V suggests the presence of tris(5-amino-1,10-phenanthroline)iron(II) on the surface. Graphite electrodes prepared after completing steps 3a and 3b showed a small redox peak at around 0.95 V vs. SCE. These peaks were ill-defined, as they appeared on the shoulder of a high-intensity background peak around 1.05 V. The background current was minimized significantly by replacing the 1.00 M KCl supporting electrolyte with a 0.50 M $NaClO_4$ solution. The redox peaks were better identified

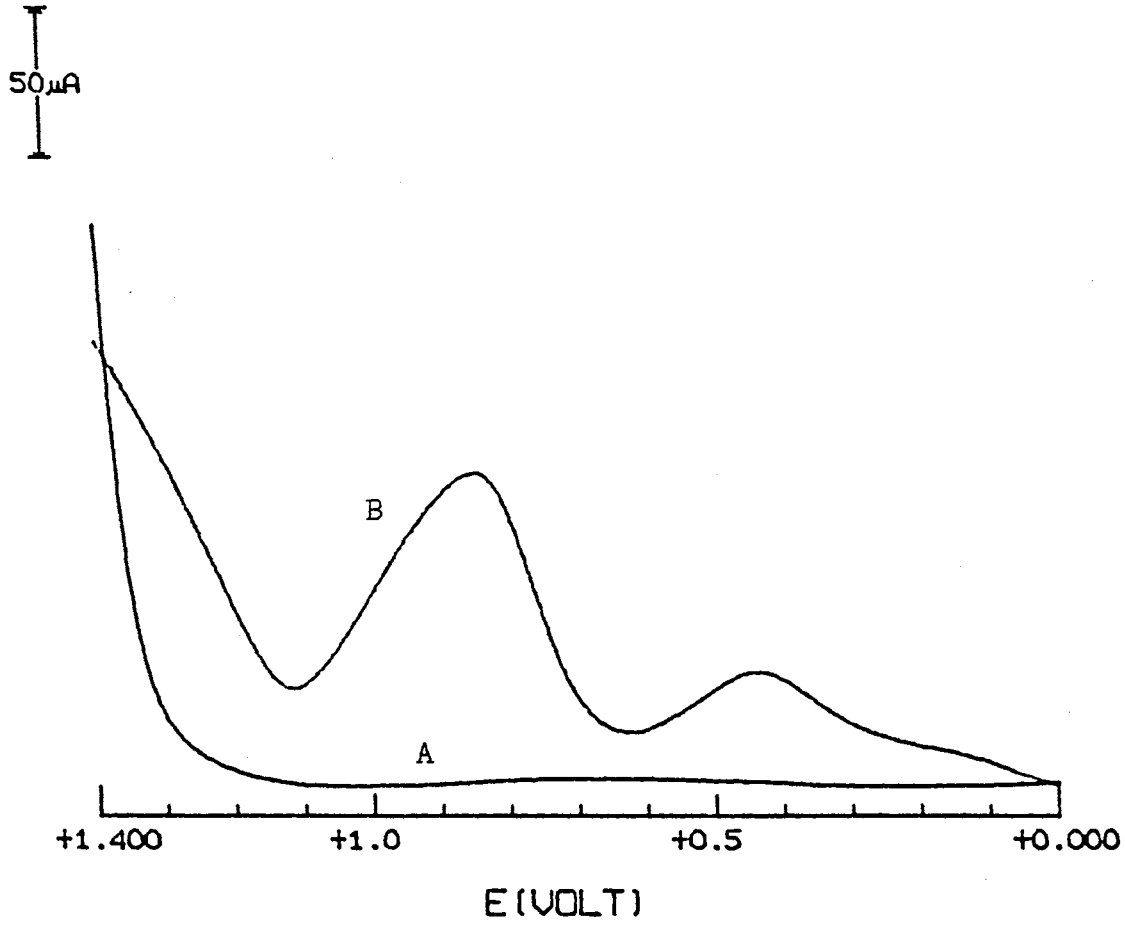

Figure 31. Voltammogramic behavior of graphite electrode modified by attachment of 5-amino-1,10-phenanthroline; (A) in solution of 1.00 M KCl, (B) after the addition of a small amount of iron(II) chloride.

by using square wave voltammetry than by cyclic Voltammetry. Figure 32 shows a typical voltammogram for the modified surfaces.

It was of practical importance to insure that the redox peaks observed were due to the tris(5-amino-1,10-phenanthroline)iron(II) covalently attached to the surface and not to simple adsorption. Graphite obtained after step 1 was treated with a boiling solution of tris(5-amino-1,10-phenanthroline)iron(II) in DMF. The experimental condition were similar to those described for step 3b. Paste electrodes made of this graphite did not show any redox peaks at about 0.95 V. This suggests that the peak appearing on Figure 32 is due to the ferroin derivative attached covalently to the surface, and not by simple adsorption.

Another verification approach was considered. Graphite generated by step 2 (reaction with $SOCl_2$) was heated in boiling aqueous iron(II) chloride solution (0.03 M) for 30 min. After treatment, the iron solution was removed by decantation and the graphite washed thoroughly with distilled-deionized water. Again, no signal was observed when the graphite was examined by cyclic voltammetry or square wave voltammetry. These observations indicate that the peak that appeared in Figure 32 was due to tris(5-mino-1,10-phenanthroline)iron(II) attached chemically to the graphite surfaces.

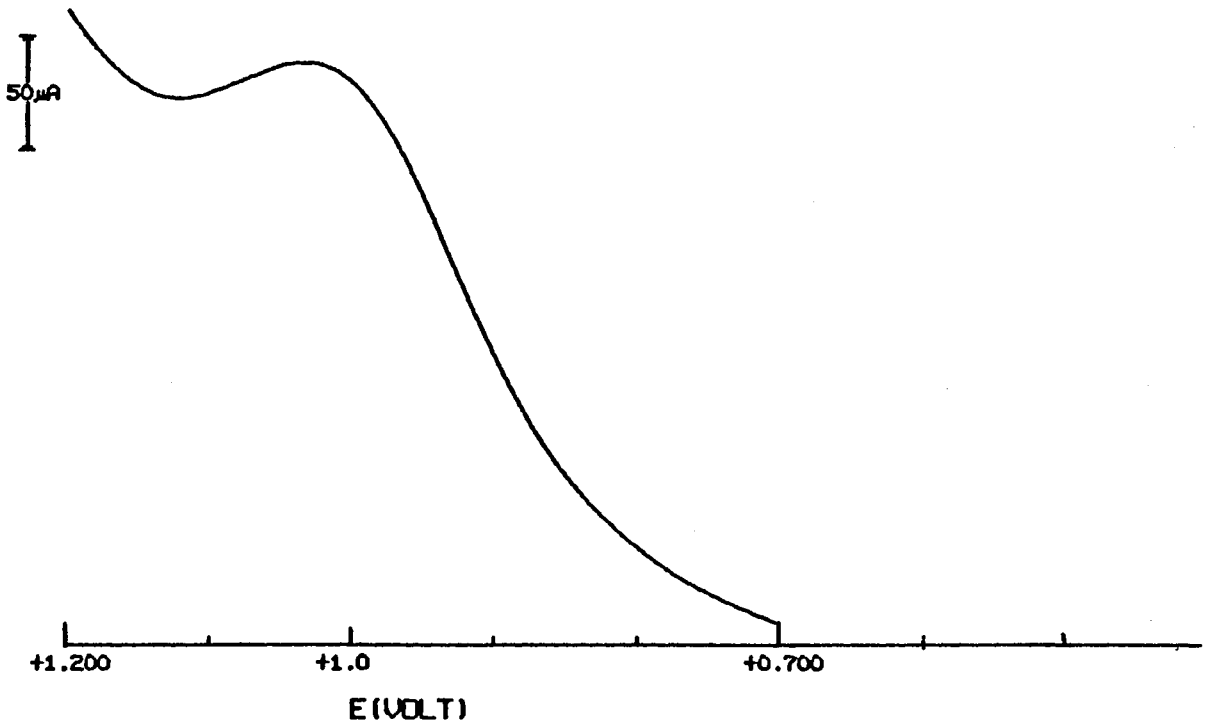

Figure 32. Osteryoung square wave voltammetric wave for the oxidation of iron(II) to iron(III) on surfaces modified by covalent attachment of tris(5-amino-1,10-phenanthroline)iron(II). Supporting electrolyte 0.50 M $NaClO_4$; initial potential +0.700 V; square wave amplitude: 25 mV; pulse frequency: 15 Hz; potential step: 4 mV.

Stability of the Modified Surfaces

The intensity of peaks due to tris(5-amino-1,10-phenanthroline)iron(II) immobilized on graphite surfaces was observed to decay after a period of 4-6 h when the electrode was continuously exposed to cyclic voltammetry scans. Such observation points to the weakness of the bond between the graphite and the modifier. It was natural to ask whether the graphite or the ferroin is contributing more to the weakness of the bond.

As has been discussed in Chapter IV, a significant number of reports indicate the success of attaching many amino compounds to graphite surfaces using procedural steps similar to those reported here. Also, it has been reported that these electrodes showed good stability (133,134). With these facts in hand, one can eliminate the possibility that the weakness of the bond is due to the usage of graphite. It seems that the modifier, tris(5-amino-1,10-phenanthroline)iron(II), is the principal contributor to the weakness of the attachment. This was further clarified when attempts were made to attach the tris(5-amino-1,10-phenanthroline)iron(II) to surfaces other than graphite. Two surfaces were selected for this purpose, oxidized polyethylene and stearic acid. The attachment steps followed were similar to those discussed here to modify graphite surfaces.

Electrodes prepared by mixing the modified polyethylene or the modified stearic acid with the electrode material did

show the redox peaks for ferroin when examined electrochemically. The intensity of the observed peaks, however, decayed in a manner similar to that observed with modified graphite. The exact factor behind the weakness of the bond is not known at present. It could be related, however, to the fact that the complex is a bulky spherical species.

Modification of Paste Electrodes via Physical Incorporating of Perchlorate Salt of Ferroin

The objective of the work reported in this chapter is to define a procedure that makes the modifier available on the electrode surfaces. In addition to modification by covalent attachment, modification by admixing is considered here. Electrode modification by admixing is not the ultimate replacement to covalent attachment, as discussed earlier. It is, however, a strong competitor to covalent attachment when stability is a problem with the latter.

Paste electrodes containing 5% (w/w) of the admixed ferroin showed well-defined redox peaks when examined by cyclic voltammetry. Figure 33 shows cyclic voltammograms for a conventional paste electrode containing 5% (w/w) ferroin. The relative rate of dissolution of the modifier was reduced appreciably by replacing the sulfate of ferroin (commonly used) by the perchlorate. The dissolution was further minimized by using 0.50 M $NaClO_4$ as a supporting electrolyte instead of 1.00 M KCl.

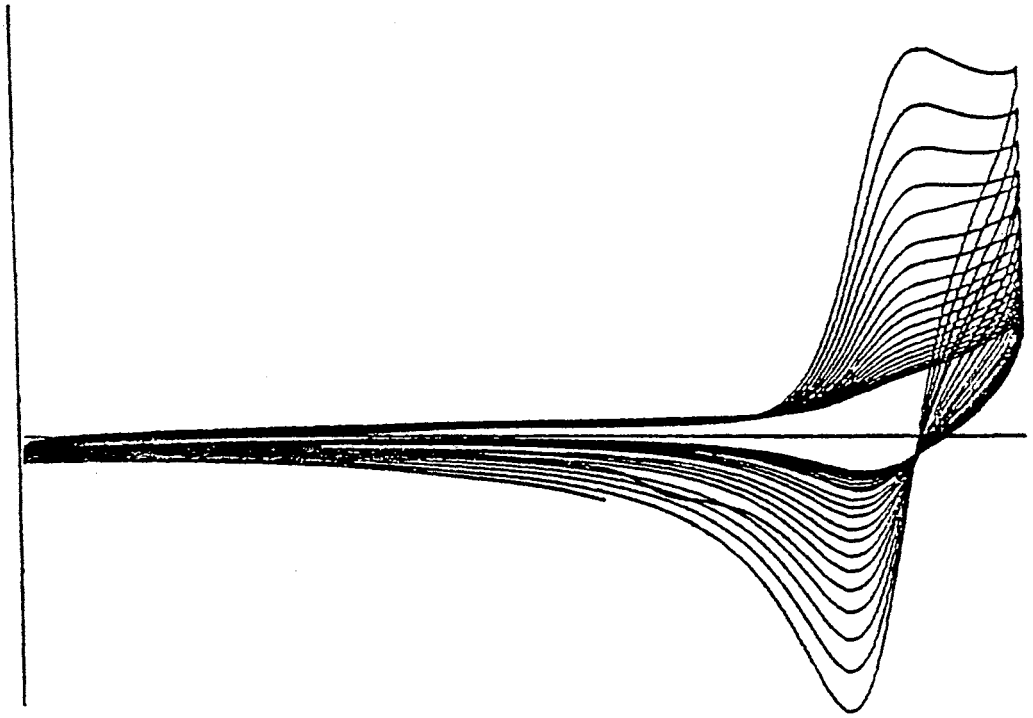

Figure 33. Cyclic voltammogram of 5% (w/w) ferroin incorporated in graphite paste electrode; supporting electrolyte was 1.00 M KCl/1.0 M H_2SO_4/0.02 N NaClO4; scan rate was 39 $mV.s^{-1}$.

A significant stabilization was effected by replacing the organic pasting liquid with a high molecular weight wax. These electrodes are not popular and are mentioned in the literature only a few times (131,132); moreover, critical evaluation of these is not reported. The remaining sections of this chapter are devoted to the characterization of these electrodes. The behavior of wax-modified electrodes is compared to that of classical paste electrode also.

Characterization of Wax-Graphite Electrodes

Wax-based graphite electrodes are interesting because they combine the advantages of classical paste graphite electrodes and another class of electrodes called wax-impregnated graphite. The latter is prepared by impregnating the pores of spectroscopic graphite rods with a high molecular weight wax. Table 11 summarizes the advantages of wax-graphite electrodes, and their drawbacks. The same problem was reported for both graphite paste electrodes and wax-impregnated graphite electrodes. The slowness of the electrode reactions limits the quality and the quantity of information available through voltammetric measurements. This information includes peak potentials, peak currents, and separation between peaks.

The electron transfer process can be enhanced drastically by pretreating the electrodes electrochemically before using them in voltammetric measurements. The electrochemical treatment is simple and makes use of

TABLE XI

ADVANTAGES AND DISADVANTAGES OF WAX-GRAPHITE ELECTRODES

Advantages

1. Very inexpensive.
2. Easy to prepare, replace, and shape.
3. Surface renewability can be achieved easly.
4. Exhibit very low residual current.
5. Display sufficient mechanical strength.
6. Can be used in aqueous and nonaqueous solutions.

Disadvantages

Electrode reaction are generally slower than at metallic or glassy carbon electrodes.

an instrumental technique called "STEP" directly available on the BAS-100 instrument used in this work. The STEP method involves applying a potential pulse of predetermined value followed by a rest period in which the potential of the electrode drops to a level where electrolysis is not expected to take place. The total time for the pulse and the rest period is called a cycle. Figure 34 shows a typical potential cycle. Table 12 lists the experimental parameters used in the STEP method.

The exact mechanism by which the potential pulse affects the electrode surface is not known. Its effect, however, is clearly seen visually and electrochemically. Visually, the electrode loses its mirror shiny surface observed after the surface smoothing process. Electrochemically, the uncompensated cell resistance, which is attributed to the electrode surface in these experiments, drops noticeably. Redox peaks observed with electrochemically treated surfaces show more informative voltammograms (compare Fig. 35a and 35f). The level of enhancement can be increased by increasing the number of cycles applied or increasing the pulse potential. Increasing the pulse potential above 1.600 V vs. SCE, however, resulted in very vigorous reactions on the surfaces of the working and the counter electrodes. Gas bubbles were generated by these reactions. It is expected that the gas generated on the working electrode surface is oxygen as the following net reaction takes place:

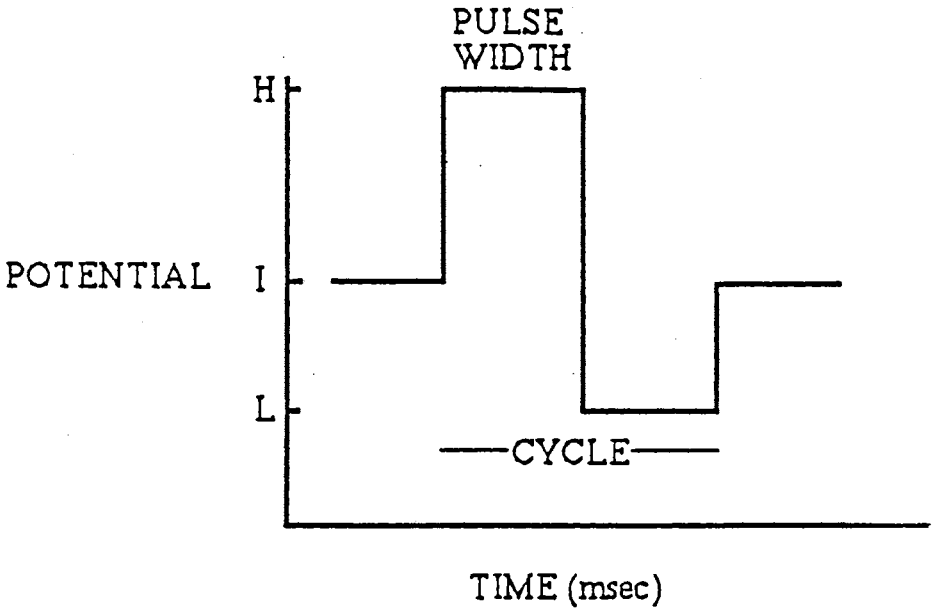

Figure 34. Typical potential cycle used for the electrochemical treatment. H: high potential; I: initial potential; L: low potential.

TABLE XII

EXPERIMENTAL PARAMETERS USED FOR STEP EXPERIMENT

Parameter	Value
Initial Potential	: 0.00 V[a]
High Potential	: 1.200 V
Low Potential	: -0.200 V
Initial Scan Direction	: Negative
Pulse Width	: 6 x 10^4 ms
Cycle Time	: Varied between 1 and 25

[a] Potential measured vs. Saturated Calomel Electrode.

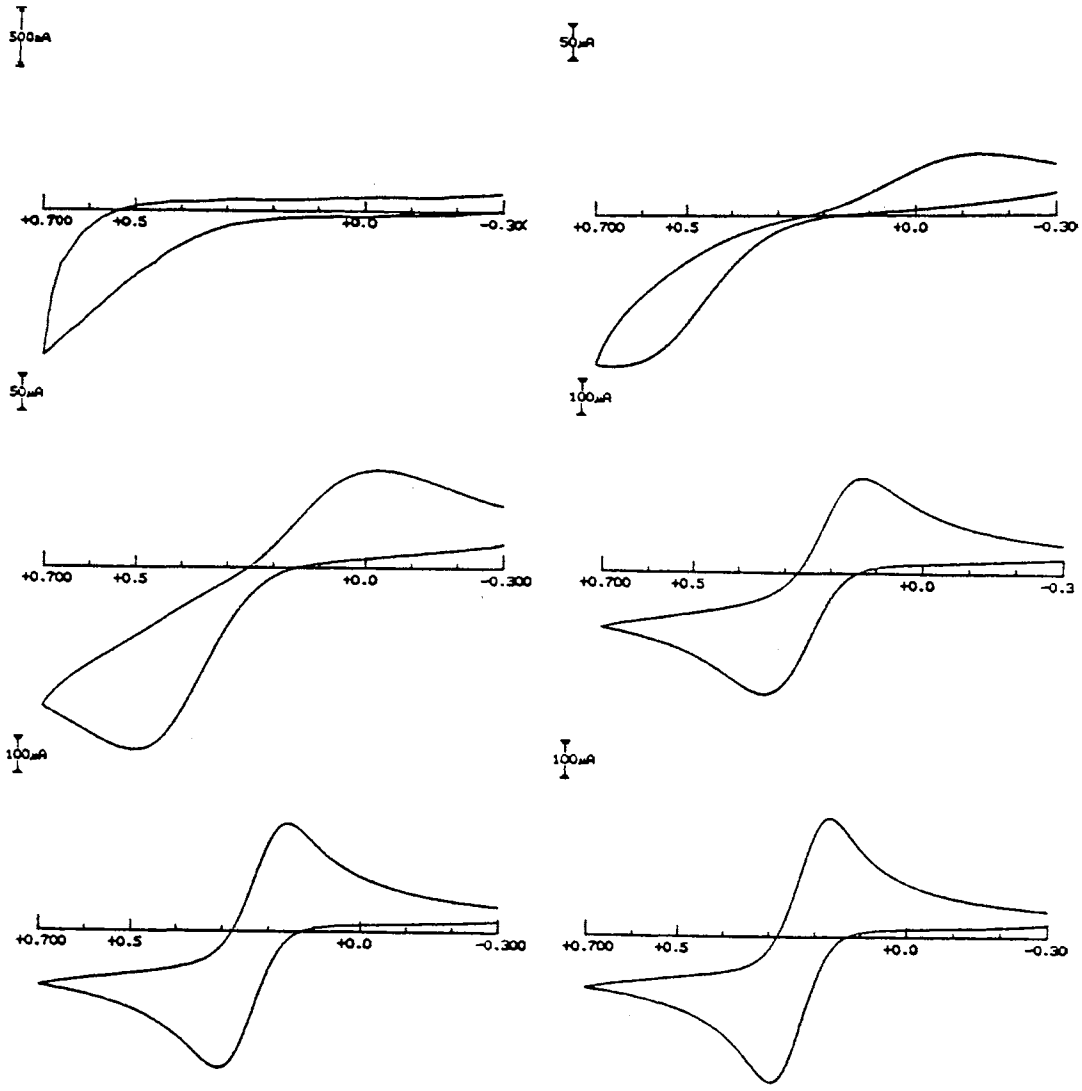

Figure 35. Effect of increasing the number of potential cycles in the STEP experiment on the cyclic voltammograms of 10 mM $K_4Fe(CN)_6$ in 1.00 M KCl. Potential scan rate 100 $mV.s^{-1}$. Scan initiated on the positive direction. (A) No treatment, (B) after one cycle, (C) after three cycles, (D) after five cycles, (E) after ten cycles, (F) after twenty five cycles.

$$2H_2O \longrightarrow O_2 + 4H^+ + 4e^- \qquad (46)$$

Protons thus generated in the solution are converted to hydrogen gas on the surface of the counter electrode:

$$2H^+ + 2e^- \longrightarrow H_2 \qquad (47)$$

The effects of increasing the number of cycles on the uncompensated cell resistance, the peak potentials, and peak currents are summarized in Table 13. The effects of number of cycles on the shape of the voltammograms are shown on Figure 35. As can be seen from the Figure, untreated surfaces did not show any redox peaks when tested in 4.0 mM $K_4Fe(CN)_6$/1.00 M KCl. The peaks start to develop, however, after the first cycle. Increasing the number of cycles to 3, 5, 10, and 25 brought a gradual enhancement in the appearance of the cyclic voltammogram. Electrodes treated electrochemically did not lose their acquired characteristics with time. Electrodes tested 12 h after the electrochemical treatment showed results similar to those tested directly after the electrochemical treatments. Wax-graphite electrodes modified with ferroin by admixing did not require the electrochemical treatment. It seems that incorporating the ferroin in the electrodes had enhanced their wettability and reduced the uncompensated resistance of the cell.

Wax-graphite electrodes are also reported to lose their performance with time (135). This problem is common for wax-impregnated graphite electrodes. No detailed

TABLE XIII

EFFECTS OF ELECTROCHEMICAL TREATMENT ON WAX-GRAPHITE ELECTRODE BEHAVIOR

No. of Cycles	ΔE_p, mV	Cell Resistance, ohm	Anodic Current, A x 10^4	Cathodic Current, A x 10^4
1	546 ± 25	TOO HIGH TO MEASURE	-2.200	1.599
5	256 ± 16	TOO HIGH TO MEASURE	-2.744	2.344
10	150 ± 10	89	-3.429	3.069
25	115	41	-4.001	3.849

experimental results were reported to verify this belief for the case of wax-graphite electrodes made by admixture. We have investigated this problem by monitoring the performance of these electrodes over a period of time. The electrode was used as a sensing element in a detector for a flow injection system. The test solution was 5.00×10^{-4} M ferroin in 1.00 M KCl. The potential of the electrode was fixed at 0.850 V vs. SCE. Such potential is high enough to insure complete electrolysis of the ferroin at the electrode surface. The response of the electrode was monitored for 88 h. Results from this experiment are summarized in Table 14. It seems from the Table that the electrode performance does not deteriorate although the electrode potential was not changed during the experimental period. Figure 36 shows typical signals obtained under flow conditions. A slight increase in peak current can be observed in the Table. It is believed that this increase is due to a behavior similar to that observed in the electrochemical pretreatments. Neither the peak shape nor the base-line level changed after 88 h. These observations invite the conclusion that the wax-graphite electrodes are stable and do not lose their performance with time. The improvement in the electrode behavior over that reported for wax-impregnated electrodes may be related to the electrode compositions. In the case of wax-impregnated graphite electrodes, melted wax is used to replace the air entraped in channels between the prefabricated graphite masses. After solidification, some

TABLE XIV

RELATIVE PEAK HEIGHTS OBTAINED FOR FERROIN (5.0×10^{-4} M) UNDER FLOW CONDITIONS BY USING A WAX-GRAPHITE ELECTRODE AS A SENSOR

Time of Exposure, h	Relative Peak Height, mm
0.5	106 ± 4%
18	111 ± 1%
40	114 ± 1%
88	116 ± 1%

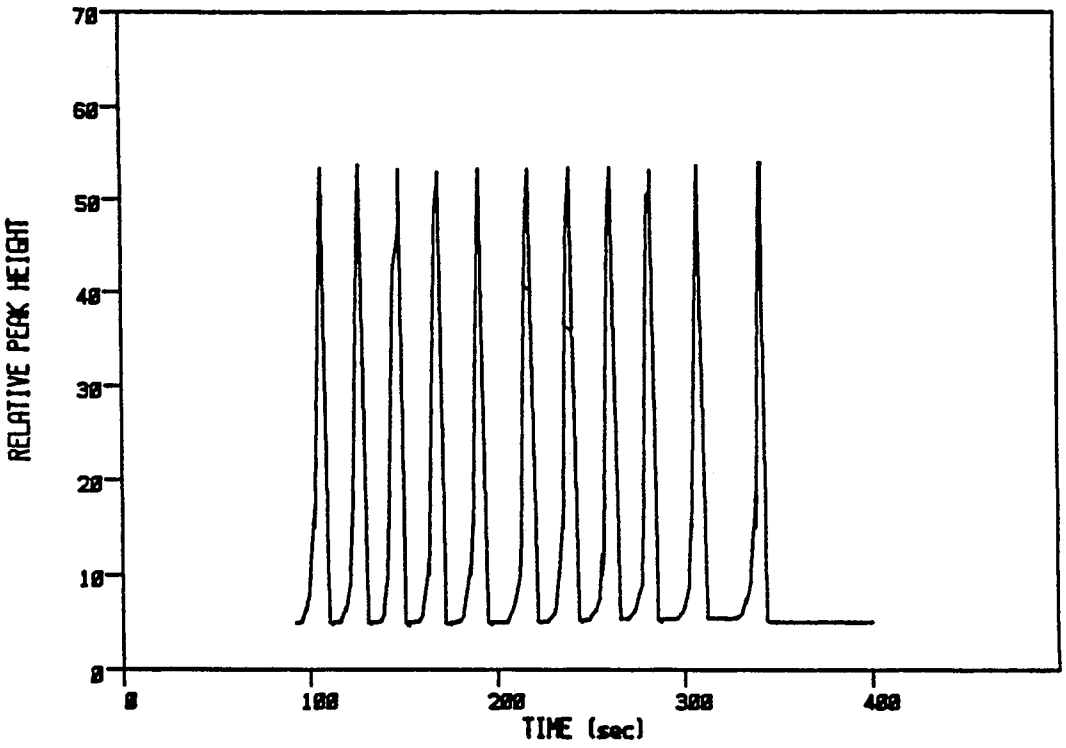

Figure 36. Typical peaks obtained with wax-graphite electrode. Test solution: 5.00×10^{-4} M ferroin; carrier solution: 1.00 M KCl; flow rate: 3.0 mL/min; electrode potential: 0.850 V vs SCE: volume of ferroin solution injected: 300 μL.

cracks start to appear and the wax can separate from the graphite substrate. Owing to the cracking process the electrodes start gradually lose their performance (136). On the other hand, the preparation of wax-graphite electrodes involves covering the fine graphite grains "uniformly" with wax and then forming the electrode. The wax content of these electrodes will be much higher than that reported for wax-impregnated graphite electrodes. The presence of the wax at higher ratios seems to minimize or eliminate the cracking process.

Performance of Modified Graphite-Wax Electrodes

As was stated earlier, graphite-wax electrodes eliminate most of the drawbacks reported for classical paste electrodes (see Table 11). But, do these electrodes minimize the diffusion of the modifier in comparison to classical paste electrodes? This behavior can be seen clearly in Figure 37, which compares the relative diffusion rates from two electrodes. The two electrodes were exactly the same except for the nature of the binder, hexadecane or wax. The modifier content in these electrodes was 16.8%, much higher than normally used. Each of these electrodes was immersed in 3.0 mL of 1.00 M KCl in a spectrophotometric cell and the absorbance at 512 nm, due to ferroin leached out of the electrodes, was monitored as a function of time. The loss of the ferroin from the graphite-wax electrode leveled off after about 20 min. In the paste

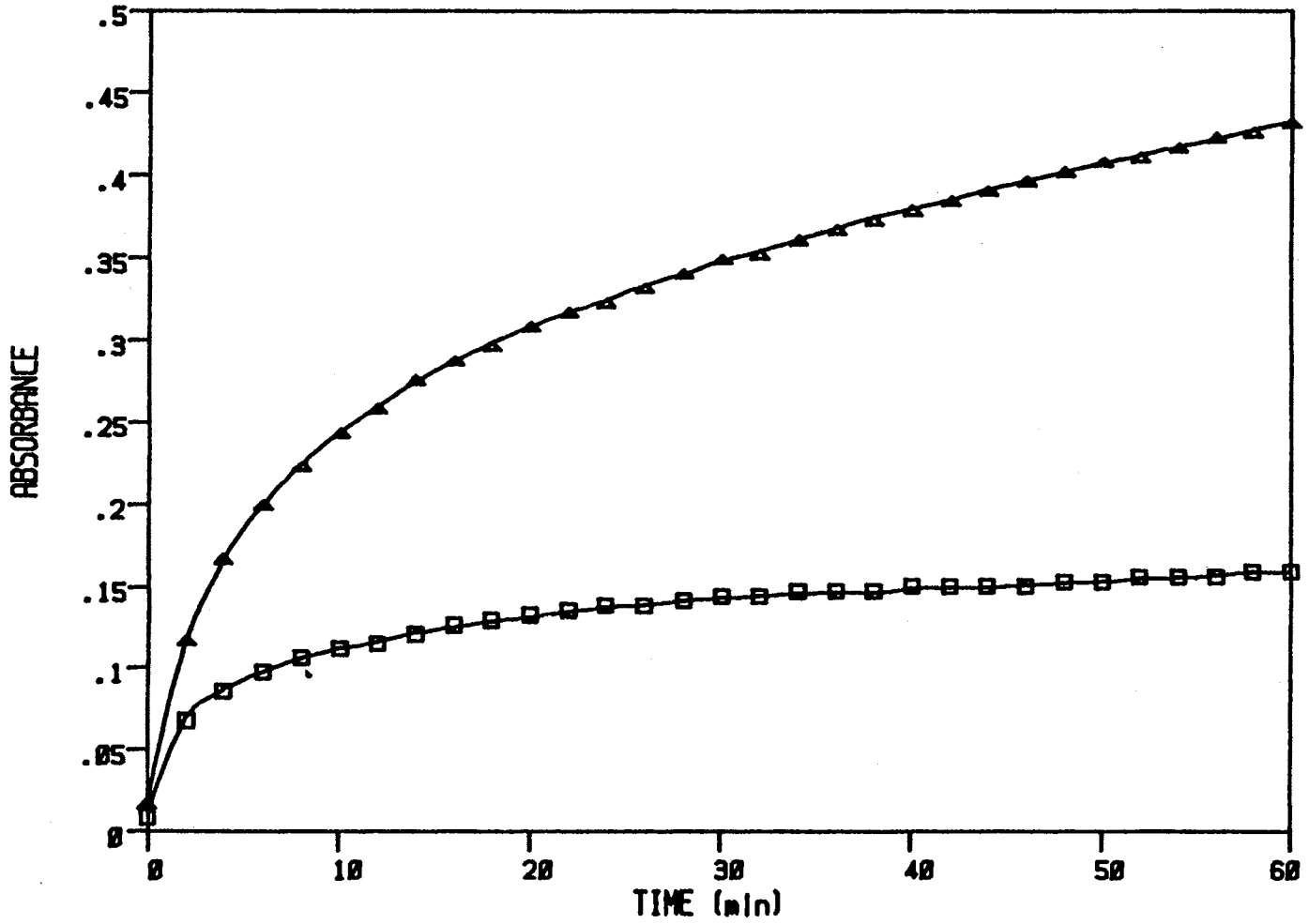

Figure 37. Relative diffusion rate of ferroin from conventional paste electrodes (triangles) and wax-graphite electrode (squares).

electrode, ferroin came out of the electrode at an appreciable rate even after one hour.

The improved stability of the modified wax-graphite electrodes was also tested in nonaqueous solvent. For this experiment ferrocene was used as the modifier. The electrodes were tested in 0.20 M sodium perchlorate in acetonitrile. The stability of the wax-graphite electrode in the organic medium was similar to that observed in aqueous medium. Figure 38 shows a typical voltammogram observed for a ferrocene-modified electrode. Modified paste electrodes were not used in nonaqueous solvents because the organic nature of the binder make it subject to loss by leaching.

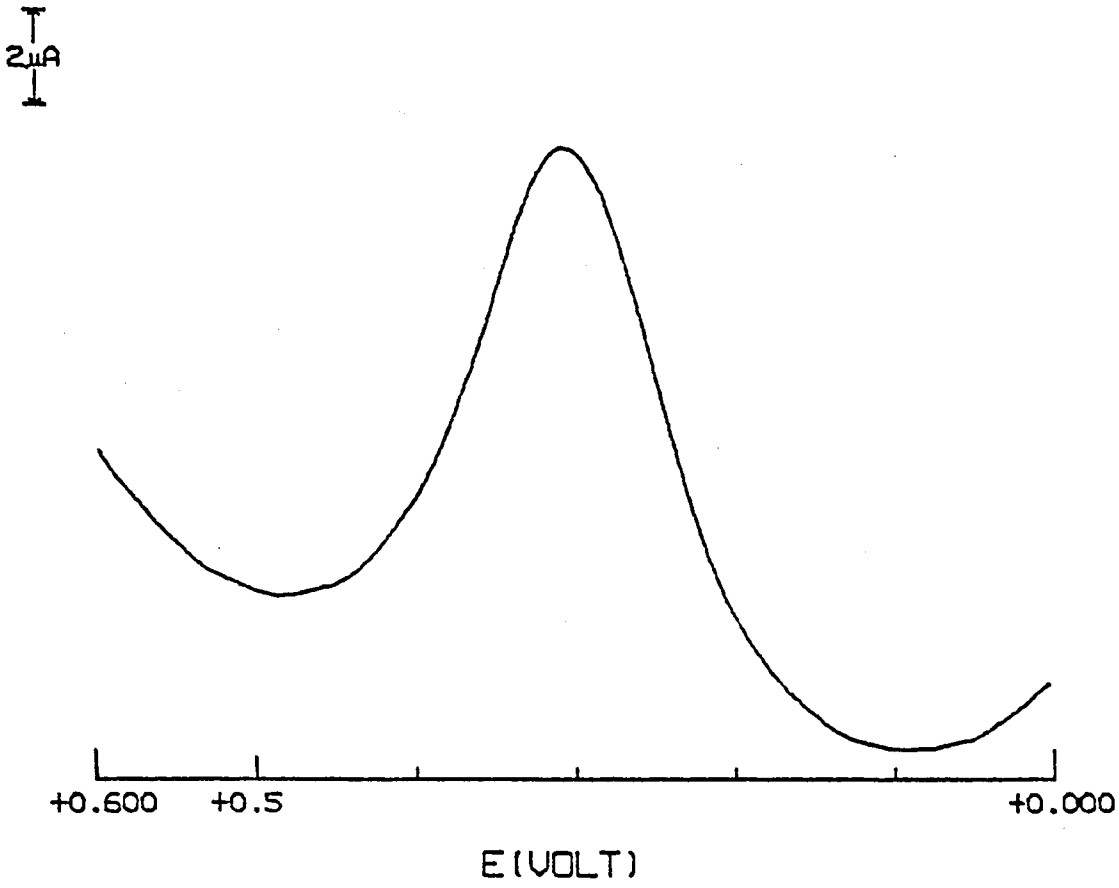

Figure 38. Square-wave voltammogram for wax-graphite electrode modified by admixng 5% (w/w) of ferrocene. Supporting electrolyte 0.20 M $NaClO_4$ in acetonitrile.

CHAPTER VI

CONCLUSIONS

This work has dealt with three related projects aimed at the design of an electrochemical input transducer. Tris(1,10-phenanthroline)iron(II), ferroin, served as the sensing element of the transducer. The first project was devoted to the electrochemical characterization of ferroin in solution. This investigation produced significant information to be considered in optimizing the redox behavior of the ferroin. The ferroin showed a reversible behavior in different acidic media at pH values from 2.0 to 5.0. Decreasing the pH below 2.0 brought a significant change in the shape and potential of the redox peaks with time. The redox peak heights for ferroin were the same in chloride and nitrate media but 20% less in sulfate.

The second project aimed for the enhancement of the electron transfer process on graphite paste electrode surfaces. This was conducted by exposing the electrodes to 0.1% surfactant solution. This procedure proved more effective than the commonly used electrochemical method. Paste electrode pretreated with surfactant supplied significantly improved quantitative and qualitative voltammogramic data. Limits of detection of SO_2 and NO_2 in

air samples (29,30) found to be lower when surfactant treated electrodes used instead of plain paste electrodes. The enhanced sensitivity of the pretreated electrode was associated with a significant increase in background current. This shortcoming, however, could be eliminated by using an electrochemical cell with a twin-working electrodes.

The third project was directed to the modification of graphite paste electrode with ferroin. It was possible to modify the electrode by chemical attachment and admixing. While both modification gave comparable results, admixing was easy to achieve and offered better control on loading the desired amount of the modifier. The performance of electrodes modified by admixing was enhanced sharply by replacing the conventional organic viscous liquids with a high-molecular-weight paraffin wax. The wax minimized the dissolution of the modifier and made it possible to construct the electrode in any desired shape. In addition, the presence of the wax extended the usefulness of graphite paste electrodes into nonaqueous media.

LITERATURE CITED

1. Blaedel, W. J.; Wang, J. Anal. Chem. 1981, 53, 78.

2. Alxender, P. W.; Hadded, P. R.; Low, G. K.; Maitra, C. J. Chromatogr. 1981, 209, 29.

3. Kissinger, P. T.; Bruntlett, G. S.; Bartin, K.; Rice, J. R. in Trace Organic Analysis: A New Frontier in Analytical Chemistry, NBS Special Publ. # 519, Washington, 1979, p. 705.

4. Weber, S. G.; Purdy, W. C. Anal. Chem. 1982, 54, 1757.

5. Fleet, B.; Little, C. J. J. Chromatogr. Sci. 1974, 12, 747.

6. Hanekamp, H. B.; Voogt, W. H.; Bos, P.; Frei, R. W. Anal. Lett. 1979, 12, 175.

7. Piblar, B.; Kosta, L.; Haristovski, B. Talanta 1979, 26, 805.

8. Kok, W. Th.; Hanekamp, H. B.; Bos, P.; Frei, R. W. Anal. Chim. Acta 1982, 142, 31.

9. Gaylor, V. F.; Elving, P. J. Anal. Chem. 1952, 25, 1078.

10. Gaylor, V. F.; Conrad, A. L.; Landerl, J. H. Anal. Chem. 1957, 29, 224.

11. Jarbawi, T. B.; Heineman, W. R. Anal. Chim. Acta 1986, 186, 11.

12. Adams, R. N. Anal. Chem. 1958, 30, 1576.

13. Marcoux, L. S.; Prater, K. B.; Prater, B. G.; Adams, R. N. Anal. Chem. 1965, 37, 1446.

14. Rice, M. E.; Galus, Z.; Adams, R. N. J. Electroanal. Chem. 1983, 143, 89.

15. Ravichandran, R.; Baldwin, R. P. Anal. Chem. 1984, 56, 1744.

16. Urbaniczky, C.; Lundstrom, K. J. Electroanal. Chem. 1984, 176, 169.

17. Albahadily, F. N.; Mottola, H. A. Anal. Chem. 1987, 59, 958.

18. Swofford, H. S.; Carman, R. L., III Anal. Chem. 1966, 38, 966.

19. Pungor, E.; Szepsvary, E.; Havas, J. Anal. Lett. 1968, 1, 213.

20. Pungor, E.; Szepsvary, E. Anal. Chim. Acta 1968, 43, 289.

21. Kissinger, P. T.; Refshauge, C.; Dreiling. R; Adams, R. N. Anal. Lett. 1973, 6, 465.

22. Klatt, L. N.; Connell, D. R.; Adams, R. E.; Honigberg, I. L.; Price, J. C. Anal. Chem. 1975, 47, 2470.

23. Anderson, J. E.; Tallman, D. E.; Chesney, D. J. Anal. Chem. 1978, 50, 1051.

24. Armentrout, D. N.; Mclean, J. D.; Long, M. W. Anal. Chem. 1979, 51, 1039.

25. Stulik, K.; Pacakova, V.; Starkova, B. J. Chromatog. 1981, 213, 41.

26. Weisshaar, D. E.; Tallman, D. E.; Anderson, J. L. Anal. Chem. 1981, 53, 1809.

27. Anderson, J. L.; Chesney, D. L. Anal. Chem. 1980, 52, 2156.

28. McLean, J. D. Anal. Chem. 1982, 54, 1161.

29. Rios, A.; Luque de Castro, M. D.; Valcarcel, M.; Mottola, H. A. Anal. Chem. 1987, 59, 666.

30. Nyasulo, F.; Mottola, H. A. J. Auto. Chem. 1987, 9,46.

31. Schilt, A. A."Analytical Application of 1,10-Phenanthroline and Related Compounds"; Pergamon: New York, 1969.

32. Gaines, A.; Hammett, L. P.; Walden, G. H. J. Am. Chem. Soc. 1936, 58, 1668.

33. Anderegg, G. Helv. Chim. Acta 1962, 45, 1643.

34. Pantani, F.; Giantelli, G. Ric. Sci. 1968, 38, 721.

35. Ogura, K.; Nahara, K.; Ueda, M. Electrochim. Acta 1976, 21, 807.

36. Ogura, K.; Miyamoto, K. Electrochim. Acta 1976, 22, 1357.

37. Anson, F. C. Anal. Chem. 1966, 38, 54.

38. Fried, I. "The Chemistry of Electrode Processes"; Acadimic: London, 1973, p. 139.

39. Kissinger, P. T.; Heineman, W. R. "Laboratory Techniques in Electroanalytical Chemistry"; Marcel Dekker: New York, 1984, p. 92.

40. Adams, R. N. "Electrochemistry at Solid Electrodes"; Marcel Dekker: New York, 1969, p. 26.

41. Kissinger, P. T.; Refshauge, C.; Dreeiling, R.; Adams, R. N. Anal. Lett. 1973, 6, 465.

42. Albahadily, F. N.; Mottola, H. A. J. Chem. Educ. 1986, 63, 271.

43. Watkins, B. F.; Behling, J. R.; Kariv, E.; Miller, L. L. J. Am. Chem. Soc. 1975, 97, 3549.

44. Operation/Installation/Maintenance Manual for the BAS-100 Electrochemical Analyzer; Bioanalytical System Inc.: West Lafayette, IN, 1983; Appendix E, p. E-1 and E-2.

45. Lindquist, J. J. Electroanal. Chem. 1974, 52, 37.

46. Rusling, J. F.; Brooks, M. Y. Anal. Chem. 1984, 56, 2147.

47. Anderson, J. E.; Tallman, D. E.; Chesney, D. J.; Anderson, J. L. Anal. Chem. 1978, 50, 1051.

48. Hohman, J. R.; Fox, Jr., M. A. Am. Chem. Soc. 1983

49. Malpas, R. E. J. electroanal. Chem. 1981, 117, 347.

50. Bard, A. J. Chem. Educ. 1983, 60, 302.

51. Bruna, H. D.; Calvert, J. M.; Denisevkh, P.; Ellis, C. D.; Meyer, T. J.; Murphy, Jr., W. R.; Murray, R. W.; Suulivan, B. P.; Walsh, J. L. "Chemically Modified Surfaces in Catalysis and Electroanalysis"; American Chemical Society; Washington, D. C., 1982, p. 133.

52. Elliott, C. M.; Murray, R. W. Anal. Chem. 1976, 48, 1247.

53. Sugawara, K. F.; Weetal, H. H.; Schucker, G. D. Anal. Chem. 1974, 46, 489.

54. Peuckert, M.; Coenen, F. P.; Bonzel, H. P. Electrochim Acta 1984, 29, 1305.

55. Peuckert, M. Electrochim Acta 1984, 29, 1315.

56. Wrighton, M. S.; Palazzotta, M. C.; Bocarsly, A. B.; Bolts, J. M.; Fisher, A. B.; Nadjo, L. J. Am. Chem. Soc. 1978, 100, 7264.

57. Lennard, J. R.; Murray, J. W. J. Electroanal. Chem. 1977, 78, 195.

58. Abruna, H. D.; Meyer, T. J.; Murray, R. W. Inorg. Chem. 1979, 18, 3233.

59. Lennard, J. R.; Rocklin, R.; Abruna, H. D.; Kuo, W. K.; Nowak, R.; Murray, R. W. J. Am. Chem. Soc. 1978, 100, 5213.

60. Hardee, K.; Bard, A. J. J. Electrochem. Soc. 1982, 123, 739.

61. Moses, P. R.; Wier, L.; Murray, R. W. Anal. Chem. 1975, 47, 1882.

62. Allerd, A. L.; Bradley, C.; Newman, T. H. J. Am. Chem. Soc. 1978, 100, 5081.

63. Ayscough, P. B.; in "Electron Spin Resonance", Ayscough, P. B. Ed.; The Royal Society of Chemistry; Burlington House, London, 1981.

64. Diaz, A. J. Am. Chem. Soc. 1977, 99, 5838.

65. White, S. H.; Murray, R. W. Anal. Chem. 1979, 51, 236.

66. Sharp, M.; Peterson, M. J. Eelectroanal. Chem. 1981, 122, 409.

67. Moses, P. R.; Murray, R. W. J. Am. Chem. Soc. 1976, 98, 7435.

68. Evans, J. F.; Kuwana, T. Anal. Chem. 1977, 49, 1635.

69. Yacynych, A. M.; Kuwana, T. Anal. Chem. 1978, 50, 640.

70. Lin, A. W.; Yeh, P.; Yacynych, A. M.; Kuwana, T. J. Electroanal. Chem. 1977, 84, 411.

71. Dautartas, M. F.; Evans, J. F.; Kuwana, T. Anal. Chem. 1979, 51, 104.

72. Ianiello, R. M.; Yacynych, A. M. Anal. Chem. 1981, 53, 2090.

73. Szentrimay, R.; Yeh, P.; Kuwana, T. in "Electrochemical Studies of Biological Systems"; Sawyer, D. T., Ed.; American Chemical Society, Washington, D. C., 1977

74. Lennox, J. C.; Murray, R. W. J. Electroanal. Chem. 1977, 78, 395.

75. Evans, J. F.; Kuwana, T. J. Electroanal. Chem. 1977, 80, 409.

76. Koval, C. A.; Anson, F. C. Anal. Chem. 1978, 50, 223.

77. Rocklin, R. D.; Murray, R. W. J. Electroanal. Chem. 1979, 100, 271.

78. Oyama, N.; Brown, A. P.; Anson, F. C. J. Electroanal. Chem. 1978, 87, 435.

79. Heinze, J. Angew Chem 1984, 23, 831.

80. Brown, A. P. Anson, F. C. Anal. Chem. 1977, 49, 1589.

81. Smith, D. F.; Willman, K.; Kuo, K.; Murray, R. W. J. Electroanal. Chem. 1978, 95, 217.

82. Laviron, E. J. Electroanal. Chem. 1974, 52, 395.

83. Wrighton, M. S.; Auston, R. G.; Bocarsly, A. B.; Bolts, J. M.; Hass, O.; Legg, K. D.; Nadjo, L.; Palazzato, M. C. J. Electroanal. Chem. 1978, 87, 429.

84. Rocklin, R. D.; Murray, R. W. J. Phys. Chem. 1981, 85, 2104.

85. Flato, J. B. Anal. Chem. 1977, 44, A75.

86. Ianniello, R. M.; Lindsay, T. J.; Yacynych, A. M. Anal. Chem. 1982, 54, 1098.

87. Smith, D. E. J. Electroanal. Chem. 1966. 1, 1.

88. Diaz, A. F.; Kanazawa, K. K. J. Electroanal. Chem. 1978, 86, 441.

89. Lennox, J. C.; Murray, R. W. J. Am. Chem. Soc. 1978, 100, 3710.

90. Baker, A. D.; Betteridg , D. "Photoelectron Spectroscopy, Chem cal and Analytical Aspects"; Permingham Press; xford; 1972, p. 119.

91. Moses, P. R.; Weir, L. .; Lennox, J. C.; Finklea, H. O.; Lennard, J. R. Murray, R. W. Anal. Chem. 1978, 50, 576.

92. Fiscker, A. B.; Wrighto , M. S.; Umana, M.; Murray, R. W. J. Am. Chem. So . 1978, 100, 3442.

93. Lennard, J. R.; Murray, R. W. J. Am. Chem. Soc. 1978, 100, 7870.

94. Proctor, A.; Castner, J F. Wingord, L. B.; Hercules, D. M. Anal. Chem. 1985, 57, 1644.

95. Finklea, H. O.; Murray, R. W. J. Phys. Chem. 1979, 83, 353.

96. Carlson, T. A. "Photoel ctron and Auger Spectroscopy"; plenum Press; New ork; 1979, p. 279.

97. Armstrong, N. R.; Lin, W.; Fujihira, M. Kuwana, T. Anal. Chem. 1976, 3, 741.

98. Willman, K. W.; Greer, .; Murray, R. W.

99. Diaz, A. F.; Kanazawa, K. IBM J. Res. Div. 1979, 23, 316.

100. Diaz, A. F.; Hetzler, .; Kay, E. J. Am. Chem. Soc. 1977, 99, 6780.

101. Diaz, A. F. "Silylated Surfaces" Leyden, D. E.; Collins, W. T. Ed ; Gordon and Breach: New York; 1980, p. 137.

102. Simonsen, M. G.; Colem n, R. V.; Hansma, P. K. J. Chem. Phys. 19 4, 61, 3789.

103. Finklea, H. O.; Vithan ge, R., NASA Report, NASA-CR-165063, 1 32.

104. Untereker, D. F.; Lenn x, J. C.; Wier, L. M.; Moses, P. R.; Murray, R W. J. Electroanal. Chem. 1977, 81, 309.

105. Srinivasan, V. S.; Lam , W. J. Anal. Chem. 1977, 49, 1639.

106. Wosilait, W. D.; Nason A. J. Biol. Chem. 1953, 206, 271.

107. Tse, D. C.; Kuwana, T. Anal. Chem. 1978, 50, 1315.

108. Kamin, R. A., Wilson, G. S. Anal. Chem. 1980, 52, 1198.

109. Gregg, M. R. Chromatographia 1985, 20, 129.

110. Firth, B. E.; Miller, L. L. J. Am. Chem. Soc. 1976, 98, 8272.

111. Osa, T.; Fujihira, M. Nature 1976, 264, 349.

112. Fujihira, M.; Ohishi, N.; Osa, T. Nature (London) 1977, 268, 226.

113. Fujihira, M.; Osa, T.; Hurh, D.; Kuwana, T. J. Electroanal. Chem. 1978, 88, 285.

114. Hawn, D. D.; Armstrong, N. R. J. Phys. Chem. 1978, 82, 1288.

115. Wrighton, M. S.; Ausin, R. G.; Bocarsly, A. B.; Bolts, J. M.; Haas, O.; Legg, K. D.; Nadjo, L.; Palazzotta, M. C. J. Am. Chem. Soc. 1978, 100, 1602.

116. Bolts, J. M.; Wrighton, M. S. J. Am. Chem. Soc. 1978, 100, 5257.

117. Sharp, M. J. Electroanal. Chem. 1978, 23, 287.

118. Wang, J. "Stripping Analysis: Principle, Instrumentation and Application"; Verlag Chem.: Deerfield Beach, 1985.

119. Cheeck, G. T.; Nelson, R. F. Anal. Lett. !978, 11, 393.

120. Ravichandran, K.; Baldwin, R. P. Anal. Chem. 1983, 54, 1586.

121. Santos, L. M.; Baldwin, R. P. Anal. Chem. 1987, 59, 1766.

122. Baldwin, R. P.; Christensen, J. K.; Kryger, L. Anal. Chem. 1986, 58, 1790.

123. Takuchi, E. S.; Murray, R. W. J. Electroanal. Chem. 1985, 188, 49.

124. Kutner, W.; Meyer, T. J.; Murray, R. W. J. Electroanal. Chem. 1985, 195, 375.

125. Yao, T.; Musha, S. Anal. Chim. Acta 1979, 110, 203.

126. Ravichandran, K.; Baldwin, R. P. J. Electroanal. Chem. 1981, 126, 293.

127. Murray, R. W. in "Electroanalytical Chemistry"; Bard, A., Ed.; Vol. 13; Marcel Dekker, Inc.: New York, 1983.

128. Barton, S. S.; Harrison, B. H. Carbon 1975, 13, 283.

129. Puri, P. R. in "Chemistry and Physics of Carbon"; Walker, P. L., Ed.; Marcel Dekker, Inc.: New York 1970.

130. Koval, C. A.; Anson, F. C. Anal. Chem. 1978, 50, 223.

131. Covington, J. R.; Lactoste, R. J. Anal. Chem. 1965, 37, 420.

132. Fenn, R. J.; Siggia, S.; Curran, D. J. Anal. Chem. 1978, 50, 1067.

133. Oyama, N.; Brown, A. P.; Anson, F. C. J. Electroanal. Chem. 1978, 87, 435.

134. Tse, D. C.; Kuwana, T. Royer, G. P. J. Electroanal. Chem. 1979, 98, 345.

135. McLaren, K. G.; Batley, G. E. J. Electroanal. Chem. 1977, 79, 169.

136. Clem, R. G.; Litton, G.; Ornelas, L. D. Anal. Chem. 1973, 45, 1307.

137. Halbert, M. K.; Baldwin, R. P. Anal. Chem. 1985, 57, 591.

2

VITA

Fakhrildeen Niema Albahadily

Candidate for the Degree of

Doctor of Philosophy

Thesis: DEVELOPMENT AND APPLICATION OF CHEMICALLY MODIFIED ELECTRODES FOR USE IN CONTINUOUS-FLOW SYSTEMS

Major Field: Chemistry

Biographical:

Personal Data: Born in Messan, Iraq, April 13, 1953, the son of Niema Albahadily and Wessila Alak. Married to Zaineb A. Attia on August 22, 1981. Sarah and Nadia were born to Zaineb and Fakhrildeen on February 1, 1983 and on December 22, 1987.

Education: Graduated from Naqabat Almoalmeen high school, Baghdad, Iraq, in June, 1972; received Bachelor of Science Degree in Chemistry from Basrah University, Iraq, in June 1976; received Master of Science from Texas A&M University in May, 1984; completed requirements for the Doctor of Philosophy degree at Oklahoma State University in July, 1989.

Professional Experience: Teaching Assistant, Department of Chemistry, Oklahoma State University, August, 1982, to May, 1987; Member of Phi Lambda Upsilon and American Chemical Society.